A UNITED STATES
DEPARTMENT OF
COMMERCE
PUBLICATION

NBS TECHNICAL NOTE 758

NBS Reactor:
Summary of Activities
October 1971 to September 1972

U.S.
EPARTMENT
OF
COMMERCE
National
Bureau
of
Standards

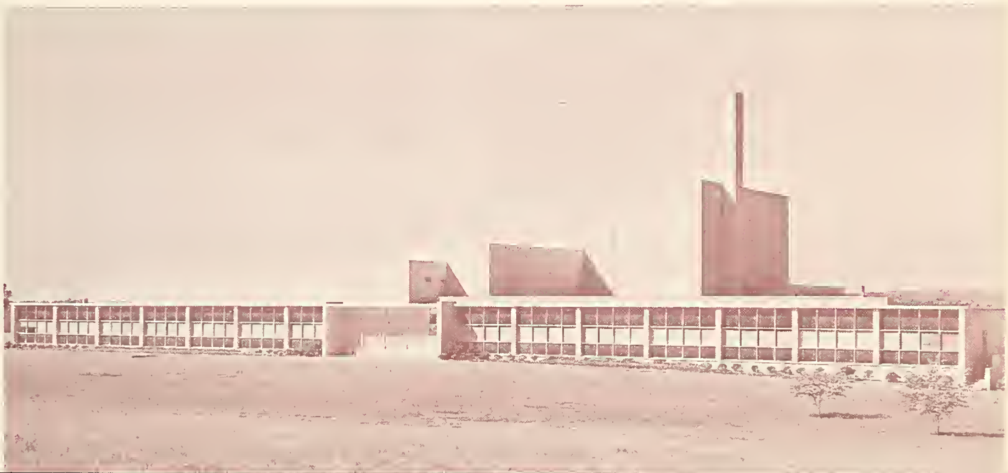

NATIONAL BUREAU OF STANDARDS

The National Bureau of Standards[1] was established by an act of Congress March 3, 1901. The Bureau's overall goal is to strengthen and advance the Nation's science and technology and facilitate their effective application for public benefit. To this end, the Bureau conducts research and provides: (1) a basis for the Nation's physical measurement system, (2) scientific and technological services for industry and government, (3) a technical basis for equity in trade, and (4) technical services to promote public safety. The Bureau consists of the Institute for Basic Standards, the Institute for Materials Research, the Institute for Applied Technology, the Center for Computer Sciences and Technology, and the Office for Information Programs.

THE INSTITUTE FOR BASIC STANDARDS provides the central basis within the United States of a complete and consistent system of physical measurement; coordinates that system with measurement systems of other nations; and furnishes essential services leading to accurate and uniform physical measurements throughout the Nation's scientific community, industry, and commerce. The Institute consists of a Center for Radiation Research, an Office of Measurement Services and the following divisions:

> Applied Mathematics — Electricity — Mechanics — Heat — Optical Physics — Linac Radiation [2] — Nuclear Radiation [2] — Applied Radiation [2] — Quantum Electronics [3] — Electromagnetics [3] — Time and Frequency [3] — Laboratory Astrophysics [3] — Cryogenics [3].

THE INSTITUTE FOR MATERIALS RESEARCH conducts materials research leading to improved methods of measurement, standards, and data on the properties of well-characterized materials needed by industry, commerce, educational institutions, and Government; provides advisory and research services to other Government agencies; and develops, produces, and distributes standard reference materials. The Institute consists of the Office of Standard Reference Materials and the following divisions:

> Analytical Chemistry—Polymers—Metallurgy—Inorganic Materials—Reactor Radiation—Physical Chemistry.

THE INSTITUTE FOR APPLIED TECHNOLOGY provides technical services to promote the use of available technology and to facilitate technological innovation in industry and Government; cooperates with public and private organizations leading to the development of technological standards (including mandatory safety standards), codes and methods of test; and provides technical advice and services to Government agencies upon request. The Institute also monitors NBS engineering standards activities and provides liaison between NBS and national and international engineering standards bodies. The Institute consists of a Center for Building Technology and the following divisions and offices:

> Engineering and Product Standards—Weights and Measures—Invention and Innovation—Product Evaluation Technology—Electronic Technology—Technical Analysis—Measurement Engineering—Building Standards and Code Services[4]—Housing Technology[4]—Federal Building Technology[4]—Structures, Materials and Life Safety[4]—Building Environment[4]—Technical Evaluation and Application[4]—Fire Technology.

THE INSTITUTE FOR COMPUTER SCIENCES AND TECHNOLOGY conducts research and provides technical services designed to aid Government agencies in improving cost effectiveness in the conduct of their programs through the selection, acquisition, and effective utilization of automatic data processing equipment; and serves as the principal focus within the executive branch for the development of Federal standards for automatic data processing equipment, techniques, and computer languages. The Center consists of the following offices and divisions:

> Information Processing Standards—Computer Information—Computer Services —Systems Development—Information Processing Technology.

THE OFFICE FOR INFORMATION PROGRAMS promotes optimum dissemination and accessibility of scientific information generated within NBS and other agencies of the Federal Government; promotes the development of the National Standard Reference Data System and a system of information analysis centers dealing with the broader aspects of the National Measurement System; provides appropriate services to ensure that the NBS staff has optimum accessibility to the scientific information of the world, and directs the public information activities of the Bureau. The Office consists of the following organizational units:

> Office of Standard Reference Data—Office of Technical Information and Publications—Library—Office of International Relations.

---

[1] Headquarters and Laboratories at Gaithersburg, Maryland, unless otherwise noted; mailing address Washington, D.C. 20234.

[2] Part of the Center for Radiation Research.

[3] Located at Boulder, Colorado 80302.

[4] Part of the Center for Building Technology.

NBS Reactor: Summary of Activities October 1971 to September 1972

Robert S. Carter, Editor

Reactor Radiation Division
Institute for Materials Research
National Bureau of Standards
Washington, D.C. 20234

NBS Technical Notes are designed to supplement the Bureau's regular publications program. They provide a means for making available scientific data that are of transient or limited interest. Technical Notes may be listed or referred to in the open literature.

U.S. DEPARTMENT OF COMMERCE, Frederick B. Dent, *Secretary*
NATIONAL BUREAU OF STANDARDS, Richard W. Roberts, *Director*

Issued March 1973

National Bureau of Standards Technical Note 758
Nat. Bur. Stand. (U.S.), Tech. Note 758, 140 pages (Mar. 1973)
CODEN: NBTNAE

For sale by the Superintendent of Documents, U.S. Government Printing Office, Washington, D.C. 20402.
Price $2.10 domestic postpaid or $1.75 G.P.O. Bookstore.

FOREWORD

The National Bureau of Standards Reactor was built not only to serve the needs of the NBS but also those of the greater Washington Scientific Community and other government agencies. The Reactor Radiation Division was established to operate the reactor and to foster its scientific and technological use. Toward this end, the Division has a small nucleus of scientists experienced in the use of reactors for a wide range of scientific and technical problems. In addition to pursuing their own research and developing sophisticated experimental facilities, they actively seek out and encourage collaboration with other scientists, engaged in challenging programs, whose work can benefit from use of the reactor, but who as yet do not have the reactor experience necessary to take full advantage of the facilities available. The Division also provides irradiation services to a wide variety of users as well as engineering and other technical services.

The reactor operates at 10 MW and is designed to provide a broad spectrum of facilities ranging from intense neutron beams to extensive irradiation facilities, making it one of the most versatile high flux research reactors in the country. Thus it is able to serve a large number of scientists and engineers in a broad range of activities both within and outside the NBS.

In previous years, this report was called "Reactor Radiation Division: Annual Report". However, since the report attempts to summarize all the work done which is dependent on the reactor including a large number of programs outside the Division, it seemed appropriate to change to the current title, "NBS Reactor: Summary of Activities". The first section summarizes those programs based primarily on Reactor Radiation Division (RRD) initiatives whereas the second and third sections summarize collaborative programs between RRD scientists and other NBS or non-NBS scientists respectively. The fourth section summarizes NBS work originating entirely outside of RRD which requires no collaboration with RRD scientists. The section entitled, "Service Programs" covers those programs originating outside NBS but for which RRD provides irradiation services. The remaining sections are self-explanatory.

Robert S. Carter, Chief
Reactor Radiation Division

ABSTRACT

This report summarizes all those programs which depend on the NBS reactor. It covers the period from October 1971 through September 1972. The programs range from the use of neutron beams to study the structure and dynamics of materials through nuclear physics and neutron standards to sample irradiations for activation analysis, isotope production and radiation effects studies.

Key Words: Activation analysis; crystal structure; diffraction; isotopes; molecular dynamics; neutron; nuclear reactor; radiation

Cover photograph: National Bureau of Standards Reactor Building, Gaithersburg, Maryland.

TABLE OF CONTENTS

TABLE OF CONTENTS

TABLE OF CONTENTS

TABLE OF CONTENTS

A. REACTOR RADIATION DIVISION PROGRAMS

ROTATIONAL DYNAMICS AND ORDER-DISORDER TRANSITIONS IN IONIC AND MOLECULAR CRYSTALS

Work has continued on detailed studies of phase transitions involving orientational disorder of ionic groups or molecules in crystals. The precise nature of the rotational disorder in the high-temperature cubic phases of broad classes of inorganic and organic solids is not in general well understood, nor is the microscopic basis of the changes in physical and thermodynamic properties associated with these order-disorder transitions. During the past year we have obtained new information concerning the dynamical and structural nature of such phase transitions in several of prototype materials (ionic and organic) by combining the results of neutron diffraction and inelastic scattering, infrared spectroscopy and Raman scattering measurements.

1. Hydrosulfide Salts - J. J. Rush and R. C. Livingston

In the past year the analysis of our previous inelastic and quasielastic scattering experiments on sodium hydrosulfide (NaSH) has been completed. In addition, samples of CsSH (whose high temperature phase has a CsCl type cubic structure) and RbSH have been synthesized and neutron spectra and neutron diffraction patterns have been measured for these compounds over a wide range of temperature. Raman spectra have also been measured for the three hydrosulfide salts at temperatures between 80 and 400K and will be discussed briefly in the next section on Lattice-Dynamics studies.

The results of our quasielastic and inelastic scattering measurements on NaSH and CsSH are illustrated in Figs. 1 and 2. In Fig. 1 we show corrected neutron spectra around the quasielastic scattering peaks (note that 1 MeV $\equiv$ 1.52 ps^{-1}) for the two hydrosulfides in their cubic phases at scattering angles of 25 and 55°. It should be noted that the width of the quasielastic peaks for both salts is considerably larger at the larger scattering angle (momentum transfer). The presence of this broadening provides direct evidence for reorientation of the SH^- ions on a time scale

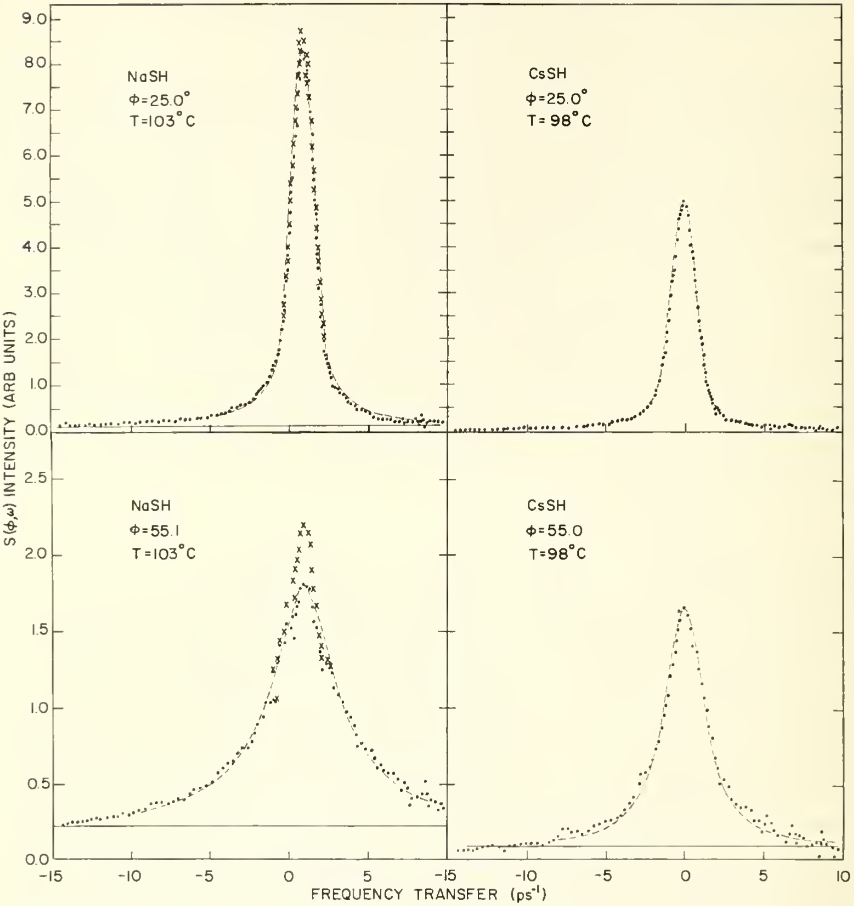

Fig. 1. Examples of quasielastic incoherent scattering spectra $S(\phi,\omega)$ for NaSH and CsSH in their cubic phases. The $S(\phi,\omega)$'s designated by (χ) represent values before correction for sodium incoherence. Model calaulations with appropriate values of τ (residence time) are indicated by dashed lines. The estimated inelastic scattering contributions and instrumental resolution (solid lines) are also shown.

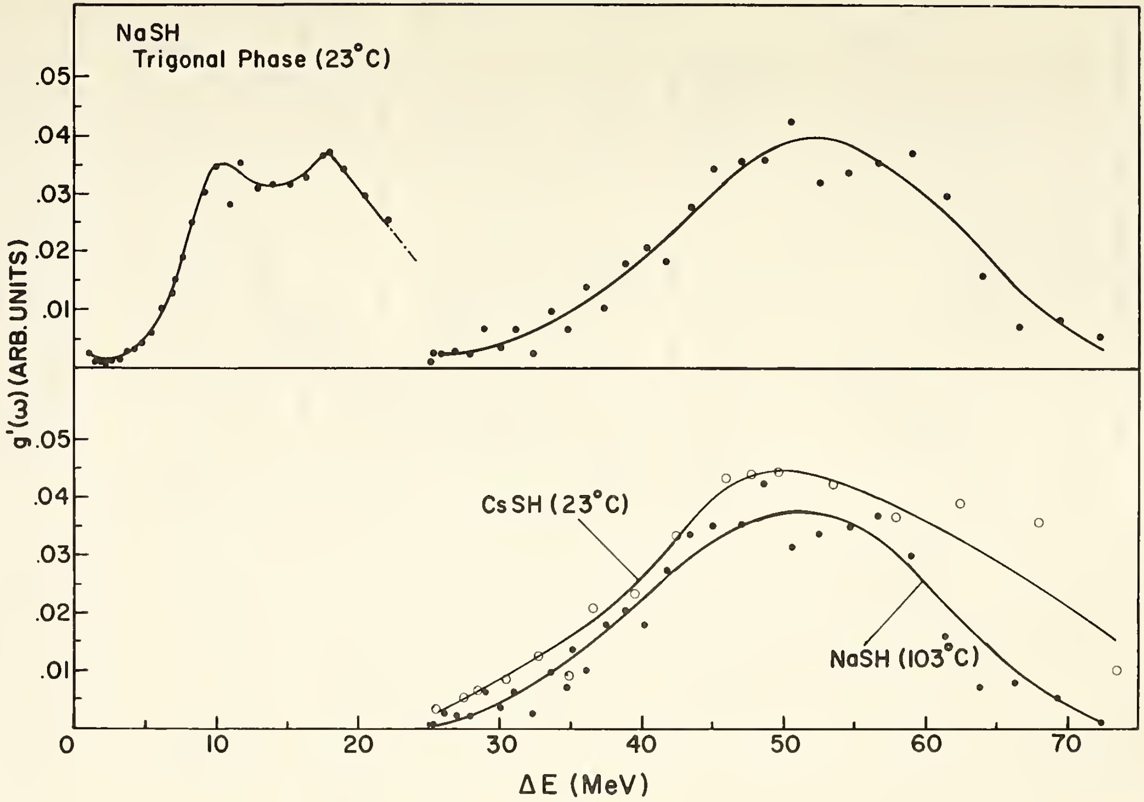

Fig. 2. "Effective" frequency distributions $g'(\hbar\omega)$ for NaSH and CsSH Only the libration bands are shown in the cubic phases.

of $\sim 10^{-12}$ sec. in the cubic phases of both compounds. No measurable broadening was observed in the elastic peak for NaSH in its trigonal phase. In Fig. 2 we show "effective" phonon energy distributions calculated from the inelastic neutron spectra for NaSH and CsSH, assuming one-phonon scattering from a cubic crystal. In each case one observes a broad "librational" band centered around an energy of 50 MeV, which clearly shows that the SH^- ions are oscillating about an equilibrium position for some time between reorientations. Moreover, the NaSH rotational bands above and below the trigonal-cubic transition are very similar, which indicates that the major dynamical change associated with the order-disorder transition is a rapid increase in reorientation rate and not a change in the equilibrium oscillations of the SH^- ions.

The widths at half-maximum ($\Delta W^{L}_{1/2}$) of the experimental quasielastic peaks for NaSH and CsSH have been measured as a function of temperature and momentum transfer, Q. These widths have been compared with theoretical calculations of quasielastic scattering behavior based on the assumption of instantaneous jumps of the SH^- ions between a limited number of equilibrium orientations, namely the [100], [110] and [111] directions in the cubic crystals. The results are shown in Fig. 3. It can be seen from the figure that each of the jump reorientation models predicts an oscillatory behavior for the observed line-widths, and such behavior is indeed observed in the experimental results. Only for the lowest-temperature results, however, is the fit for any of the model calculations close to satisfactory over the entire range of Q. The observed line-widths at $Q>3\mathring{A}^{-1}$ are generally larger than predicted from our simple jump diffusion models. This lack of fit can be attributed to several factors, including the fact that the reorientation jumps are not "instantaneous" as assumed in the theory but in some cases have jump-times comparable to the residence times between jumps.

In spite of the above uncertainties, however, our results lead us to the following conclusions concerning the disordered phases in NaSH and CsSH. First it is clear from the oscillatory behavior of the experimental widths and the observation of "librational" bands, that the disorder involves

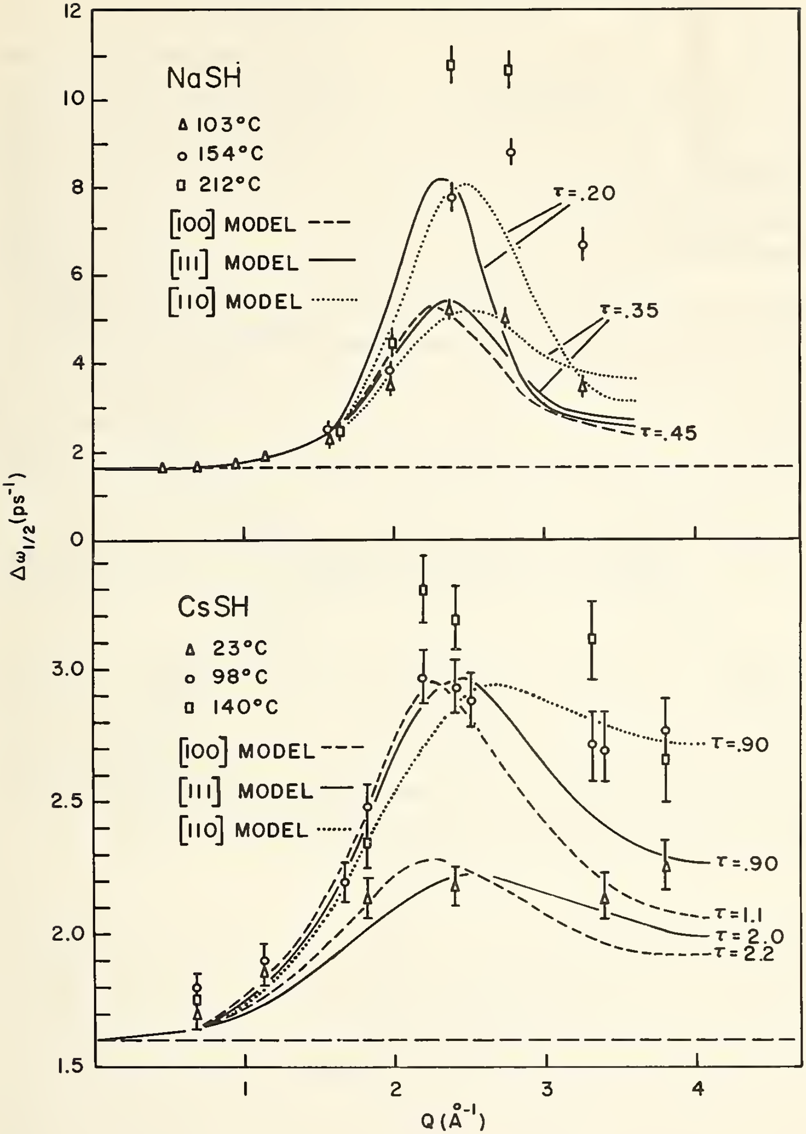

Fig. 3. Full widths at half-maximum $\Delta W_1^L/2$ vs. Q of the experimental $S(\phi,\omega)$'s for cubic NaSH and CsSH at several temperatures. Also shown are theoretical widths calculated for SH^- reorientations assuming random jumps between 6[100], 12[110] or 8[111] crystal directions. Residence times (τ) between jumps are also indicated for the theoretical curves.

SH^- ion orientation among a finite number of quasiequilibrium sites. The results thus rule out any kind of "static" disorder (on the neutron time scale) or the existence of anything approaching free or isotropic reorientation. The residence times between jumps range from 0.4 to 0.2 for NaSH in the temperature range 100 to 200°C and from 2.0 to 0.75 ps for CsSH in the range from 23 to 140°C. Comparisons of the theoretical and experimental line-widths do not lead to a definite conclusion concerning equilibrium SH^- orientations, but they do suggest that the [100] and [111] directions are least likely for NaSH and CsSH, respectively. It should be noted here that we have recently measured quasielastic neutron spectra for CsSH and RbSH at four times the instrumental resolution used in the experiments discussed here. These new measurements are in collaboration with J. M. Rowe at Argonne National Laboratory and the results are currently being analyzed in the hope of obtaining new information on the disordered phases.

During the past year we have also measured neutron powder patterns for NaSH, CsSH and RbSH at temperatures down to 80 K. These results combined with our Raman scattering spectra discussed below have revealed the existence of new crystal phases at low temperature for each hydrosulfide salt, which involve further ordering of the SH^- ions.

2. Sodium and Potassium Cyanide - J. J. Rush

NaCN and KCN are members of a broad group of polymorphic compounds M^+XY^- (which includes the hydrosulfides discussed above) whose crystal phase below the melting point has a cubic structure requiring that the linear XY^- ions assume effective spherical symmetry, either by rotation or some kind of random orientation. Attempts to study the details of the disorder in the cubic phases of the cyanides by x-ray and neutron powder diffraction have been largely unsuccessful. To obtain more definitive information on the structure of these phases, we have, in collaboration with J. M. Rowe and D. L. Price of Argonne National Laboratory, measured the neutron diffraction pattern of a single crystal of NaCN at 295K. The data was collected on a 4-circle diffractometer, using an incident wave-

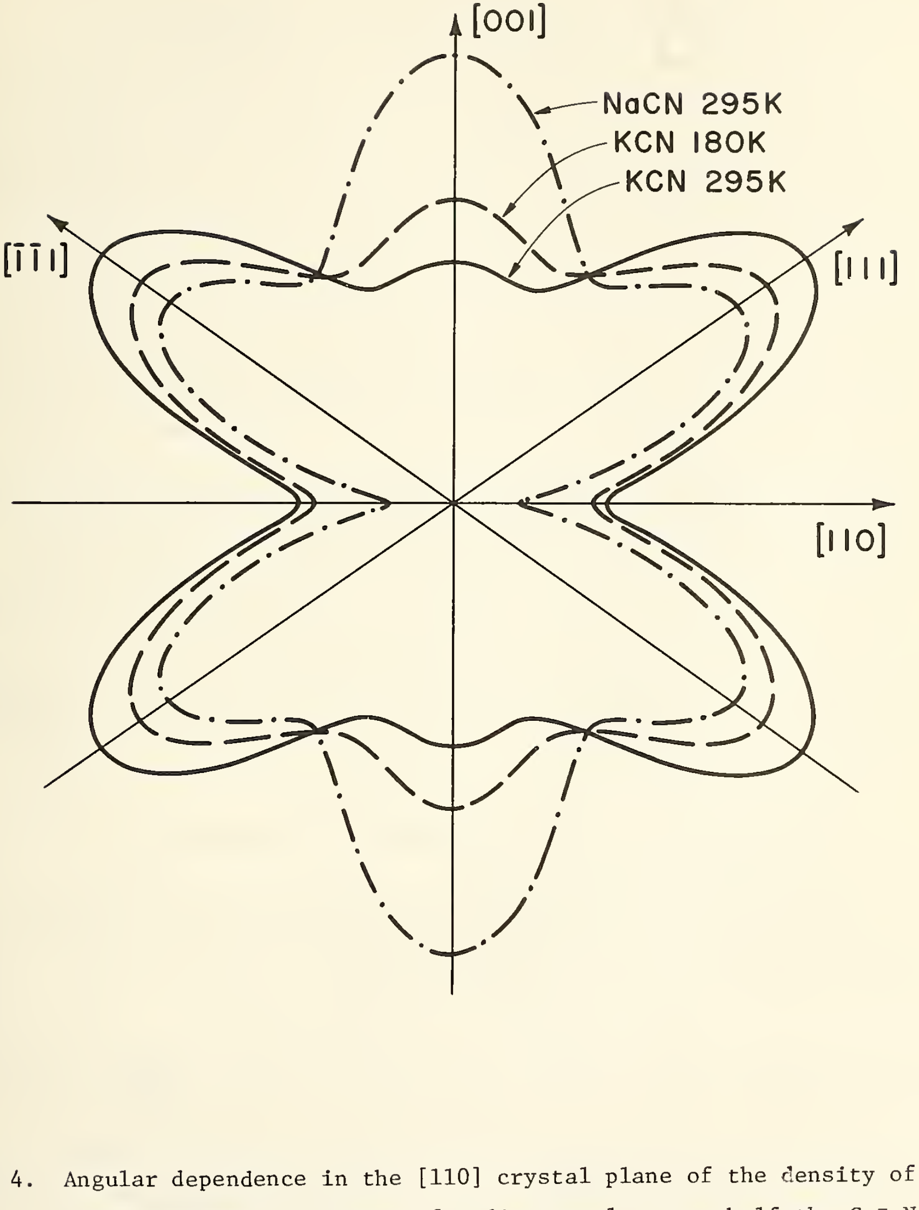

Fig. 4. Angular dependence in the [110] crystal plane of the density of C and N atoms on a sphere of radius equal to one half the C $\equiv$ N bond length.

length of 1.232Å. In our measurement 26 independent reflections were accessible; measurable intensity was found for 19 of these.

The NaCN diffraction results and our earlier diffraction patterns for KCN have been analyzed in terms of a model which expands the angular orientation of the CN^- ions in a series of symmetry-adapted spherical harmonics. This model enables us to obtain a fit to the observed diffraction intensities using as adjustable parameters a scale factor, an extinction correction, the $C \equiv N$ bond length, Debye-Waller factors for the metal and cyanide ions, and the coefficients $a_{\ell\nu}$, of the expansion in spherical harmonics. The results of these model fits to the several sets of diffraction data can be summarized as follows: Weighted R-factors of between 2-3% were obtained in each case. The derived cyanide angular distributions indicate a monotonic trend in the series KCN(295K) through KCN(180K) to NaCN(295K) involving a shift in preferential orientation from the [111] toward the [100] direction in the crystal. A view of these angular distributions is shown in Fig. 4. Unusually large translational Debye-Waller factors ($\approx 0.06 - 0.07 Å^2$) have also been derived for NaCN and KCN from the fitting procedure, in agreement with an earlier analysis of the KCN data. In addition, an average $C \equiv N$ bond distance of 1.18Å was obtained from the three fits.

3. Infrared and Raman Band Shape Analysis of Neopentane -

R. C. Livingston and J. J. Rush

The correlation functions for the infrared and anisotropic Raman bands of a spherical molecule such as neopentane are given by

$$\langle u(o)\cdot u(t)\rangle \text{ and } 1/2\langle 3[u(o)\cdot u(+)]^2-1\rangle$$

where u(t) is a vector along one of the two-fold axes. These functions are the Fourier transforms of infrared and depolarized Raman bands, respectively. They yield detailed information on the time behavior of rotational motion of a molecule. In addition both correlation functions arise in a diffent way in the theory of neutron scattering so that a comparison of the optical results with those of neutron scattering can in principle yield more information about the rotational behavior.

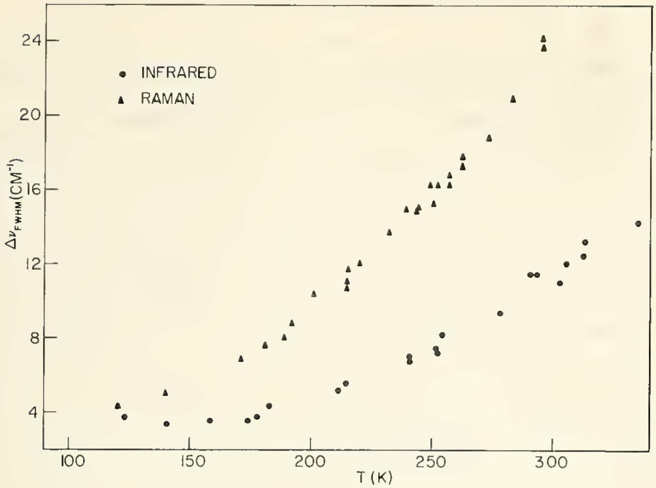

Fig. 5. Raman and infrared bandwidths (full widths at half maximum) of the 924 cm^{-1} rotation-vibration band of neopentane as a function of temperature.

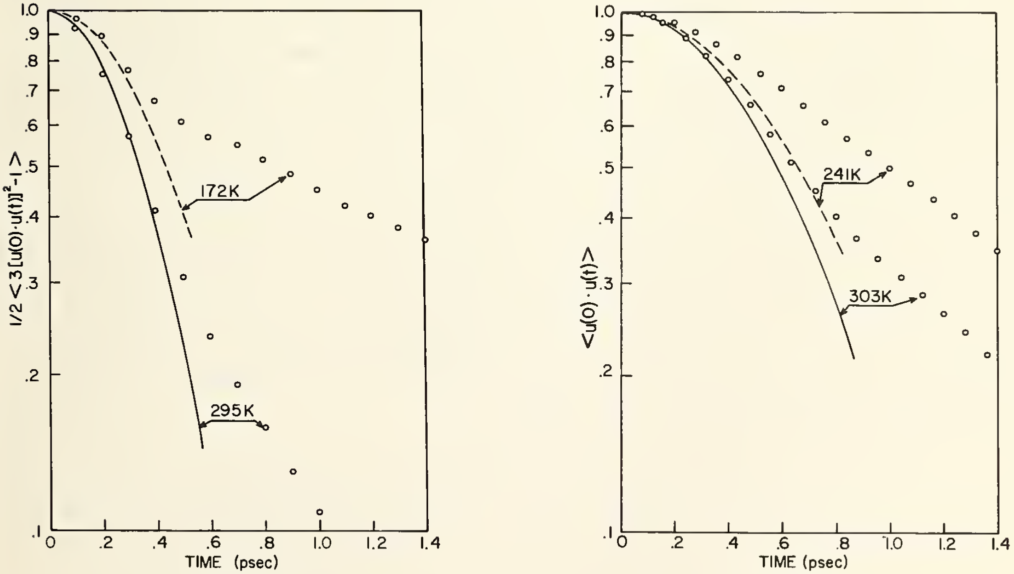

Fig. 6. Correlation functions of the 924 cm^{-1} Raman band of neopentane The curves represent the free-rotor decay.

Since the last reporting period, Raman spectra of the F_2 vibration-rotation band (923 cm^{-1}) of neopentane have been measured at temperatures in both the solid and liquid phases. Also, the previously reported infrared measurements have been extended a wider range of temperatures. These experiments are being done in collaboration with W.G. Rothschild of the Ford Scientific Company. The full widths at half maximum for the infrared and Raman bands from 140 K to 300 K are plotted in Fig. 1. In this region neopentane has two phase transitions: liquid-plastic at 253 K and plastic-solid II at 140 K. As indicated in Fig. 1 there is no discontinuity at 253 K in either infrared or Raman bandwidths, which indicates a large degree of molecular mobility in the plastic phase of neopentane. At the plastic-solid II phase transitions both infrared and Raman bands show an abrupt splitting into several (≈6) unresolved peaks with a total width of approximately the same magnitude as that at the lowest temperature in the plastic phase. This crystal field splitting strongly suggests that the mobility exhibited in the liquid and plastic phases has disappeared. In Fig. 2 correlation functions calculated by Fourier transforming the infrared and Raman spectra at two temperatures are plotted along with the behavior expected for a free rotor at the same two temperatures. On comparing the experimental data with that of the free rotor, one sees that both the Raman and infared data indicate that at room temperature neopentane rotates freely for approximately .4 ps which corresponds to an angle of rotation before a "collision" of approximately 40 degrees. A plot of the relaxation time ($\tau \doteq 1/\pi c \Delta\nu$) vs 1/T yields an activation energy in the high temperature region of about 1.3 kcal/mol. This is in good agreement with the activation energies determined by quasielastic neutron scattering, NMR and entropy data. A full manuscript of this work will be prepared and submitted as a publication.

REACTOR RADIATION DIVISION PROGRAMS

NEUTRON SCATTERING STUDIES OF HYDROGEN IN TRANSITION METALS

The behavior of hydrogen in metals is of considerable theoretical and practical interest. Important aspects of metal-hydrogen systems include the details of diffusion processes, the nature of the M-H bonds, phase transitions, and the effects of hydriding on intermetallic forces and on electrical, magnetic, and thermodynamic properties. In this section we summarize the progress made over the past year in our continuing neutron scattering studies of the diffusion and vibration of hydrogen in transition metals. Work completed during the past year, including our first results in the investigation of hydrogen in metallic single crystals, has yielded important information on the mechanism of hydrogen diffusion in several systems.

1. Tantalum Hydride - J. J. Rush and R. C. Livingston

In collaboration with H. E. Flotow and J. M. Rowe of Argonne National Laboratory, measurements have been completed on a study of hydrogen dynamics in tantalum hydride, including the temperature and concentration dependence of the hydrogen diffusion. This work represents a natural extension of our previous studies on hydrogen in vanadium (another Group V-A metal). Neutron spectra have been measured for both $TaH_{0.15}$ and $TaH_{0.50}$ at momentum transfers (for quasielastic scattering) between $Q = 0.5A^{-1}$ and $Q = 4.1A^{-1}$ over a temperature range from 22 to 340°C. These results, and a comparison with various theoretical model for hydrogen diffusion, lead us to the tentative conclusion that jumps between tetrahedral sites are predominent in the diffusion process. In Fig. 1 we present the experimental full-widths at half-maximum $(\Delta\omega\ L\frac{1}{2})$ in $ps^{-1}(10^{12}s^{-1})$ derived from our measurements on $TaH_{0.15}$, plotted vs. Q^2. Also shown are theoretical line-width curves calculated from models assuming instantaneous near-neighbor jumps between octahedral and tetrahedral interstitial sites in the bcc metal lattice. The residence times between jumps assumed in these calculations are listed in the figure caption. The residence times obtained for $TaH_{0.15}$ vary from 3.4 to

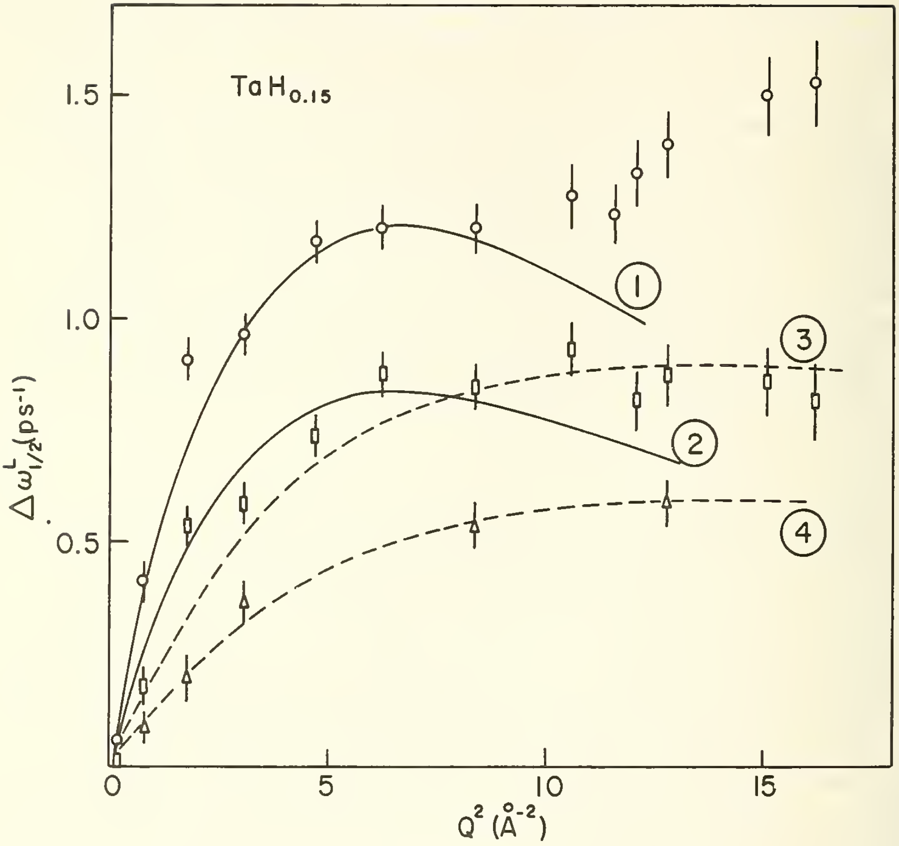

Fig. 1. The measured widths of the quasielastic peaks for $TaH_{0.15}$ compared with the predictions of several theoretical models. Curves <u>1</u> and <u>2</u>; jumps between nearest-neighbor octahedral sites; 1: τ=1.8 ps; 2: τ=2.5 ps; Curves <u>3</u> and <u>4</u> jumps between nearest neighbor tetrahedral sites; 3: τ=2.3 ps, 4: τ=3.4 ps.

1.5 ps between 148 and 340°C while an activation energy off 10.5±1.7 kJ/mol is derived for hydrogen diffusion at this concentration. The analysis of the $TaH_{0.5}$ data is not yet complete. However the results so far appear to confirm the predominence of tetrahedral jumps, and the residence times are roughly double those for $TaH_{0.15}$ at comparable temperatures. Hydrogen vibration spectra have also been obtained for $TaH_{0.50}$ and a detailed comparison with nmr results is being made.

Comparison of the tantalum hydride results with our previous results on VH_x also provides some additional insights on hydrogen diffusion in these systems. The VH_x results showed a significant increase in quasielastic line width at $Q \geq 3 Å^{-1}$, whereas the jump diffusion theory predicts little change in line-width in this region of Q. These results were attributed qualitatively to the influence of partial gas-like behavior in the hydrogen diffusion due to the fact that the jump times in the (bcc) phase of $VH_X K$ at high temperatures (~0.1 ps) are not instaneous but are comparable to the observed residence times (τ) between jumps (~0.5 to 1 ps). The slower diffusion rates in TaH_x (τ's between 1.3 and 4 ps) should minimize these effects, and offer an excellent chance to test this suggestion by examining the large Q behavior of the quasielastic scattering in this system. The results in Fig. 1 show little increase in the quasielastic line widths above Q = 3 (except for $TaH_{0.15}$ at the highest temperature) and are thus quite consistent with our previous suggestions on the influence of "gas-like" behavior. It should also be noted that the unusually high proton Debye-Waller factors which are observed for VH_x are also absent in the tantalum hydride system.

We are in the process of extending these experiments to the measurement of quasielastic and inelastic scattering by hydrogen in a single crystal of tantalum. This will enable us to examine in greater detail the diffusion of hydrogen in various crystal directions and hopefully will provide a more critical test of various diffusion models.

2. Palladium Hydride - J. J. Rush and G. A. Ferguson (Naval Research Laboratory)

In collaboration with J. M. Rowe of Argonne National Laboratory we have continued our study of the diffusion of hydrogen in a single crystal of palladium (3% H in Pd) by the quasielastic scattering of cold neutrons. The use of a single crystal in these measurements eliminates the averaging over crystallite orientations which complicates theoretical comparisons for experiments with polycrystal samples and enables us to determine the neutron momentum transfer (Q) quite well with respect to crystal direction. Measurements were obtained at T = 305°C at a series of crystal orientations and over a Q range of 0.4 to 2.5Å^{-1}. The linewidth results at every crystal orientation are in good agreement with a simple theory (Chudley-Elliott) which assumes that the migration of individual hydrogens in the fcc Pd lattice can be well described as instantaneous jumps between adjacent octahedral sites, with a residence time of 2.8 ps at 350°C. In fact the results provide the best evidence yet obtained for the applicability of a simple jump model of hydrogen diffusion in a metal. The widths at half-maximum derived for diffusion along the [110] crystal direction are shown in Fig. 3, along with theoretical widths calculated for jumps between near-neighbor octahedral and tetrahedral sites. Our results confirm the conclusions of Skold and Nelin concerning octahedral site occupations in $PdH_{0.03}$, but the hydrogen Debye-Waller factors derived from our neutron intensities ($\rho=0.05\text{Å}^2$ in the [110] direction and $\rho=0.09\text{Å}^2$ in the [100] direction are considerably lower than those obtained by these workers in their neutron spectral measurements on palladium hydride powder.

Experiments on both single-crystal and powdered palladium hydride samples are continuing. We will try to accurately measure the energy and width of the local (hydrogen vibration) mode. We have also prepared a single crystal sample of $PdD_{0.025}$, so that isotope effects on the hydrogen dynamics can be investigated. Attempts are also being continued to prepare a single crystal sample of β-PdH_x (above x = 0.6) for diffusion and lattice dynamics studies.

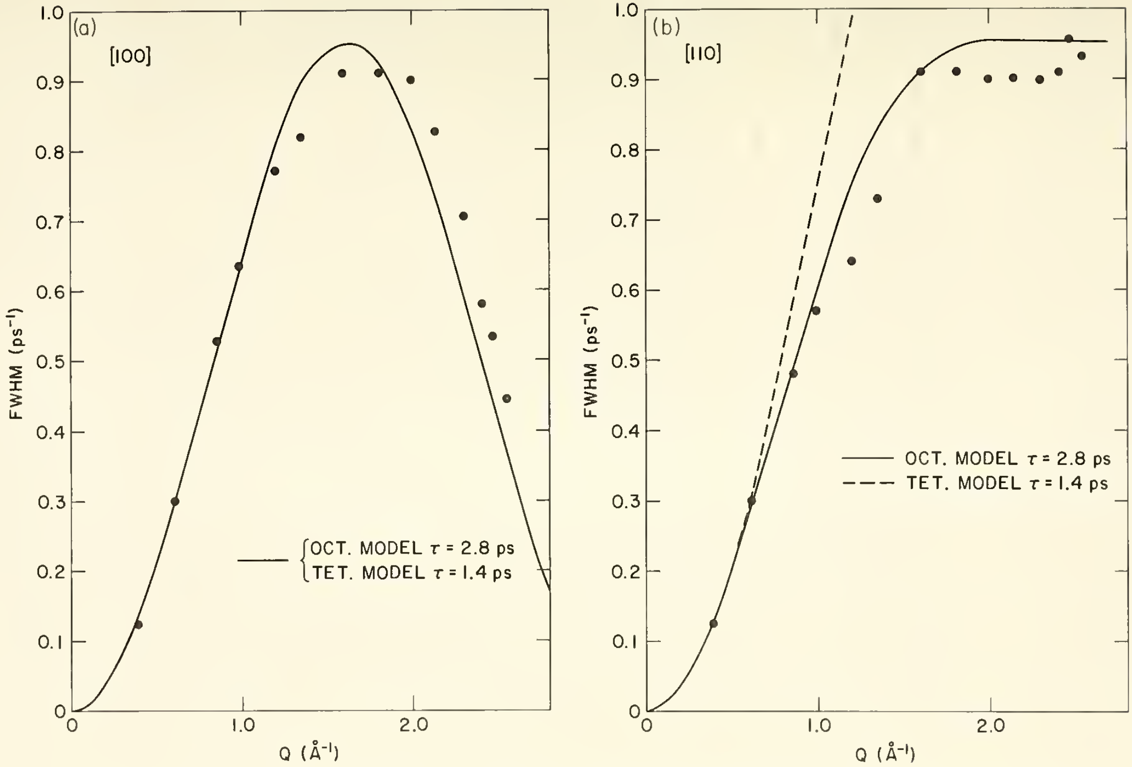

Fig. 2. (a) Full widths at half-maximum for momentum transfer ($\vec{Q}$) along the [100] direction. The predictions of a simple jump model for the two possible interstitial sites are shown as smooth curves. (b) Same as (a) for $\bar{Q}$ along the [110] axis.

LATTICE DYNAMICS STUDIES

1. KCN and Alkali Hydrosulfides - J. J. Rush and R. C. Livingston

Preliminary neutron scattering measurements of the phonon dispersion curves for acoustic branches in a single crystal of KCN have been obtained in collaboration with J. M. Rowe and D. L. Price of Argonne National Laboratory. The phonon branches measured thus far show no evidence of unusually low frequencies which might be suggested by the unusually large translational displacements derived from our diffraction data as discussed above. This is an indication that the very large "Debye-Waller" factors may reflect a random displacement of the ions from cubic lattice positions, which is not directly related to lattice vibrational motions. Further phonon measurements are planned during the coming year to obtain information about the dynamics and crystal forces in the cyanide cubic phases.

In collaboration with G. J. Rosasco of the Inorganic Materials Division, the lattice vibrational modes (at $q = o$) of NaSH, RbSH and CsSH have been investigated in three crystal phases, using the new Raman scattering instrumentation in the IMR Central Laboratory. Dramatic changes in the number, shape and frequency of the librational, translatory and S-H stretching modes of the hydrosulfide crystals have been associated with varying degrees of ordering of the SH^- ions. These results correlate quite well with the neutron diffraction and inelastic scattering results discussed above. A similar Raman study of the lattice modes of KCN and NaCN at temperatures down to 30 K has also been completed in collaboration with R. Khanna of the University of Maryland. Again very interesting effects associated with order-disorder transitions are observed. The spectroscopic results from both of these experiments are currently in the final stage of analysis and a more complete report will be presented in the next progress report.

2. Metal-Hydrogen Systems - J. J. Rush

Work has continued, in collaboration with J. M. Rowe and H. E. Flotow at Argonne National Laboratory and G. L. Ferguson of NRL, on attempts to prepare large single crystal samples of β-$PdH(D)_x$, up to a concentration of x = 0.8. If and when they are prepared these crystals will be used in a study of the lattice dynamics and local modes of this system. As mentioned above, single crystals of tantalum have also been obtained which will be loaded with hydrogen to study the effects of interstitial hydrogen on the lattice dynamics and intermetallic forces in transition metals.

CRYSTAL STRUCTURE AND THERMAL MOTION IN DURENE BY CONSTRAINED LEAST-SQUARES REFINEMENT

E. Prince and J. J. Rush
and
L. W. Schroeder

The work on the crystal structure of durene (1,2,4,5-tetramethyl benzene) described in the 1970 and 1971 progress reports has been continued further during this year. Previous efforts to refine the structure from diffraction data has produced a clear picture of overall features of the structure, but the refined structure contained a number of physically impossible details, particularly in the thermal parameters. The technique of refinement with constraints on the thermal parameters described elsewhere in this report was applied to this problem with satisfactory results. Figure 1 shows two views of the molecule as determined from two different refinements, one with and one without constraints. The two pictures are very similar, but the constrained one is preferable on physical grounds. The constrained refinement leads to values for the meansquare amplitudes of the principal librational modes of oscillation. Table 1 shows a comparison of the frequencies inferred from these amplitudes with those determined by Raman scattering and neutron inelastic scattering. The agreement is qualitatively satisfactory, and in particular the order of the frequencies of the various modes is in agreement.

TABLE 1. Librational oscillation frequencies as calculated from mean square amplitudes found in the constrained refinement, compared with frequencies measured by Raman and neutron inelastic scattering.

Axis of Libration	$I(10^{-40} g\text{-}cm^2)$	Mean Square Amplitude (radians^2)	Frequency (cm^{-1})	
			Rigid Body	Spectroscopic
Methyl Torsion	5.24	0.142	130	144,179*
OX	390	0.0115	50	72[†]
OY	803	0.0034	65	103[†]
OZ	1172	0.0085	34	32[†]

*From Livingston, et. al. (1972).

[†] From Sanquer and Meinnel (1972).

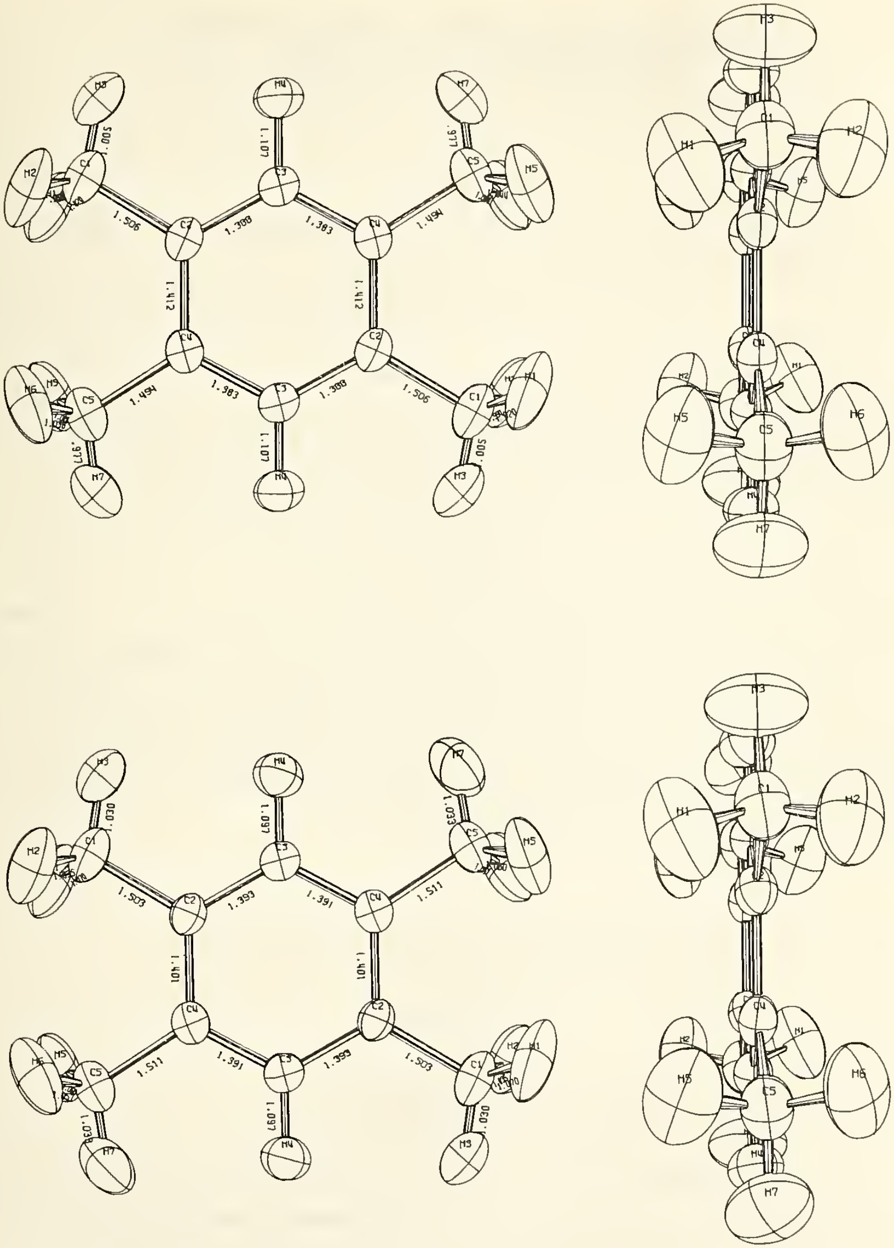

Fig. 1. Two views of the durene molecule resulting from a) the unconstrained refinement and b) the constrained refinement.

USE OF RIGID BODY CONSTRAINTS IN LEAST-SQUARES CRYSTAL STRUCTURE REFINEMENT

E. Prince

and

L. W. Finger
(Carnegie Institution of Washington, Washington, D.C. 20008)

Recently G. S. Pawley, of the University of Edinburgh, and various co-workers have drawn attention to the possibilities of using systems of constraints, particularly on thermal parameters, as a way of utilizing information in addition to diffraction information in the refinement of crystal structures. Following this approach we have derived a set of equations which relate the temperature factor coefficients for individual atoms in a molecule to rigid-body motion parameters of the molecule as a whole, thereby making it possible to express the structure factor formula in terms of the rigid-body parameters and to fit these parameters to the data by means of least-squares refinement. The equations have been further extended to allow for the attachment to the rigid molecule of side groups which are free to librate around a single bond. The results have been incorporated into a computer program and employed in a study of the crystal structure of durene.

DERIVATIVE LATTICES AND THEIR APPLICATIONS

A. Santoro

and

A. D. Mighell
(Inorganic Materials Division)

As part of a study of the geometrical properties of crystal lattices, derivative lattices have been defined and methods for their calculation have been found.[1] These lattices are not infrequently related to important properties of crystals and, therefore, find applications in many fields of crystallography, for example in (1) the study of regular aggregates such as twins and epitaxis and syntaxic intergrowths; (2) the study of the geometrical conditions controlling the mutual orientation of crystals forming grain-boundaries in many materials of metallurgical interest; (3) the study of some phase transitions, such as order-disorder transformations; (4) the study of derivative structures; (5) the automatic determination of the diffraction symmetry in single-crystals studies; (6) the critical evaluation of Crystal Data. We will now summarize some of the work in this area during the past year.

1. Theory

Let us consider a lattice Λ and let us describe it in terms of a triplet of non-coplanar translations $\vec{a}_i$ $(i = 1,2,3)$ defining a primitive cell. Let us now perform the transformation

$$\vec{b}_i = \mathop{}_{j} S_{ij}\,\vec{a}_j$$

with $|\underset{\sim}{S}| = 0$. The translations $\vec{b}_i$ can be regarded as the edges of a primitive cell defining a new lattice Γ which we have called "derivative lattice". Derivative lattices have been classified on the basis of the properties of the transformation matrix $\underset{\sim}{S}$. Specifically if the S_{ij}'s are integers and if $|\underset{\sim}{S}|>1$, Γ is a superlattice of Λ. If matrix $\underset{\sim}{T}$ is the inverse of $\underset{\sim}{S}$, and if the T_{ij}'s are integers and $|\underset{\sim}{T}|>1$, Γ is a sublattice of Λ. If one or more of the T_{ij}'s are fractional, Γ is a composite lattice of Λ.

It can be shown that all the possible superlattices associated with a lattice Λ can be generated, without duplications, by using a restricted class of matrices $\underset{\sim}{S}$, i.e. only those matrices whose coefficients are integers which satisfy the conditions, $|\underset{\sim}{S}|>1$; $0 \leq S_{ij} < S_{jj}$ for $i<j$; $S_{ij} = 0$ for $i>j$. It can also be shown that the unique sublattices can be generating superlattices. The matrices generating composite lattices can be obtained by multiplying in any order and in any combination matrices generating superlattices and sublattices.

The theoretical work on this subject has been completed and a paper has been published in Acta Crystallographica.

2. Applications

a. Heterotaxy

The term "heterotaxy" describes a regular aggregate of two or more crystals of different crystalline species grown with a well-defined mutual orientation. The formation of a regular aggregate is possible if the lattices of the constituent crystals are related to each other in a simple manner (specifically, if they can be transformed into each other by matrices with rational elements). Heterotaxy can be two or three dimensional. In the first case the intergrowth is called "epitaxic", in the second "syntaxic". The possibility of heterotaxy can be predicted on the basis of derivative lattice theory. In fact, if two crystals are related so that the lattice of one is a derivative of the other, then the geometrical conditions for syntaxic intergrowth are satisfied. For example, the unit cell of the mineral Ewaldite can be transformed into the cell of the mineral Mackelveyite by means of the transformation $\bar{1}10/210/00\bar{k}$ with $k = 2/3$.[2] The lattice of Mackelveyite is a composite of the lattice of Ewaldite and the relationship in the basal plane (00.1) is illustrated in Fig. 1. The two minerals frequently form polycrystals in syntactic intergrowth. It is also worthwhile to note that Mackelveyite and Ewaldite have the same chemical composition and that the first goes into the second by an ordering phase transformation. If k were not a simple rational number, we would have had an epitaxic, rather than a syntaxic, intergrowth. Work on this subject is now in progress.

b. Coincidence-Site Lattices

Field-ion and electron-microscopy studies have shown that in many materials of metallurgical interest the two crystals forming a grain-boundary are often mutually oriented so that they have a common superlattice which continues without disturbance from one crystal to the other. This superlattice is called coincidence-site lattice and the two crystals adjacent to the boundary are said to be in a coincidence-side relationship or coincidence-site related.[3,4,5]

The concept of coincidence-site lattice has been used in the study of the "structure" of grain-boundaries and in connection with such subjects

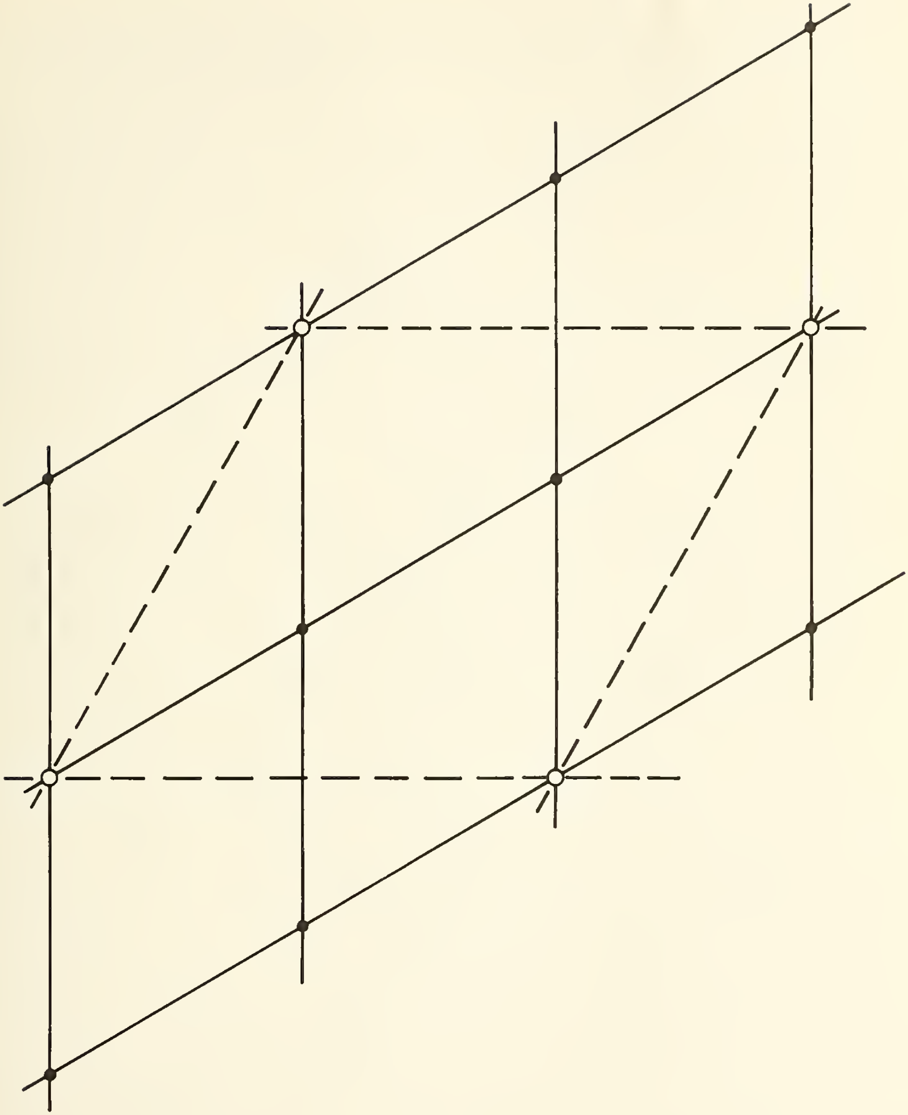

Fig. 1. Relationship between the lattices of Ewaldite and Mackelveryite which frequently form syntactic intergrowths.

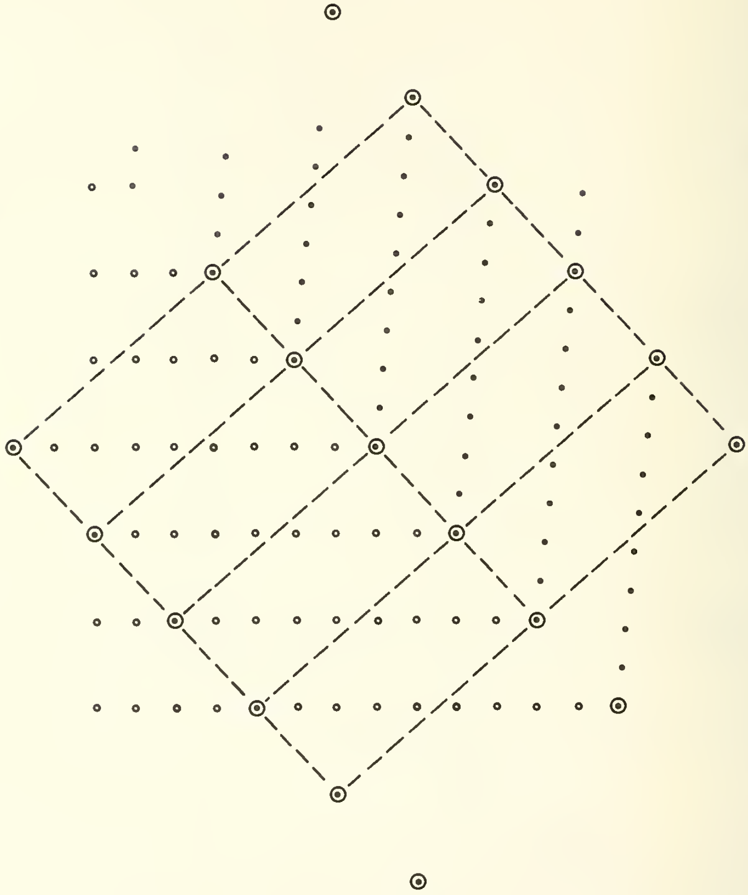

Fig. 2. Two-dimensional example of coincidence-site related lattices. The two lattices indicated by small circlets are identical and are mutually oriented so that they have in conversion the superlattice indicated by the large circlets.

as grain-boundary migration in high purity materials and nucleation and growth of boundary precipitates.[6,7]

The interpretation of experimental results in terms of the coincidence-site lattice model requires the knowledge of the geometrical conditions under which two crystals are coincidence-site related. The characterization of a coincidence-site lattice can be made by applying the theory of derivative lattices because the original lattices are sublattices of the coincidence-site lattice. An example of the geometry involved in coincidence-site relationships is given in Fig. 2. Work on this subject has been completed and a paper for Acta Crystallographica is in press.

c. Automatic Determination of Diffraction Symmetry

If three reflections from non-parallel planes are determined in a single-crystal diffraction experiment, we may calculate a set of provisional lattice parameters from the settings necessary to bring the planes into reflecting position.[8] These parameters define the true lattice of the crystal only if the reciprocal cell obtained from the three reflections is primitive. If this is not the case, the provisional cell defines a sublattice of the true lattice, i.e. the reciprocal cell determined experimentally is multiple primitive.

The true crystal lattice can be found by the following method based on the results of derivative lattice theory. A powder pattern can be obtained from the same crystal being used for intensity measurements (with a Gandolfi's camera, for example). If the pattern cannot be indexed with the provisional parameters, then we systematically generate the superlattices of the provisional lattice unitl the one which indexes the powder pattern is found. This superlattice is the true crystal lattice.

The metric symmetry of the crystal can then be found by means of known reduction procedures.[9] The crystal symmetry, which is the same for a subgroup of the metric symmetry, can then be determined from intensity measurements of reflections supposed to be equivalent. Work on this subject is still in progress.

---

[1] Santoro and Mighell, *Acta Cryst.* A28, 284 (1972).

[2] Donnay and Donnay, *Tschermaks Min. Petr. Mitt.* 15, 201 (1971).

[3] Ranganathan, *Acta Cryst.* 21, 197 (1966).

[4] Acton and Bevis, *Acta Cryst.* A17, 175 (1971).

[5] Brandon, *Acta Met.* 14, 1479 (1966).

[6] Aust and Rutter, *Trans. A.I.M.E.* 215, 119 (1959).

[7] Unwin and Nicholson, *Acta Met.* 17, 1379 (1969).

[8] Busing and Levy, *Acta Cryst.* 22, 457 (1967).

[9] Mighell, Santoro and Donnay, *Int. Table for X-ray Crystallography*, 1, 530 (1969).

GROUP THEORETICAL SELECTION RULES IN INELASTIC NEUTRON SCATTERING WITHIN THE RIGID-MOLECULE MODEL

R. C. Casella
and
S. F. Trevino
(Picatinny Arsenal, Dover, N. J.)

The general program for considering the effects of crystal symmetry on the structure function for inelastic neutron scattering, the implementation of which was mentioned in the last Annual Progress Report, is continuing. We have obtained extensive theoretical results for the rigid-molecule model and work on applications has begun (See S. F. Trevino, H. Prask, and R. C. Casella in Interagency and University Collaborative Programs, Sec. C). A paper on the general theory has been submitted for publication and an invited talk was presented at the AEC Summer Institute on Neutron Spectroscopy at MIT in August 1972. A brief discussion of this work follows:

The verification and exploitation of symmetries in nature permeates modern physics. As applied to the phonon spectra of crystals inelastic thermal neutron scattering plays a major role in elucidating these symmetries.

However, for sufficiently complex crystals with many atoms in the unit cell the number of phonon modes at a given wave vector $\vec{q}$ is so large that the experimentalist's task of assigning symmetry types to the various phonon branches becomes increasingly difficult. The problem is compounded further by the fact that for such crystals the symmetry is generally lower than for simple crystals resulting in fewer symmetry types (irreducible representations, IR) to which one must assign the phonon modes. That is, the effects of symmetry tend to wash out.

There are, nonetheless, situations where the symmetry effects remain indelible even for complex crystals. When one deals with molecular units whose internal vibrations lie at sufficiently high energies so as to decouple effectively from the intermolecular vibrations, one can greatly reduce the number of potentially active modes via energy discrimination. This simplification is embodied in the well known rigid-molecule approximation in which only translations of the molecular centers of mass (c.m.) and rotations about the c.m. are allowed.

Another simplification in identifying lattice-mode symmetries was introduced several years ago by Elliott and Thorpe (ET) who devised a model-independent technique for assigning IR's to the phonon modes when the atoms are allowed to vibrate without special constraints.

We have achieved a union of these two simplifications which we believe permits handling considerably more complex crystals than was heretofore possible. The generalization of ET's work to apply to the rigid-molecule model involves the resolution of several points of principle. These have been resolved to yield simple and useful results. The ET structure function $F^{(r)}(\vec{k})$ can be written as the sum of two non-negative terms:

$$F^{(r)}(\vec{k}) = F^{(r)}(\vec{k}|R) + F^{(r)}(\vec{k}|\Theta).$$

Here, $\vec{k}$ refers to the momentum transfer to the neutron, R denotes translations of the molecular c.m., Θ rotations about the c.m., and r labels the IR. Closed expressions have been found for these quantities both in the Brillouin-zone interior and at the boundary.

THERMAL NEUTRON FLUX MEASUREMENTS

V. W. Myers and M. Ganoczy

A manganese sulfate bath is being used at a beamport for determining the thermal neutron intensity of the beam. Cobalt glass beads activated in the beam can then be used for calibrating a NaI well detector. An unknown thermal flux can be measured by activating a cobalt glass bead in the flux and then counting it in the calibrated well detector.

INTERCOMPARISON OF NEUTRON DIFFRACTOMETERS

V. W. Myers

Collaboration is continuing in a program of the International Union of Crystallography for the comparison of neutron flux at various neutron spectrometers. Gold foils are activated in the diffracted beam and sent to one of the following laboratories for counting: Australian AEC; Kjeller, Norway and NBS. Foils will be counted at NBS for irradiations at spectrometers at the following reactors: Brookhaven HFBR, NBSR, Oak Ridge HFIR, and Puerto Rico Nuclear Center. There may be irradiations made at other facilities also and then counted at NBS. This study will probably be completed by June 1973.

TIME REVERSAL VIOLATION IN K^o MESON DECAYS

R. C. Casella

Since the discovery of CP violation in the decays of neutral kaons into pions by Christenson, Cronin, Fitch, and Turlay in 1964, a convincing microscopic explanation which maintains contact with the rest of physics has been lacking despite a highly successful phenomenological framework due to Wu and Yang. Assuming CPT symmetry the CP violation immediately implied T (time reversal) violation. In 1968-9, on the basis of still quite crude data, Casella was able to show that T is violated independently of the assumption of CPT symmetry. Based upon vastly improved data the violation of T and the validity of CPT (within reasonable accuracy) are now independently established in kaonic decays quite apart from any microscopic explanation.

In addition, the new data point increasingly towards the equality of the Wu-Yang parameters η_{+-} and η_{oo} characterizing the CP violation in the $\pi^+\pi^-$ and $\pi^o\pi^o$ channels, an equality predicted much earlier by Wolfenstein (1964) who assumed that CP is conserved in the weak interactions and that the observed CP violation results from a mixing of the pure CP-even and CP-odd states formed from the K^o and its antipartical, $\overline{K}^o$. A new "superweak" interaction, essentially decoupled from the rest of physics, was postulated as the CP-violating mechanism inducing the mixing.

We are investigating the possibility that the experimentally acceptable "superweak" force which breaks time reversal invariance is not a new one, but is instead related to the cosmic "time arrow" inherent in the Hubble expansion of the universe. Earlier (1964) attempts at a global explanation of T violation had focused attention on the diagonal elements of the 2 x 2 mass matrix M describing the K^o-$\overline{K}^o$ complex, assuming (contrary to Einstein's equivalence principle) that the K^o and $\overline{K}^o$ interact slightly differently with gravitational fields. Such theories predict Lorentz-factor velocity dependences and CPT violation in disagreement with experiment. It is now clear that the T violation must occur in the off-diagonal elements of M where changes in the strong-interaction quantum number S (strangeness) also occur. This aspect and the smallness of the Hubble expansion over a K^o lifetime present obstacles which must be overcome if we are to obtain a theory along these lines which is consistent with (1) the equivalence principle, (2) CPT symmetry, and (3) other aspects of the data.

COLD-NEUTRON TIME-OF-FLIGHT FACILITY

R. S. Carter, A. A. Cinquepalma, D. H. Fravel,
and J. B. Sturrock

The cold neutron time-of-flight facility is designed for inelastic neutron scattering studies of solids and liquids. A neutron beam from the reactor is filtered through polycrystalline beryllium to eliminate neutrons with wavelengths shorter than 3.92Å. The beam then passes through a four rotor phased chopper systems which chops the beam into short bursts of neutrons of selected energy. The sample to be studied is placed immediately after the choppers and the scattered neutrons are detected in a large bank of detectors arranged along the arc of a circle with a 2.4 meter radius. The detectors are located in a shielding room. The detector information is fed into a multi-channel analyzer and the neutron energy determined from the flight time of the neutrons from the sample to the detectors.

The only remaining item to be completed is the shielding room and the installation of the detector bank. The shielding room is mounted on a steel frame that floats on air pads to enable the whole room (∿9' x 12' x 14') to be moved to provide access to the choppers. The base and side walls have been completed and assembled. The supporting framework for the detectors has been installed. The top sections will be completed shortly. Then the detectors will be mounted on the frame to complete the system.

COLD-NEUTRON SOURCE

R. S. Carter, E. M. Guglielmo, and F. J. Shorten

The NBS reactor includes a special port, 22" in diameter, which penetrates the reflector up to the edge of the fuel elements. This large opening was designed to provide space for the insertion of a cold neutron source close to the core. By inserting a large, low temperature moderator it is possible to significantly increase the available intensity of very low energy neutrons ($\lambda > 4$Å) which are very useful for many types of molecular dynamic studies.

The moderator will be a cylinder of D_2O ice 14" in diameter by 12" long. A small amount of H_2O may be added to optimize the moderating property of the source. The source will have a reentrant hole 4" deep by 8" in diameter for beam extraction. The hole will be filled with beryllium which has the property of reflecting the higher energy neutrons back into the moderator while passing the lower energy neutrons. The moderator will be maintained at 25 K by cold helium gas passing through tubing in the moderator. The vacuum cryostat containing the moderator will be constructed of thin-walled aluminum to minimize heating by capture gamma rays. The cryostat will be mounted on a shielding plug and the whole assembly will roll inside a second plug and shield assembly which itself will roll into the special port of the NBSR. The shield mounted on the second plug surrounds the cryostat and consists of about 4" of lead and bismuth which greatly reduces the gamma ray heating of the moderator. Two 6" and two 2" diameter beams can be extracted from the cold source through the reactor shield. One of the 6" beams will be used for the cold neutron time-of-flight facility while the others await future development.

The helium for cooling is provided by an all helium regrigerator using a turbine expansion engine developed by the NBS cryogenic laboratory in Boulder. It has a one kilowatt capacity at 25 K which is sufficient to handle the heat generated in the moderator at twice the current reactor power.

The bismuth tip and cryostat are the only items which remain to be installed. The cryostat has been received and extensive testing is underway. The bismuth tip again failed to pass its acceptance tests and had to be rejected. The contract with the vendor has been terminated since the damage to the cooling tubes done either during fabrication or during repair attempts is too extensive to be reliably repaired. A completely new bismuth tip must now be fabricated.

B. RRD-NBS COLLABORATIVE PROGRAMS

THE STRUCTURE OF $Ca(H_2PO_4)_2$

B. Dickens, L. W. Schroeder
(Polymers Division)

and

E. Prince

The work on the crystal structure of $Ca(H_2PO_4)2$ described in the 1971 report has been completed this year. The neutron data suffered serious extinction effects which were insufficiently accounted for by a simple isotropic correction. A model which includes the effects of anisotropic extinction gave more precise parameters. This model suggests that extinction in $Ca(H_2PO_4)_2$ is dominated by the domain size and anisotropy.

A successful refinement including anisotropic extinction allowed a more detailed analysis of the hydrogen positions and motions. The variation of the mean-square-amplitudes of the nominally centered hydrogens (H_4 and H_5 of Fig. 1) with their displacement from the center of symmetry along the O...O vector was studied. This showed that these protons must be within .15 Å of the center in order to fit the diffraction data with reasonable parameters. A consideration of these results and the infrared spectrum of $Ca(H_2PO_4)_2$ allows one to conclude that these protons are in symmetric potential wells with zero-point energies greater than any central barrier that may exist.

Figure 1 shows that the structure of $Ca(H_2PO_4)$ exhibits complex and unusual hydrogen bonding. The linking of PO_4 groups via symmetrical hydrogen bonds (H_4,H_5) to form chains is the most novel feature. These chains are linked to form sheets which are separated by sheets of Ca^{++} ions forming a layer structure. Another feature is the linking of phosphate groups via hydrogen bonds (H_2, see lower left corner of Fig. 1) in a dimeric configurations which are further joined by hydrogen bonds (H_1,H_3) to the chains.

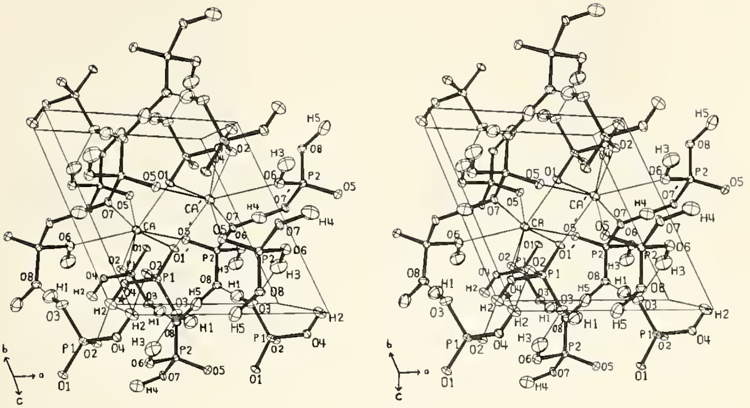

Fig. 1. Stereographic pair showing the atomic structure of $Ca(H_2PO_4)_2$.

THE CRYSTAL AND MOLECULAR STRUCTURE OF DINITRATOTETRATHIAZOLE COPPER (II), $[Cu(C_3H_3NS)_4](NO_3)_2$

A. D. Mighell and C. W. Reimann
(Inorganic Materials Division)

and

A. Santoro

As a continuation of our study of compounds containing metal-organic complex cations, the structure of dinitratotetrathiazole copper(II), $[Cu(C_3H_3NS)_4](NO_3)_2$, has been determined. The thiazole molecule, which acts as ligand in this compound, has considerable biological interest, as it is part of the molecule of thiamine (Vitamin B_1). The purpose of the present study is to obtain accurate parameters of the thiazole ring and of the NO_3^- anions, and to compare the packing of the $[Cu(C_3H_3NS)_4]^{2+}$ cations with that of analogous complexes of imidazole and pyrazole whose structures have been previously determined.

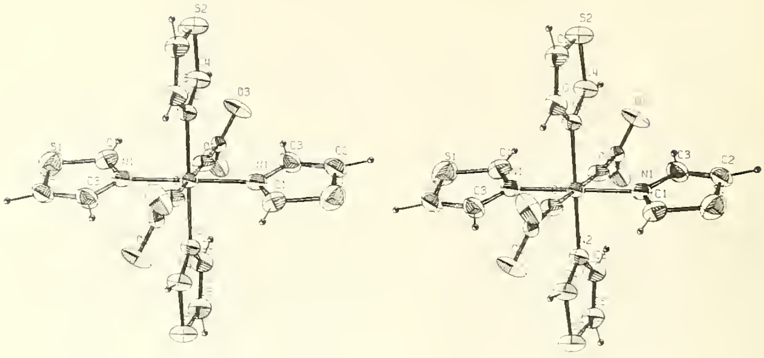

Fig. 1. Stereo view of the molecule $[Cu(C_3H_3NS(_4](NO_3)_2$.

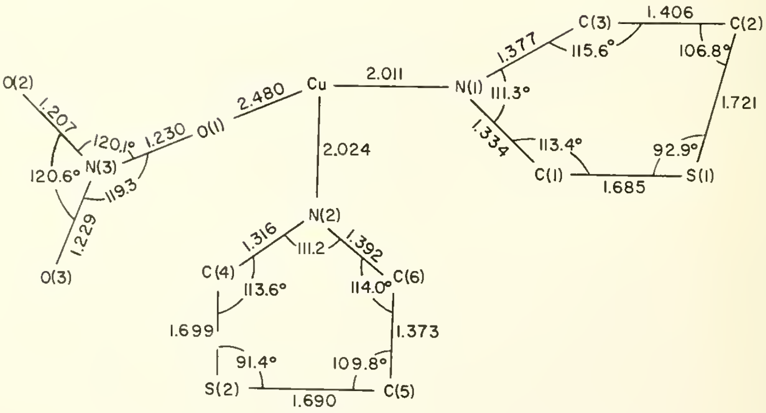

Fig. 2. Unique bond distances and angles in the molecule of $[Cu(C_3H_3NS)_4](NO_3)_2$.

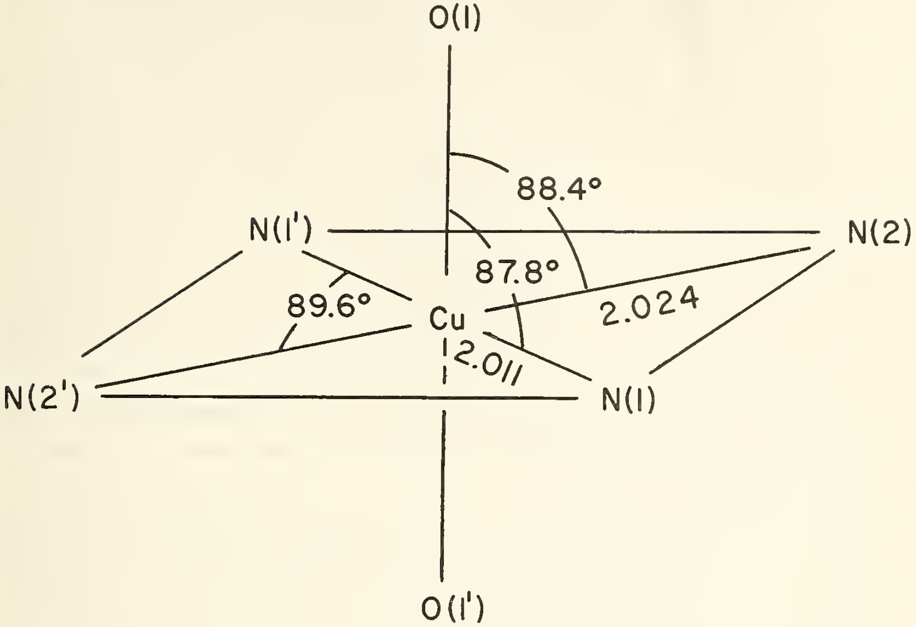

Fig. 3. Coordination of the copper atom in the structure of $[Cu(C_3H_3NS)_4](NO_3)_2$. The coordination polyhedron is a distorted octahedron.

Dinitratotetrathiazole Copper(II) is monoclinic, space group C2/c, and lattice parameters a = 14.38Å, b = 10.116Å, c = 14.603Å, β = 112.9°. Single crystal x-ray intensities were measured with a counter diffractometer and the structure was solved by Patterson and Fourier methods. There are four molecules of complex per unit cell. The complex is centrosymmetric with the copper atom located at the center of symmetry of the space group. All the other atoms occupy general positions. There are two thiazole ligands and one nitrate ion in the structure which are crystallographically independent. Figure 1 is a stereo view of the molecule of the complex. Unique bond distances and angles are given in Figs. 2 and 3. The copper atom sits at the center of a distorted octahedron and is coordinated by four nitrogen atoms of the thiazole rings and by two oxygen atoms of the nitrate groups. Preliminary calculations have shown that the thiazole rings are planar.

The packing of this structure resembles that of Dichlorotetrapyra zolenickel(ii), $[Ni(C_3H_4N_2)_4]\ Cl_2$.[1] This analogy suggests that internal hydrogen bonding may be present also in the structure of the copper complex. Such bonding would involve hydrogen atoms bonded to carbon atoms. (C-H...O) bonding has been observed in numerous structures[2] As the positions of the hydrogen atoms have not been determined unambiguously in the present analysis, we have no direct evidence to support the previous hypothesis. Neutron diffraction work is contemplated, if crystals of the appropriate dimensions can be grown.

---

[1] Reimann, Mighell and Mauer, *Acta Cryst.*, 23, 135 (1967).

[2] See for example, Sutor, *Nature*, 195 (1962).

NEUTRON DIFFRACTION DETERMINATION OF THE LIQUID HELIUM STRUCTURE FACTOR AND RELATED CORRELATION FUNCTIONS

B. Mozer
(Inorganic Materials Division)

and

B. LeNeindre
(CNRS, Bellevue, France)

and

L. A. deGraaf
(Interuniversitair Reactor Insituut, Delft, The Netherlands)

In a previous paper[1] we reported measurements of liquid neon structure factors at fixed temperature and several densities. These measurements were performed to allow one to obtain an isothermal density derivative of the liquid structure factor or the isothermal density derivative of the radial distribution function which contains information about correlations of three particles in the liquid.[2] There is sufficient interest in the correlation of three helium atoms in liquid helium and some aspect of this three-body correlation can also be obtained from an isothermal density derivative of the liquid helium radial distribution function obtained from neutron scattering measurements of the liquid helium structure factor. Furthermore, there has been a suggestion that a measure of the condensate fraction of liquid helium could be obtained from measurements of the structure factor at several temperatures above and below the λ transition temperature.[3]

Neutron diffraction measurements of high statistical accuracy have been obtained for liquid helium at three densities, 0.1528, 0.1567, and 0.1628 g/cm^3. These structure factors were measured at two temperatures, one above the λ transition at 2.86 Kelvin, and the other below the λ transition in the neighborhood of 1.90 Kelvin. The measurements were performed using three different wavelength neutrons of 0.845, 1.063, and 2.428Å to cover "momentum transfer" regions of $K = \frac{4\pi}{2} \sin \theta/2$ of 3.5 to 7.0, 1.5 to 4.6, and 0.2 to 2.2Å^{-1} respectively. Statistical accuracy of the data after background and other corrections was 0.4% using the shortest wavelength neutrons and 0.1 to 0.2% in the other two wavelength measurements. The data were corrected for the background contribution, multiple scattering, and inelastic neutron scattering. The resolution of the instrument as determined by the diffraction pattern of copper powder was ΔK = 0.1, 0.255 and 0.31Å^{-1} for the (111) copper peak for the three wavelengths of 2.428, 1.063, and 0.845Å respectively. Instrumental resolution was removed by a calculation using an iterative procedure in order to insure proper joining of the data in the overlap regions in K. The result of this calculation was to confirm our hypothesis that the joining of the data can be accomplished by using the integrated intensity factors in the overlap region.

The resultant structure factor is obtained by setting the corrected data in the asymptotic region (K = 6. to 7. Å^{-1}) to unity and then working toward the small kappa region by joining the data via integrated intensities and unfolding the spectra for instrumental resolution. These results for the structure factors show a linear region for small kappa, the main peak at about 2.05Å^{-1} then two highly damped oscillations about unity which eventually lead to a flat asymptotic behavior from about 5.5Å^{-1} and greater. These features can be seen in figures 1, 2, and 3. Changes in peak position with density are observed. One also notes that the extrapolation of the linear region at small kappa agrees well with calculated values of the structure factor at K = 0 obtained from the bulk compressibility and other known quantities. Also observed are significant differences in the structure factor above or below the λ for a given density. The radial distribution function, g(r), for each density and each temperature has been obtained from a Fourier transform calculation of Dr. R. Mountain of the Heat Division. A representative radial distribution function is shown in figure 4. What is observed is a pattern very similar to that for the structure factor. In the region 0 to about 2Å where g(r) should be zero we see structure indicative of the noise in our spectrum for S(K) at large K. This structure can be reduced by a small (0.2%) change in our asymptotic region but this is within our accuracy in this region of 0.4%. The structure observed in the region

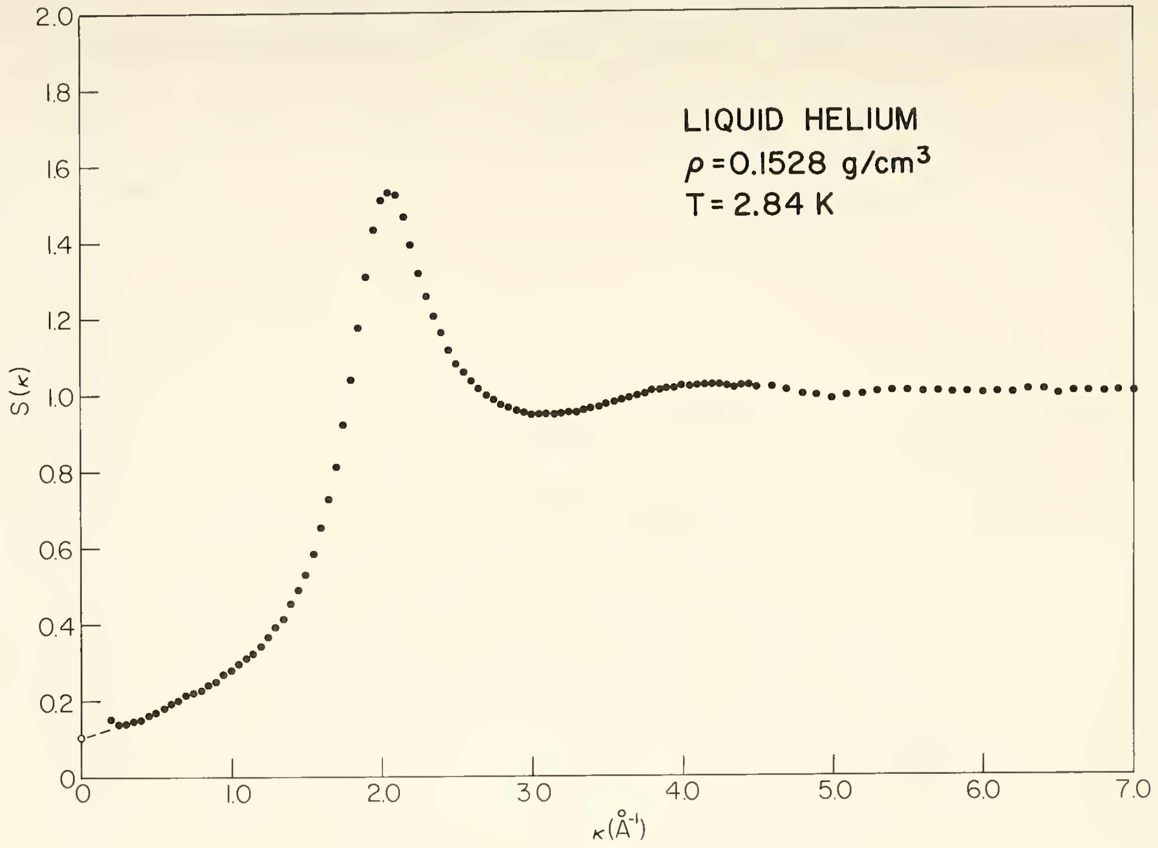

Fig. 1. Structure factor of liquid helium at a density of 0.1528 g/cm^3 and temperature 2.84K.

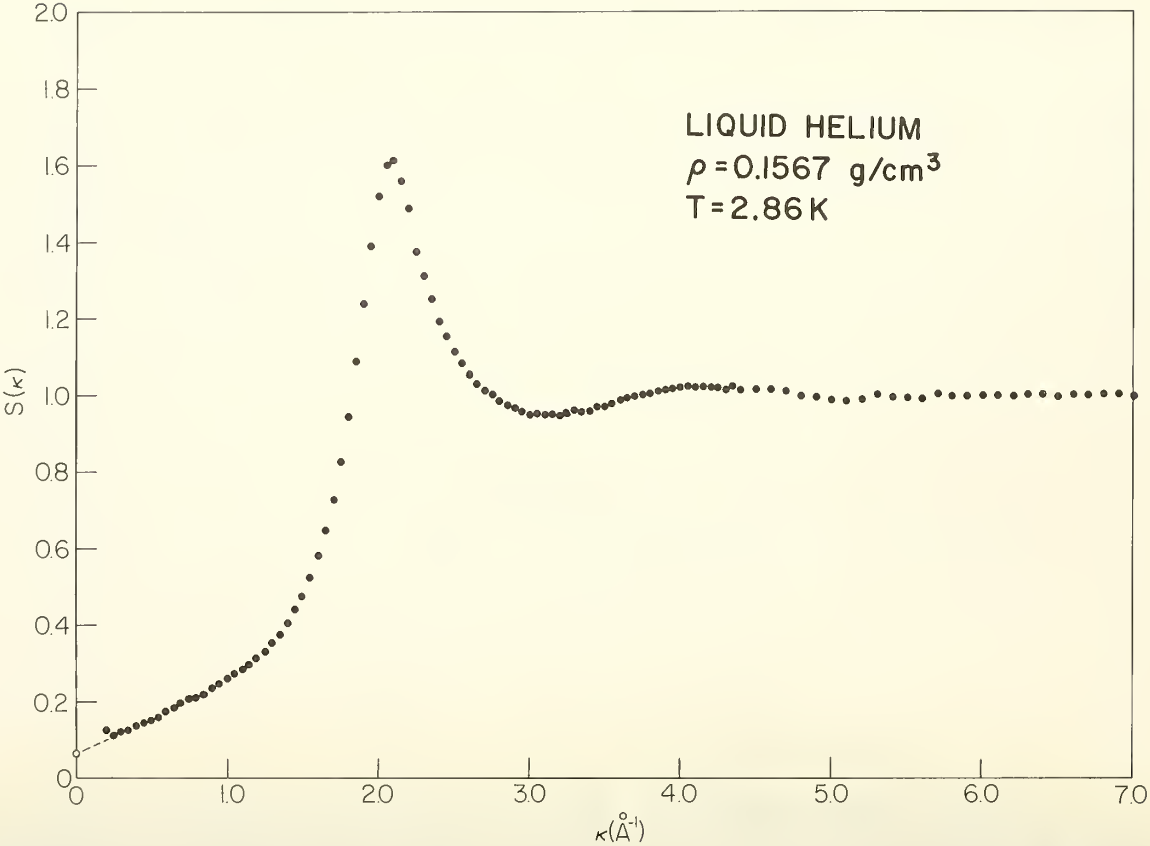

Fig. 2. Structure factor of liquid helium at a density of 0.1567 g/cm^3 and temperature 2.86K.

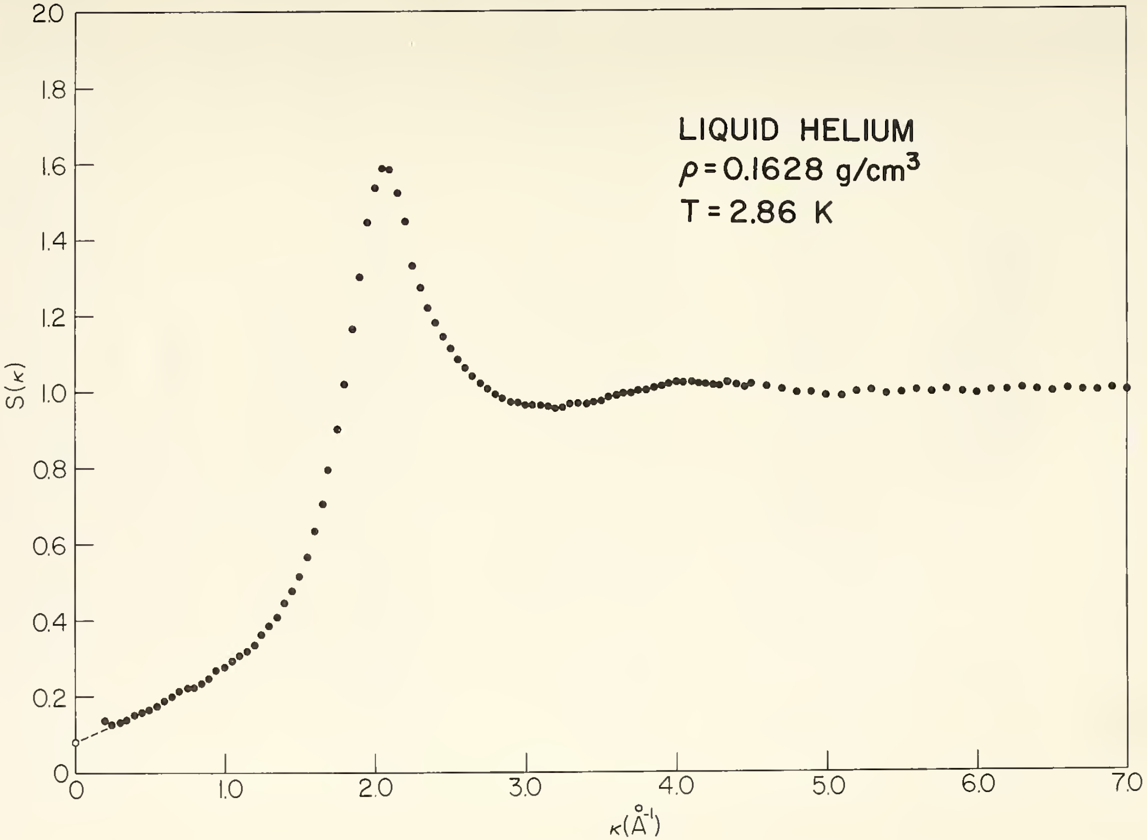

Fig. 3. Structure factor of liquid helium at a density of 0.1628 g/cm^3 and temperature 2.86K.

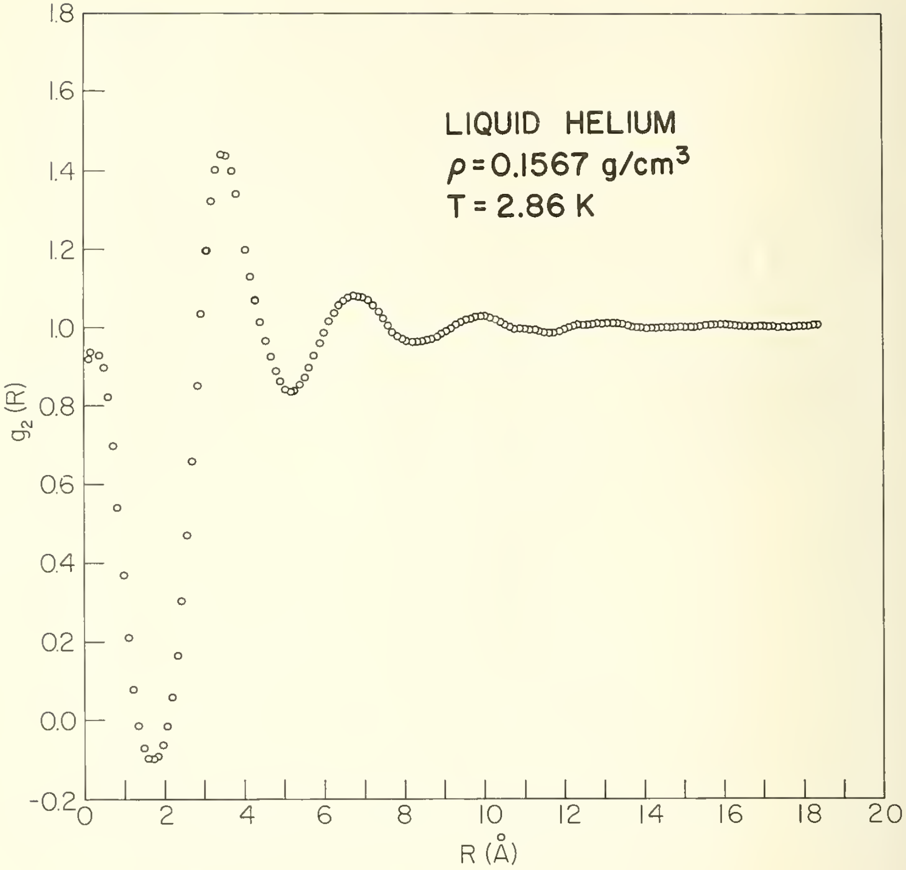

Fig. 4. Radial destribution function, $g_2(R)$, for liquid helium at a density of 0.1567 g/cm^3 and a temperature 2.86K.

r>2 is very smooth with only a few characteristic excursions about unity such as was noted for S(K). The smoothness of g(r) and the size of the structure at small r yield support for the reliability and accuracy of the structure factors.

A preliminary calculation of the three body correlations in liquid helium has been obtained from our measurements of the structure factor. These calculations indicate sizable three-body correlations in liquid helium with significant differences above and below the λ transition temperature. Detailed results of the calculation of three-body correlations for liquid neon are given in a separate note in this report by Raveche and Mountain and a corresponding study for liquid helium will be reported later.

---

[1] L. A. de Graaf and Bernard Mozer, *J. Chem. Phys.* 55, 4967 (1971).

[2] H. J. Raveche and R. D. Mountain, *J. Chem. Phys.* 53, 3101 (1970).

[3] G. J. Hylands, G. Rowlands, and F. W. Cummings, *Phys. Letters*, 31A, 465 (1970).

TEMPERATURE DEPENDENCE OF THE LIQUID HELIUM STRUCTURE FACTOR AT FIXED DENSITY

B. Mozer
(Inorganic Materials Division)

and

B. LeNeindre
(CNRS, Bellevue, France)

It has been suggested that information about the condensate fraction in liquid helium below the λ transition temperature can be obtained from measurements of the liquid helium structure factor.[1] We observed in our previous measurements on the liquid helium structure factor changes when the temperature was above or below the λ transition temperature at fixed density. The temperature above the λ transition was too high to critically evaluate the suggestion offered in reference (1). We therefore thought it would be of value to have a careful scan of the structure factor at fixed density and several temperatures both above and below the λ transition temperature. We obtained structure factors for liquid helium using neutron diffraction at a fixed density of 0.1528 g/cm^3 and at 6 temperatures, 1.86, 2.04, 2.33, 2.83 kelvin and just above and below the λ transition temperature for this density, 2.132. The measurements were performed using two different neutron wavelengths of 2.406Å and 0.986Å to cover the region of momentum transfer 0.2 to 3.5 and 1.5 to 7.0Å^{-1}. Resolution of the instrument was improved over the previous experiment by using a Soller slit collimator in front of the neutron counter and stopping down the monochromatic beam impinging on the specimen. The resolution was determined from copper powder diffraction peaks and was less than 0.1Å^{-1} for both wavelengths where the data overlaps. Statistical accuracy of the measurements was maintained to better than 0.4% except at small values of the momentum transfer.

S(K) was determined from the raw data after correcting for background, multiple scattering and inelastic scattering. The structure factor is observed to decrease with temperature in the small momentum transfer region corresponding to the decrease in the structure factor at zero momentum given by $S'(o) = \rho k_B T \chi_T$ where χ_T is the isothermal compressability as observed by Hallock in x-ray measurements. The most significant change observed in the structure factor occurs at the main peak when one approaches the λ transition. From our highest temperature to slightly above the λ transition we note a slight increase in the intensity of the major peak. The intensity decreases slightly as the temperature goes just below the λ transition and then decreases more rapidly as the temperature decreases. The change in the intensity from the lowest temperature to the temperature at the λ transition is 5% whereas the intensity changes from slightly above the λ transition to the highest temperature is about 1%.

These results will be used to test the hypothesis of Cummings, Hyland and Rowlands[1] about the relation of the condensate fraction to the liquid structure factor in helium.

---

[1] F. W. Cummings, G. J. Hyland, and G. Rowlands, *Phys. kondens, Materie*, 12, 90 (1970).

DISPERSION OF EXCITATIONS IN LIQUID HELIUM AT FIXED DENSITY

B. Mozer
(Inorganic Materials Division)

and

B. LeNeindre
(CNRS, Bellevue, France)

Preliminary inelastic neutron scattering experiments on liquid helium at the fixed density of 0.1528 g/cm^3 have been performed in order to provide both the structure factor and excitation spectrum for a critical evaluation of recent theories on liquid helium. We used the time-of-flight system to observe excitations in kappa regions from 0.09 to 2.56Å^{-1} and at temperatures above the below the λ transition temperature. Our measurements cover the phonon region, rotor region and single particle excitation region of the spectra.

Preliminary analysis of the data shows dispersion of the excitations in agreement with other measurements. Temperature effects are quite striking just below the λ transition to just above.

THREE ATOM CORRELATIONS IN LIQUID NEON

H. J. Raveche

and

R. D. Mountain
(Heat Division)

De Graaf and Mozer have recently published[1] very accurate neutron diffraction measurements in liquid neon. We have used these results to discuss the correlation of three atoms in liquid neon and to consider several approximate forms for the triplet correlation function.

(The structure factor, $S(\kappa)$, was measured by De Graaf and Mozer for three pressures, 21.4, 79.0 and 140.0 atm along the 35.05 K isotherm of liquid neon; these pressures correspond to densities of 0.0317, 0.0334 and 0.0347 atom/$\mathring{A}^3$ respectively. The experiment was designed to construct the isothermal density derivative of the radial distribution function. The quantity is a measure[2] of both magnitude and range of the correlation between three atoms and can be readily determined from the experimental results by using the relation,

$$g_2(r_{12}) = 1 + (2\pi^2 \rho r_{12})^{-1} \int d\kappa \, \kappa \sin \kappa \, r_{12}\{S(\kappa)-1\} \tag{1}$$

From the isothermal density derivative, we computed[3] a measure of three atom correlations through the functional

$$F(r_{12}|g_3) \equiv \int d\underset{\sim}{r}_3 g_2(r_{13}) g_2(r_{23})\{g_3(r_{12},r_{13},r_{23})-1\} \quad , \tag{2}$$

where $g_3(r_{12},r_{13},r_{23})$ is the triplet correlation function. The results of the diffraction data and two approximate representations of the triplet correlation function are shown in Figure 1. The solid curve in the experimental result and the dashed-dotted curve were evaluated from the convolution approximation,

$$g_3(r_{12},r_{13}r_{23}) \simeq 1 - \frac{h(r_{12})h(r_{13})h(r_{23}) + \rho \int d\underset{\sim}{r}_4 h(r_{14})h(r_{24})h(r_{34})}{g_2(r_{12})g_2(r_{13})g_2(r_{23})} ; \tag{3}$$

the dashed curve was computed from

$$g_3(r_{12},r_{13},r_{23}) \simeq 1 - \frac{h(r_{12})h(r_{13})h(r_{23})}{g_2(r_{12})g_2(r_{13})g_2(r_{23})+1} \quad , \tag{4}$$

where $h(r) = g_2(r)-1$. Several other approximations were also computed. The small structure of the solid curve, in the vicinity of 4 and 4.8Å, represents the uncertainty in the data. The results in Figure 1 show a substantial amplitude (solid curve) in $F(r_{12}|g_3)$ for distances of nearly two atomic diameters and, since the coefficients of $g_3(r_{12},r_{13},r_{23})$ in $F(r_{12}|g_3)$ are positive, the oscillation of $F(r_{12}|g_3)$ about zero requires the triplet function to oscillate about unity in value, as the distance between three atoms vary.

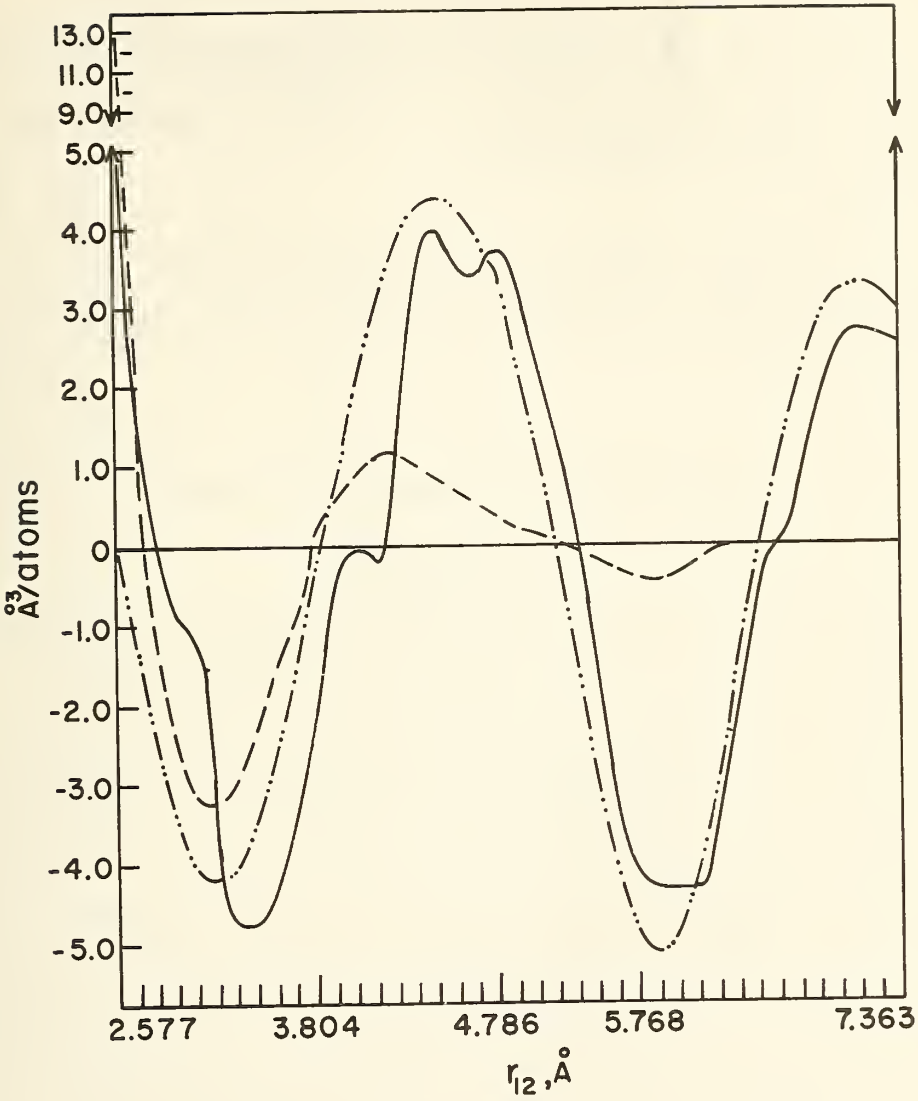

Fig. 1. $F(r_{12}|g_3)$ at T = 35.05, ρ = 0.0334 atoms/Å^3 as a function of r_{12}. The solid curve is the experimental result, the dashed-dotted curve was computed from Eqn. (3) and the dashed curve from Eqn. (4).

The relative agreement of the experimental results and those obtained from the approximations (3) and (4), are discussed in reference (3) in terms of finding a representation for the triplet correlation function which is accurate at liquid densities.

---

[1] L. A. deGraaf and B. Mozer, *J. Chem. Phys.* 55, 4967 (1971).

[2] H. J. Raveche and R. D. Mountain, *J. Chem. Phys.* 53, 3101 (1970).

[3] H. J. Raveche and R. D. Mountain, to appear in *J. Chem. Phys.*, Nov. 1, 1972.

THF "ROTATOR" PHASE TRANSITIONS IN N-ALKANES

John D. Barnes
(Polymers Division)

Analysis of our neutron inelastic scattering data from n-nonadecane in terms of a circular random walk model has been completed and the results submitted for publication. The circular random walk model describes the kinematics of the alkane molecule as a series of rotational jumps about the long axis of the molecule, represented by a random walk among a number, N, of sites distributed at equal intervals on the circumference of a cube. The remaining parameters which describe the kinematics of the molecule are the dipole relaxation time, τ, and the radius, d, of the circle. In Fig. 1 we show an example of the values of the half-width at half-maximum derived from our theoretical scattering low calculations for several values of the parameters defined above. A detailed comparison of our theoretical and experimental scattering laws shows that the following parameter set is consistent with our quasielastic scattering results at $T = 301K$: $3.5 \times 10^{-12}s < \tau < 4.0 \times 10^{-12}s$, $N \geq 8$.

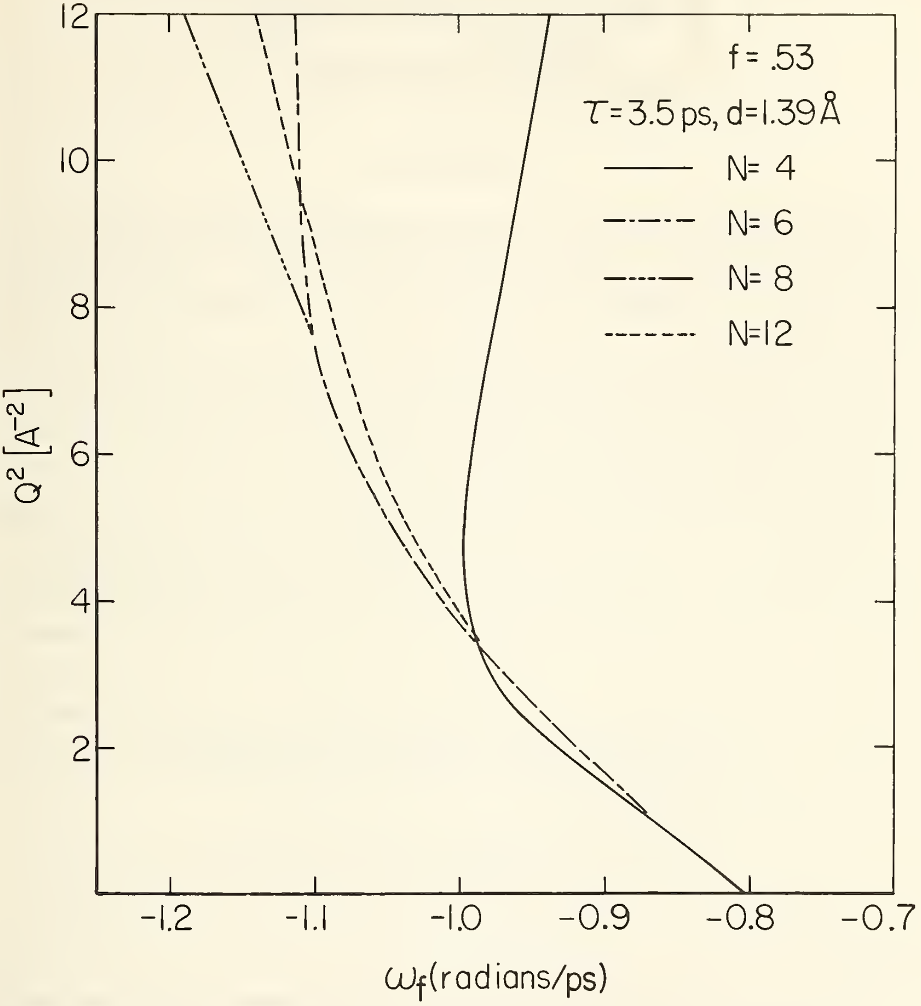

Fig. 1. Theoretical contours of half-width at half-maximum of the quasielastic scattering law calculated from the Circular Random Walk Model. Note how the choice of different values for the number of sites leads to differences in the shapes of the contours.

C. INTERAGENCY AND UNIVERSITY COLLABORATIVE PROGRAMS

THE LATTICE DYNAMICS OF $NaNO_3$

S. Trevino and H. Prask
(Picatinny Arsenal, Dover, N.J.)

and

R. C. Casella

Sodium nitrate crystallizes in a rhombohedral unit cell ($R\bar{3}C$) containing two formula units, and has been the subject of considerable spectroscopic study, including some coherent neutron inelastic scattering measurements.[1]

The room-temperature lattice dynamics of single-crystal $NaNO_3$ are now being examined using the Picatinny Arsenal-NBS three axis neutron spectrometer recently made operational at the NBSR.

The present work is aimed at completing the characterization of the external lattice modes with particular emphasis on the high-symmetry C-axis direction. The dispersion curves of all of the relatively low-energy modes ($\hbar\omega \lesssim 18$ MeV) have been measured and characterized in the C-direction. Assignment of symmetry species at $q = o$ from the neutron scattering selection rules of Casella and Trevino, discussed elsewhere in this report, agree with assignments inferred from optical spectroscopic data for optically-active modes.

On completion of the room-temperature studies, the external mode lattice dynamics will be examined above and below the specific heat anomaly at 275°C.

---

[1] K. W. Logan, S. F. Trevino, R. C. Casella, W. M. Shaw, L. D. Muhlestein and R. D. Mical, in "Phonons", ed. M. A. Nusimovici, Flammarion Sciences Press (Paris) 1971, p. 104.

DYNAMICS OF AMMONIUM PERCHLORATE

H. Prask and S. Trevino
(Picatinny Arsenal, Dover, N. J.)

and

J. J. Rush

As part of a planned detailed study of the dynamics, structure and rotational behavior of ammonium perchlorate, we have measured preliminary neutron inelastic scattering spectra for NH_4ClO_4 powder at 5, 78 and 295K. Spectra were measured at scattering angles of 18.5, 71.5 and 107°, so that the Q dependence of the "quasielastic" and inelastic scattering could be surveyed. The results are presently being analyzed to assess their implications concerning the possible quasifree rotation of the NH_4^+ ions in this crystal. Future neutron scattering and diffraction measurements are planned on both powder and single crystal samples. Low temperature Raman spectra will also be measured to complement the neutron scattering experiments.

LATTICE DYNAMICS STUDIES OF COMPLEX CRYSTALS CONTAINING LINEAR TRI-ATOMIC GROUPS

R. S. Singh, S. F. Trevino and H. J. Prask
(Picatinny Arsenal, Dover, New Jersey)

Metal azide salts are materials which exhibit a broad range of crystal stabilities and are thus of a considerable interest for explosive applications. In the monovalent-metal azide salts, the azide ion (N_3) is linear and symmetric, whereas in the divalent-metal salts the azide groups tend to be asymmetric and nonlinear; it is the latter type which are considerably less stable.

The present program is aimed toward gaining an understanding of the interatomic forces in metal azide salts in order to correlate differences in bonding and stability. Earlier results have included lattice-dynamical calculations and preliminary neutron-scattering studies of NaN_3[1] and KN_3.[2] Reasonably complete infra-red reflection spectra for NaN_3 (D_{3d}^5)

Crystals	A_{2u}		E_u			
	TO	LO	TO	LO	TO	LO
NaN_3	195*		175*			
			173	243		
KN_3	138	196	130	154	166	192
	140*		130*			
RbN_3			91	109	123	163
			93*		127*	
C_sN_3			85	107	123	163
			91*		126*	

*IR thin film transmission

TABLE I. $\vec{k}\sim0$ TO and LO phonons of Na-, K-, Rb- and C_sN_3. Polarized reflectivity spectra of single crystals of KN_3 and unpolarized spectra of the pressed pellets of the others were obtained. Thin film transmission measurements are also included. Resolution was 2 cm^{-1} with all quantities in cm^{-1}.

and KN_3, RbN_3 and CsN_3 (all D^{18}_{4h}) have now also been obtained at room temperature, and are presented in Table I. Infrared reflection data have been obtained and are being analyzed for Na and K bifluoride salts, which are isomorphous to the corresponding metal-azide salts. High resolution neutron scattering studies are also planned (with J. J. Rush, NBS) for these salts.

---

[1] H. A. Rafizadeh, S. Yip and H. Prask, *J. Chem. Phys.* 56, 5377 (1972).

[2] K. R. Rao, S. F. Trevino, H. J. Prask and R. D. Mical, *Phys. Rev.* 4B, 4551 (1971).

THE CRYSTAL STRUCTURE OF CYCLOTRIMETHYLENE-TRINITRAMINE

C. S. Choi
(Picatinny Arsenal, Dover, N.J.)

and

E. Prince

The compound cyclotrimethylene-trinitramine, commonly known as RDX, is a well-known explosive. The crystal structure of RDX has been investigated previously by other people using x-ray photographic data. The present neutron diffraction study was undertaken to complete the crystal structure by determining the hydrogen positions and refining overall structural details. A total of 836 reflection data points were collected within the limiting sphere of 100° in the 2θ angle. The structure was refined with anisotropic temperature factors for all atoms to the final R index, wR = 0.21 and R = 0.039. The final least squares parameters are given in Table 1.

The compound crystallizes in orthorhombic space group Pbca, a = 13.182(2)Å, with eight molecules per unit cell. The molecule consists of alternate CH_2 and $N\text{-}NO_2$ groups in a puckered ring (Fig. 1), the environment of the carbon atoms is essentially tetrahedral, and the $N\text{-}NO_2$ groups are planar. The molecule possesses a plane of approximate mirror symmetry perpendicular to the plane defined by the three carbon atoms of the C-N ring. It is interesting to compare the crystal structure of RDX to those of both α- and β-HMX (cyclotetramethylene-tetranitramine), in view of the close similarity in chemical composition and explosive nature. The bond lengths and angles of RDX agree well with those of α- and β-HMX, except for the C-N-C angles, which are approximately 8° smaller in RDX than in HMX. In both compounds, the $N\text{-}NO_2$ group planes are bound tightly to the molecular ring by strong O...H as well as O...C interactions. Very short intermolecular distances including weak hydrogen bonds of the type C-H...O occur in both compounds. The thermal motions of both compounds may be described by rigid body motion of the ring and separate rigid body motion of the nitro groups.

Table 1. Final least squares parameters for the structure of RDX. Thermal parameters are the coefficients, B_{ij} ($\mathring{A}^2$), of the form exp - 1/4 ($B_{11}a^{*2}h^2 + B_{22}b^{*2}k^2 + B_{33}c^{*2}\ell^2 + 2B_{12}a^*b^*hk + 2B_{13}a^*c^*h\ell + 2B_{23}b^*c^*kl$). The estimated standard derivations are in parenthesis.

Atom	x/a	y/b	z/c	B_{11}	B_{22}	B_{33}	B_{12}	B_{13}	B_{23}
C(1)	.1839(3)	.3578(3)	.4400(3)	3.22(15)	2.97(13)	2.06(14)	-.70(13)	-.69(11)	.07(12)
C(2)	.0503(2)	.2440(2)	.3395(3)	2.33(15)	1.45(11)	3.44(13)	.08(13)	-.01(13)	-.17(11)
C(3)	.1487(2)	.3813(3)	.2159(3)	2.52(14)	3.32(16)	1.75(14)	-.34(13)	.34(11)	-.31(12)
N(1)	.1761(2)	.4360(2)	.3330(2)	2.67(8)	2.66(8)	2.51(9)	-1.09(8)	.01(8)	.00(8)
N(2)	.0877(2)	.2996(2)	.4537(2)	2.95(9)	2.10(8)	2.50(9)	.14(8)	.33(8)	.09(7)
N(3)	.0536(1)	.3222(2)	.2329(2)	2.11(9)	2.28(8)	2.74(9)	.15(8)	-.35(7)	-.37(7)
N(4)	.2260(2)	.5379(2)	.3346(2)	2.17(8)	2.41(9)	3.48(10)	-.55(8)	.79(9)	-.26(9)
N(5)	.0155(2)	.3525(2)	.5294(2)	4.55(14)	3.22(10)	2.56(10)	1.57(10)	1.04(9)	.77(9)
N(6)	-.0333(2)	.3875(2)	.2078(2)	2.84(11)	3.06(10)	3.16(10)	.72(9)	-.72(9)	-.53(8)
O(1)	.2270(3)	.5932(3)	.2388(4)	5.66(23)	3.30(17)	4.07(19)	-1.22(18)	.82(17)	.68(16)
O(2)	.2649(3)	.5687(3)	.4338(4)	3.42(16)	3.30(17)	4.17(19)	-.86(15)	-.13(16)	-1.31(14)
O(3)	-.0693(3)	.3142(4)	.5262(4)	3.33(21)	7.18(26)	4.26(20)	1.38(21)	1.53(17)	1.56(19)
O(4)	.0454(4)	.4271(3)	.5990(3)	8.94(32)	3.81(21)	2.58(16)	2.51(22)	.57(20)	-.53(15)
O(5)	-.1121(3)	.3534(4)	.2504(4)	2.46(16)	5.72(25)	5.84(25)	.44(17)	-.62(16)	.22(21)
O(6)	-.0236(4)	.4691(4)	.1390(4)	6.44(27)	4.41(23)	4.15(20)	1.85(21)	-.91(20)	.62(18)
H(1)	.2401(6)	.2944(7)	.4226(7)	3.72(33)	5.32(36)	5.64(37)	-.14(30)	-1.28(31)	1.41(32)
H(2)	.2013(6)	.4068(6)	.5244(6)	7.62(43)	5.60(37)	2.70(29)	-2.01(34)	-1.27(29)	-.59(28)
H(3)	-.0261(5)	.2117(6)	.3540(6)	3.71(34)	4.33(33)	5.97(35)	-1.46(29)	-.18(31)	.16(27)
H(4)	.1015(5)	.1728(5)	.3192(7)	4.64(30)	2.63(26)	5.94(37)	.89(27)	-.16(27)	-1.14(27)
H(5)	.2052(5)	.3166(6)	.1917(6)	3.14(28)	6.02(37)	5.24(37)	.46(30)	.80(25)	-2.25(30)
H(6)	.1440(6)	.4432(7)	.1413(7)	6.37(44)	6.02(39)	3.63(35)	-1.70(35)	.17(28)	1.08(31)

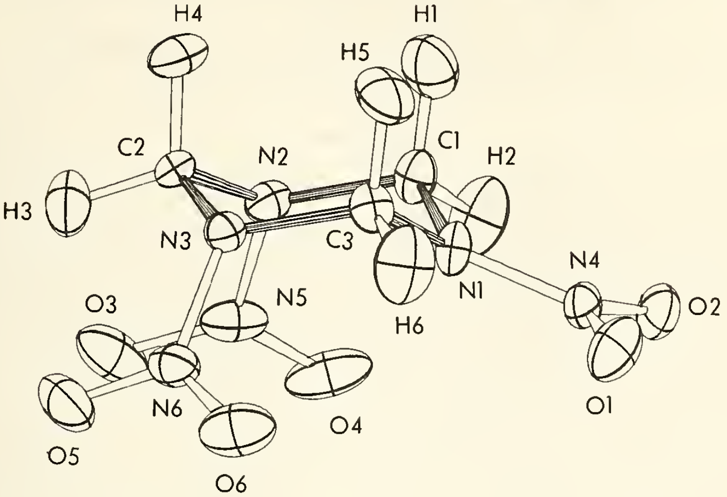

Fig. 1. A perspective view of RDX molecule.

THE STRUCTURE OF ANDALUSITE AND SILLIMANITE

L. W. Finger
(Carnegie Institution of Washington, Washington, D.C.)
and
E. Prince

Anadusite and sillimanite are alunimum silicate minerals both of which have the nominal composition Al_2SiO_5. Nuclear magnetic resonance measurements of the electric field gradients at the aluminum nuclear positions were in significant disagreement with values computed from the crystal structures previously determined by x-ray diffraction. The neutron diffraction study was undertaken to see if more accurate values for oxygen positions in the structures would resolve the discrepancies. A highly accurate data set was obtained for andalusite and refined to a weighted R index of .026. Because of unavoidable characteristics of the sample the sillimanite data were less accurate, and the final weighted R was .045. In both cases there were small shifts in atomic coordinates which resulted in better fits to the nmr data. A notable feature of the results was that M-O interatomic distances for the neutron structures were almost invariably shorter by significant amounts, than the corresponding distances in the x-ray structure. This can be seen in Table 1, which compares the corresponding distances in andalusite. This result suggests that there may be a systematic displacement of the electron clouds around the oxygen atoms so as to make their centers further away from the cations. It is hoped that a careful x-ray study on andalusite will allow an accurate determination of the electron density distribution.

TABLE 1 Andalusite Interatomic Distances - Interatomic distances in andalusite, as determined from x-ray and neutron diffraction.

	Neutron Value, Å	X-Ray Value, Å	Δ(N - X)
Si tetrahedron			
Si-O(b)	1.635(2)*	1.635(5)	0.000
Si-O(c)	1.609(2)	1.615(6)	-0.006
Si-O(d) (2x)	1.623(1)	1.631(4)	-0.008
Mean Si-O	1.623	1.628	-0.005
O(b)-O(c)	2.525(2)	2.514(7)	+0.011
O(b)-O(d) (2x)	2.690(2)	2.704(5)	-0.006
O(c)-O(d) (2x)	2.659(1)	2.681(6)	-0.022
O(d)-	2.663(2)	2.658(4)	0.005
Mean O-O	2.648	2.657	-0.009
Al octahedron			
Al_1-O(a) (2x)	1.817(2)	1.829(4)	-0.012
Al_1-O(b) (2x)	1.885(2)	1.892(4)	-0.007
Al_1-O(d) (2x)	2.079(1)	2.085(3)	-0.006
Mean Al_1-O	1.927	1.935	-0.008
O(a)-O(a)	2.445(3)	2.476(7)	-0.031
O(a)-O(b) (2x)	2.780(1)	2.780(1)	0.000
O(a)-O(d) (2x)	2.770(2)	2.793(6)	-0.023
O(a)-O(d) (2x)	2.739(2)	2.738	0.001
O(b)-O(d) (2x)	2.835(2)	2.854	-0.019
O(b)-O(d) (2x)	2.791(2)	2.794(6)	-0.003
O(b)-O(b)	2.445(3)	2.469(7)	-0.024
Mean O-O	2.727	2.739	-0.012
Five-coordinated aluminum			
Al -O(a)	1.800(3)	1.816(6)	-0.016
Al -O(c)	1.871(3)	1.886(6)	-0.015
Al -O(c)	1.833(3)	1.843(5)	-0.010
Al -O(d) (2x)	1.814(2)	1.818(3)	-0.004
Mean Al -O	1.826	1.836	-0.010
O(a)-O(c)	2.483(2)	2.515(7)	-0.032
O(a)-O(d) (2x)	2.748(1)	2.761(5)	-0.013
O(c)-O(c)	2.233(3)	2.247(7)	-0.014
O(c)-O(d) (2x)	2.668(2)	2.677(5)	-0.009
O(c)-O(d) (2x)	3.253(2)	3.265	-0.012
O(d)-O(d)	2.896(2)	2.901(4)	-0.005
Mean O-O	2.772	2.785	-0.013

*The estimated standard deviation of the final digit is given in parentheses.

DISTRIBUTION OF ALUMINUM AND SILICON CATIONS IN A FELDSPAR MINERAL

E. Prince

and

G. Donnay and R. F. Martin
(McGill University, Montreal, P.Q., Canada)

In the 1971 Progress Report we described a structure refinement carried out on a crystal of the feldspar mineral orthoclase. The distribution of aluminum and silicon between two sites with slightly different, tetrahedral, oxygen environments is commonly used by geologists as a means of studying the thermal history of the rocks in which the mineral crystals are found. Because of the similarity of their atomic scattering factors for x-rays, the distribution of Si and Al cations cannot be determined directly from x-ray diffraction data, and mean M-O distances in the tetrahedron have commonly been used as an indirect measure of this distribution. Our values for these distances, together with the commonly accepted curve, implied an Al content for the site designated T(2) of about 0.09. However it came to our attention that Brown and co-workers of SUNY, Stony Brook, working at Brookhaven, had successfully determined the distribution directly, in a similar mineral, by neutron diffraction. We therefore tried a direct refinement with our data, constraining the total Al and Si contents for the two sites to conform to the overall chemical analysis. This refinement resulted in a small but highly significant reduction in the weighted R index, and gave an essentially zero value for the Al content in the T(2) site. Figure 1 shows a plot of the mean M-O distances against Al content for the two sites in our crystal and the two sites in the Brown et al study, which all lie, perhaps fortuitously, on a straight line. The dashed line is the one previously used by the feldspar geologists. This result suggests that the mean M-O distance is not sufficient information to determine the cation distribution.

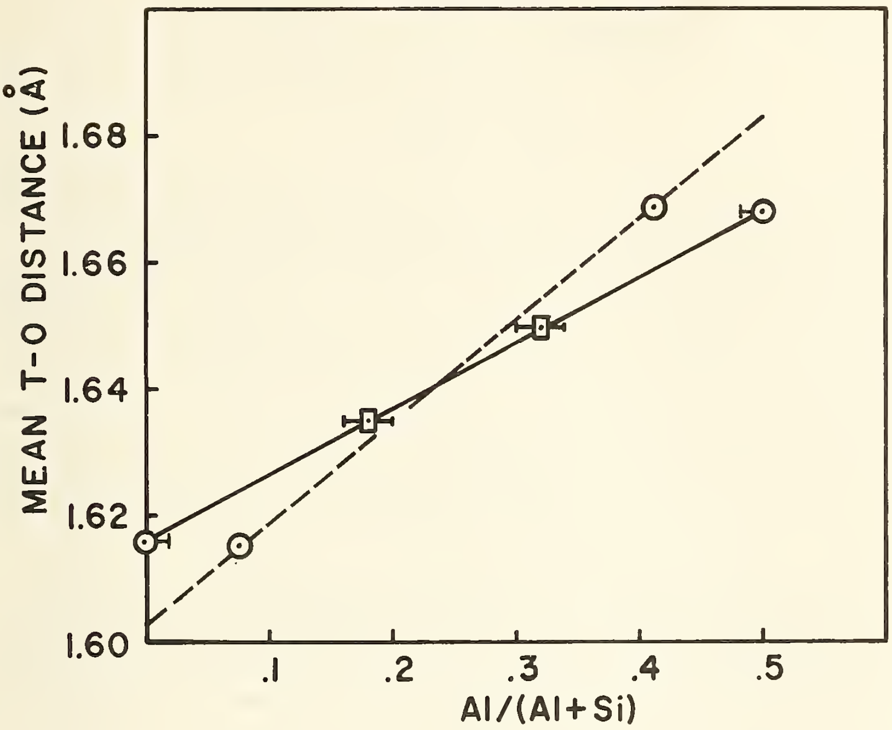

Fig. 1. Mean metal-oxygen distances as a function of Aluminum content in the tetrahedral sites, for two feldspar studies. The dashed line has been used by geologists to relate the mean M-O distance to the cation distribution.

THE CRYSTAL STRUCTURE OF 1,3,5,7,TETRACETO-1,3,5,7,TETRAZACYCLO-OCTANE

C. S. Choi
(Picatinny Arsenal, Dover, N. J.)

and

B. Dickens
(Polymer Division)

The compound 1,3,5,7,tetraceto-1,3,5,7,tetrazacyclo-octane (TAT) is a key intermediate in the production of HMX (cyclotetramethylene-tetranitramine), and commonly labeled as TAT. Preliminary investigation by precession photographs with MoKα radiation revealed that the crystal belongs to tetragonal space group $P4_12_12$ (enantiomorphous to $P4_32_12$) with four molecules per unit cell. An automated 4-circle x-ray diffractometer equipped with a graphite monochromator to reflect MoKα radiation was used for the measurement of reflection intensities and for precise determination of the unit cell dimensions, i.e. $a = b = 10.540(2)$ Å and $C = 12.137(2)$ Å. The structure was solved by direct methods and refined to a final R-index $wR = 0.037$ and $R = 0.039$ for 1244 observed reflections. The molecule consists of alternate CH_2 and $N\text{-}CO\text{-}CH_3$ groups in a puckered C-N ring, having boat-shape configuration with a two fold rotation axis through the center of the C-N ring (see Fig. 1). The heavy atoms of each acetyl group are essentially coplanar with the neighboring nitrogen atom. The TAT molecule is very similar to α-HMx which also has a boat-shape configuration. The bond lengths and angles found here for the C-N ring generally agree with those of α- and β-HMX. The rigid body thermal motion analysis by using the aniostropic temperature factors indicate that the molecular thermal motion is represented by three motions, i.e. a libration about the two-fold rotation axis and two intramolecular bending motions about the diagonal of the C-N ring.

Table 1. Final least squares parameters for the structure of TAT. Thermal parameters have the form, exp-1/4 $(B_{11}a^{*2}h^2 + B_{22}b^{*2}k^2 + B_{33}c^{*2}l^2 + 2B_{12}a^*b^*hk + 2B_{13}a^*c^*h\ell + 2B_{23}b^*c^*k\ell)$.

ATOM	X	Y	Z	B_{11}	B_{22}	B_{33}	B_{12}	B_{13}	B_{23}
C1	.3792(1)	.4718(1)	.1353(1)	3.49(36)	2.61(32)	2.60(37)	-.02(32)	-.07(31)	-.48(29)
C2	.5372(1)	.3235(2)	.0575(1)	2.45(30)	3.22(34)	3.00(39)	-.05(28)	.06(29)	-.11(31)
C3	.4580(2)	.2981(1)	.2497(1)	3.76(40)	3.24(37)	2.91(38)	-.65(32)	-.41(34)	.09(32)
C4	.1803(1)	.4022(1)	.0443(1)	2.70(32)	2.49(32)	3.68(42)	.20(26)	.45(33)	-.33(32)
C5	.5447(2)	.1870(2)	.2660(2)	4.99(54)	3.87(47)	3.74(52)	-.04(41)	-.72(45)	.71(43)
C6	.1491(2)	.3249(2)	.1444(1)	3.92(44)	3.07(38)	4.34(54)	-.45(33)	.83(41)	.03(41)
N1	.4548(1)	.3568(1)	.1492(1)	3.07(28)	2.71(28)	2.56(32)	-.05(22)	-.04(26)	-.13(24)
N2	.2917(1)	.4680(1)	.0429(1)	2.59(27)	2.54(26)	2.59(31)	-.05(22)	.13(24)	-.22(23)
O1	.3917(1)	.3359(1)	.3255(1)	6.00(41)	5.26(36)	2.86(31)	.26(33)	.57(31)	.35(30)
O2	.1107(1)	.4035(1)	-.0360(1)	3.13(27)	4.71(32)	4.51(37)	-.51(27)	-.78(28)	.06(31)
H1	.334(2)	.484(2)	.198(1)	1.76(32)					
H2	.436(2)	.543(2)	.119(1)	1.89(32)					
H3	.587(1)	.398(2)	.039(1)	1.34(29)					
H4	.593(2)	.251(2)	.082(1)	1.68(33)					
H5	.555(3)	.168(3)	.336(2)	6.03(62)					
H6	.640(2)	.211(2)	.253(2)	5.34(55)					
H7	.525(2)	.121(2)	.217(2)	3.81(47)					
H8	.211(2)	.246(2)	.150(1)	4.35(50)					
H9	.062(2)	.291(2)	.142(2)	4.29(51)					
H10	.153(2)	.366(2)	.209(2)	4.89(57)					

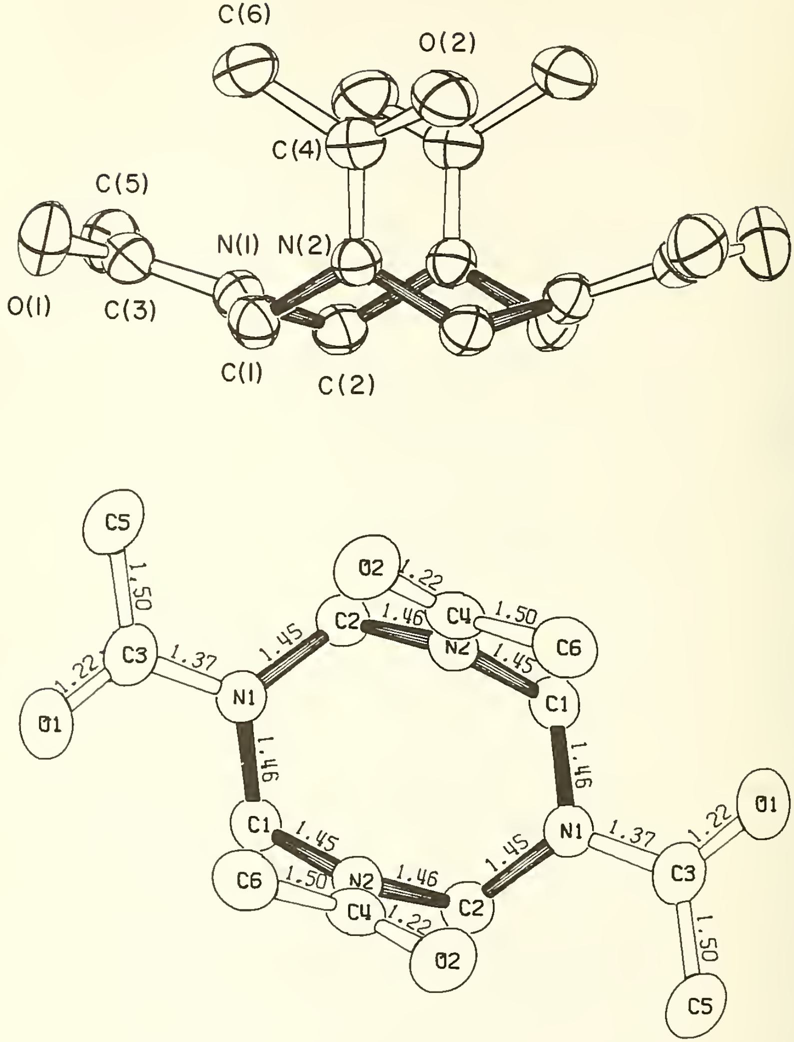

Fig. 1. The TAT molecule viewed from side and top of the molecule.

MAGNETIC STRUCTURES OF $Eu_{1-x}Gd_xS$

S. Pickart and H. A. Alperin
(Naval Ordnance Laboratory, White Oak, Md.)

The rare-earth chalcogenide EuS is a ferromagnetic insulator, while GdS is a metallic antiferromagnet. Mixtures of these two materials therefore offer an opportunity to study magnetic behavior of a system showing a complete range of transport properties. Furthermore, the system has a simple face-centered cubic lattice with both rare earth atoms having identical spin-only magnetic moments (in a half-filled 4-f shell), thus encouraging theoretical analysis.

Our previous neutron diffraction measurements[1] showed that GdS has the second type of antiferromagnetic order, with both first and second neighbor interactions negative. This is presumably because of the s-electron polarization (RDDY exchange), while the ferromagnetic alignment in EuS is believed to result from localized (Heisenberg) exchange forces. Magnetic measurements[2] on the mixed system $Eu_{1-x}Gd_xS$ showed drastic changes for small x in the ordering temperature, but the saturation magnetization behaved as though the Gd moment were not contributing, i.e. as simple dilution.

To understand this effect we investigated the magnetic alignment by means of neutron diffraction in samples with $x = 0.1$, 0.2, 0.3, 0.6 and 0.8. The results, some of which are plotted in Fig. 1, show three ranges of different behavior: only ferromagnetic alignment for $x = 0.1 - 0.3$, only antiferromagnetic (GdS type) for $x = 0.8$, and negligible long-range order of any type for $x = 0.6$. Small angle scattering, due to short-range order, was observed in all samples. Consequently, we must conclude that the magnetic structures in this mixed system are inhomogeneous, probably forming clusters of Gd spins that are locally anti-parallel (and thus do not contribute to the net moment), but with the clusters not correlated on a long-range basis.

---

[1] T. McGuire, R. Gambino, S. Pickart and H. Alperin, *J. Appl. Phys.* 40, 1009 (1969).

[2] T. McGuire and F. Holtzber, *AIP Conf. Proc.* 5, 855 (1972).

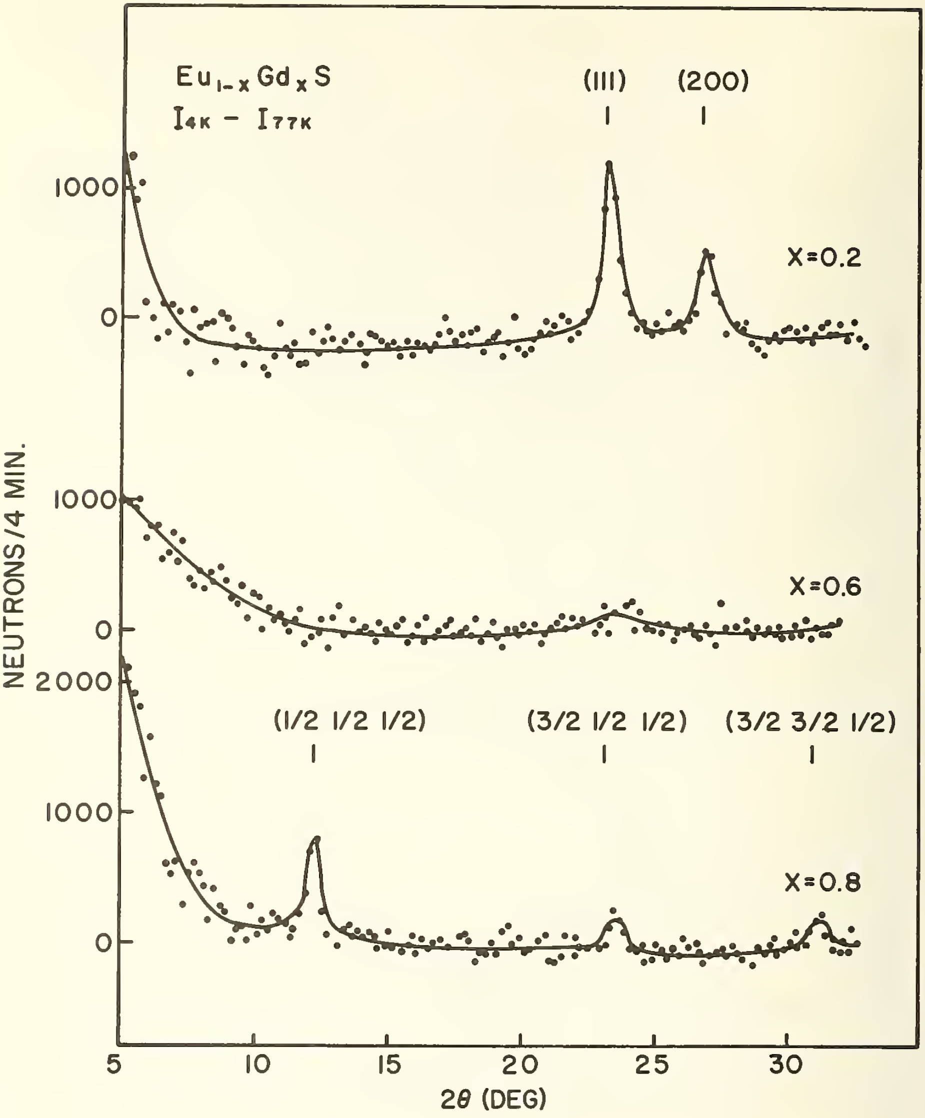

Fig. 1. Magnetic intensity (data at 77K subtracted from data at 4K) for three samples in the $Eu_{1-x}Gd_xS$ system. Reflections with integral Miller indices are due to ferromagnetism, those with half-integral indices to antiferromagnetism of the type found in pure GdS.

PHONON DISPERSION IN hcpBe

H. Alperin, S. Pickart and J. Rhyne
(Naval Ordnance Laboratory, White Oak, Md.)

Be metal has a very high strength-to-weight ratio and heat capacity; it is therefore useful in aerospace applications, and would be even more so were it not so brittle. The ductility of polycrystal Be is known to go through a marked maximum at 440°C, and this has recently been correlated with an anomaly in the lattice expansion[1] in a single crystal. In order to search for the microscopic origin of these phenomena, we have begun a study of the temperature dependence of the phonon spectra in single crystal Be using neutron inelastic scattering. Correlation of interatomic force constant changes with ductility might conceivably suggest methods of enhancing the desirable properties of Be.

Room temperature measurements have been completed for two propagation directions, along the c-axis (shown in Fig. 1) and in the $[11\bar{2}0]$ direction in the basal plane. These data are much more accurate than previous measurements[2] and show no evidence of the Kohn anamolies predicted by a recent pseudopotential calculation[3] (in contrast to the tensor force constant model, which predicts smooth curves). High temperature measurements are now in progress.

---

[1] F. Wang (private communication).

[2] C. Thaper et al., *Proc. Intl. Conf. in Rennes, 1971;* R. Schmunk, *Phys. Rev.* 149, 450 (1966).

[3] W. King and P. Cutler, *S. S. Comm.* 7, 295 (1969).

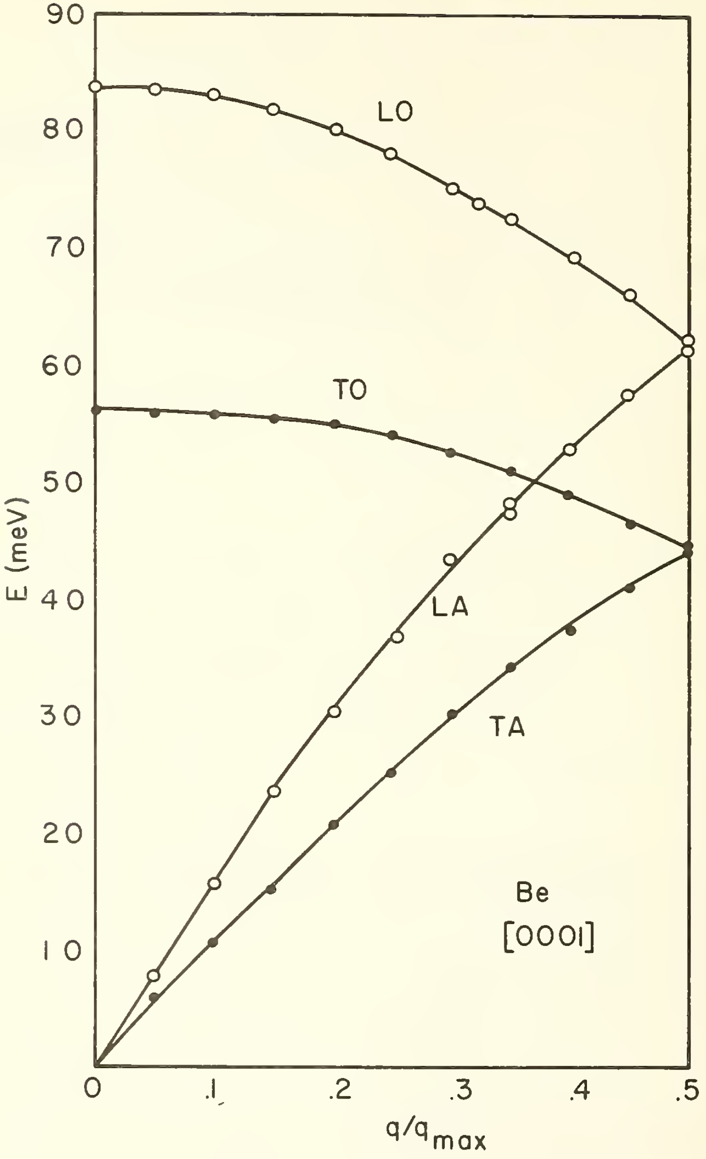

Fig. 1 Energy transfer (E) vs. reduced wavevector for longitudinal and transverse acoustic and optic phonons propogating along the c-direction in hcp/Be.

SOFT-PHONON MODE BEHAVIOR IN PbTe

H. Alperin, S. Pickart and J. Rhyne
(Naval Ordnance Laboratory, White Oak, Md.)
and
V. Minkiewicz
(University of Maryland, College Park, Md.)

In recent years, a controversy has arisen as to whether or not the compound semiconductor PbTe exhibits paraelectric behavior, i.e., a Curie-Law temperature dependence of the dielectric constant. This characteristic, which might ultimately lead to a ferroelectric transition, would be important for potential dielectric-constant related applications. Cochran's theory of ferroelectricity relates the spontaneous polarization acquired in the ferroelectric state to the tendency for certain types of lattice vibrations to lower their energy or become "soft" as the temperature is lowered, ultimately becoming "frozen in" at the transition. Since inelastic neutron scattering is the only direct method of observing these effects, we have carried out a study of the PbTe vibrational spectrum over an extended temperature range (300 to 4.2 K), using this technique.

Our results, summarized for the [111] propagation direction in Fig. 1, reveal that the longitudinal optical mode vibration is essentially temperature independent, while the corresponding transverse optical mode decreases strongly as the temperature is lowered. The latter does not reach zero, however, so that the PbTe behavior is paraelectric, but not ferroelectric. These measurements confirm the temperature dependence of the static dielectric constant in PbTe which had been implied by an earlier experiment, and they explain how carrier mobilities in PbTe can reach such unusually high values at cryogenic temperatures.

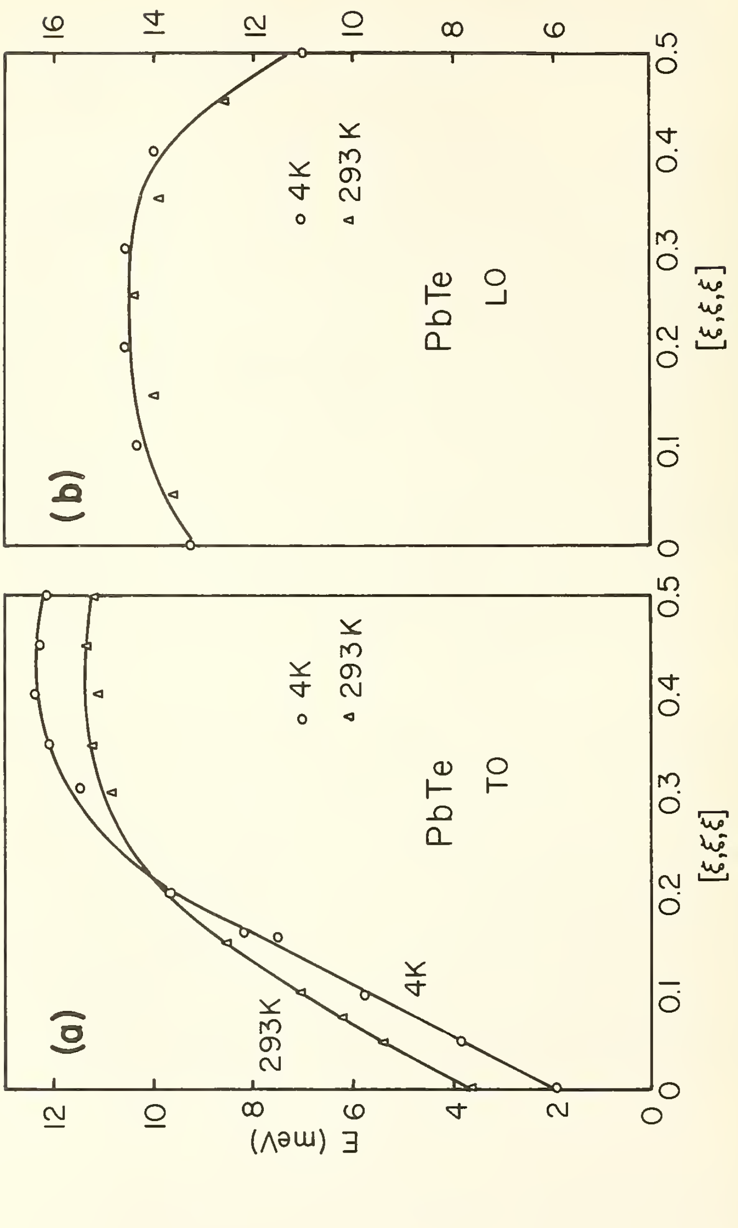

Fig. 1. Phonon dispersion curves in PbTe at two temperatures:
a) Transverse optic branch b) Longitudinal optic branch.

OBSERVATION OF AN AMORPHOUS SPIN DISTRIBUTION

J. Rhyne, S. Pickart and H. Alperin
(Naval Ordnance Laboratory, White Oak, Md.)

Neutron diffraction measurements made on a sputtered sample of composition $TbFe_2$ have provided the first direct evidence for an amorphous spin distribution, i.e. a magnetically polarized state formed from atomic spins with no spatial periodicity.

Previous classes of materials believed to be amorphous magnets are transition metal-loaded phosphorus glasses[1] and ternary Fe-Pd-C alloys[2] prepared by a variation of splat cooling. Neutron diffraction measurements made on the first class were either inconclusive or showed microcrystalline phases; the ternary alloys can be prepared only in thin foils of micrometer thicknesses and are not suitable for the neutron scattering technique (which is unique in that it measures the spin distribution directly by the interaction of the neutron spin with the atomic moments).

Magnetic measurements on the sputtered $TbFe_2$ sample show a well-defined Curie point at 388K and a saturation moment at OK of 2.8 μ_B per molecule, both substantially lower than the values for the crystalline $TbFe_2$ phase. Neutron data were taken at 423K, in the paramagnetic region, and at 4K, where maximum polarization is attained, both patterns showing a broad diffuse maximum characteristic of amorphous materials but shifted significantly at lower temperatures. The difference between these two patterns, seen in Fig. 1, is due to the magnetic scattering alone.

These data show unequivocally that the spatial distribution of the magnetization in this material is amorphous or liquid-like. Without further involved analysis, not much can be said about its exact nature, other than that it is not simply ferromagnetic (each atom having the same average moment) or ferrimagnetic (rare earth and iron moments antiparallel), as in the crystalline phase.

Of particular interest is the small angle scattering in Fig. 1, which is not observed in the data taken above the Curie point. It indicates an inhomogeneity or clustering in the magnetic structure which is not related to any inhomogeneity in the atomic structure, perhaps intrinsic to the magnetic amorphous state. Further measurements with applied magnetic fields are in progress, and attempts will also be made to observe critical scattering and spin-wave scattering to get information concerning the dynamics in amorphous magnets.

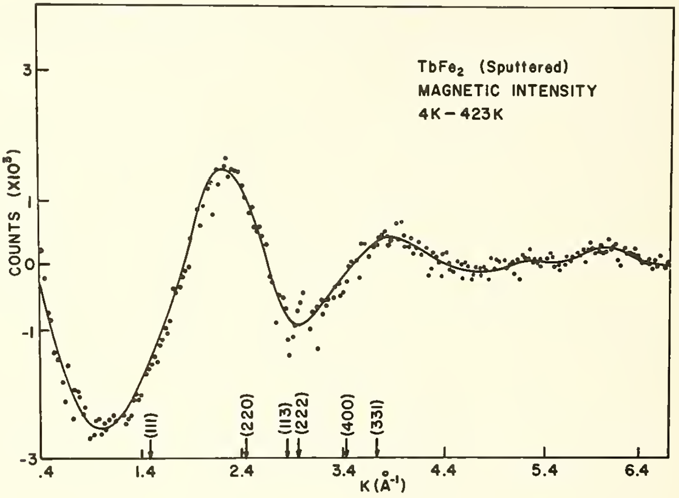

Fig. 1. Magnetic vs. scattering vector (low temperature data minus high) in sputtered $TbFe_2$. Arrows show the location of the principal peaks in the crystalline $TbFe_2$ phase.

---

[1] T. Egann et al., *J. Phys. C: Solid State* 5 (to be published).

[2] T. Sharon and C. Tsuei, *Phys. Rev.* B5, 1047 (1972).

CRYSTALLINE ORDERING IN SILICA AND GERMANIA GLASSES

J. H. Konnert, J. Karle, and G. A. Ferguson
(Naval Research Laboratory, Washington, D.C.)

Two limiting models have been proposed for glasses; in one model[1] the material is depicted as composed of small regions of crystalline-like order bonded together in essentially random orientations and, alternatively, another model of glass structure is described as a random network[2] in which the distribution of only the shortest interatomic distances corresponds throughout the material to those present in a crystalline phase. Diffraction analyses performed on the glasses of silica[3-6] and germania[5,7] have been generally interpreted in terms of the random network model.

X-ray diffraction data were collected with MoK_α radiation using fused quartz and fused silica from vapor phase hydrolysis of pure silicon compounds ("infrasil" and "suprasil", respectively, prepared by Amersil Inc.). All data sets produced nearly identical radial distribution functions (RDF's). Neutron diffraction data were collected at a wavelength of 0.84Å. The RDF's are illustrated in Fig. 1. Significant deviations from a uniform distribution of distances are present out to at least 20Å.

Full details of the data reduction will be published elsewhere. However, since this procedure has revealed previously undetected details in the RDF's, the main points of the procedure will be mentioned. The basic considerations concern the imposition of constraints on the RDF.[8] That portion of the total intensity function that contains interatomic distance information, i(s), is isolated in a manner described for electron diffraction.[9] The truncation problem is handled by recognizing that in the usual experiments only the shortest distances are sufficiently ordered to contribute to i(s) beyond the experimental limit of data collection. These short distance (SD) contributions are removed from i(s) by a least squares procedure that minimizes the spurious detail in the RDF at small and large values of r. The equation employed is:

$$r^2D(r)=4\pi r^2(\rho(r)-\rho_o) = \frac{2\pi}{r}\int^{s_{max}} s\ Ki(s)-\sum_{SD} \frac{N_{ij}f_if_j\exp(-\ell_{ij}^2 s^2/2)}{sr_{ij} \quad \underset{UC}{} f^2} \sin sr_{ij}\ \sin srds$$

$$+\ SD\ contributions$$

where $s = (4\pi\sin\theta)/\lambda$, λ is the wavelength, 2θ is the angle between the incident and diffracted beam, K places the intensity on an absolute scale, r_{ij} is the distance between the ith and jth atoms, N_{ij} is the coordination number, ℓ_{ij} is the disorder parameter, UC is the unit of composition (SiO_2 or GeO_2), s_{max} is the experimental limit of data collection, the f's are the atomic scattering factors, ρ_o is the density parameter, and $4\pi r^2\rho(r)$ is the probability weighted by the scattering factors of finding atoms in the sample separated by the distance r. The short distances are reintroduced without associated truncation effects into the final RDF.

RDF's were calculated for crystalline forms by broadening the Bragg maxima in the powder patterns to correspond to an 11A particle size for 3/4 of the sample and a 20Å size for 1/4. Such broadening reduces the amplitudes of the RDF without altering the positions of the peaks, thus affording a suitable approximation to the RDF corresponding to small ordered regions. If the dimensions of these regions are less than the unit cell dimensions, this corresponds to all configurations in the unit cell being represented by different particles.

Atomic parameters obtained from crystal structure analyses were used to calculate the diffraction patterns for quartz[10] and cristobalite.[11] Since tridymite forms highly twinned crystals with a variety of unit cells (all with a sub-cell of approximate dimensions a = 8.7Å, b = 5.0Å, c = 8.2Å), accurate atomic parameters are not available. The average structure has been determined at 250°C and provides evidence for the bonding topology.[12] A powder diffraction pattern collected with a sample of tridymite from Diamond Lake, Douglas Co., Oregon showed orthorhombic diffraction symmetry with a = 81.97Å, b = 9.94Å, c = 17.23Å. The approximate weight percent of impurities, as indicated by electron probe analysis, are Al∿2%, Na∿1%, and K∿1%. Accurate atomic positions have not been determined for the crystalline polymorphs of germania. The neutron powder diffraction patterns for quartz-like and cristobalite-like germania were calculated with the use of the atomic coordinates of quartz and cristobalite and the appropriate scattering factors for neutrons.

The $r^3D(r)$ curves are illustrated in Fig. 1. The x-ray RDF for silica glass is quite similar to the RDF obtained from the powdered tridymite, but quite different from the RDF's derived from cristobalite and quartz. The positions of the maxima in the silica glass RDF's obtained from neutron and x-ray diffraction data are nearly the same, indicating that the distances tend to cluster similarly. The germania glass RDF obtained from the neutron diffraction data is very similar to the silica glass RDF obtained from the x-ray data. The Ge and O atoms scatter neutrons with approximately the same relative efficiency as Si and O atoms scatter x-rays, as illustrated by the similarity of the neutron diffraction RDF's calculated for quartz-like and cristobalite-like germania to x-ray RDF's of quartz and cristobalite. Thus the RDF's strongly suggest that silica glass, germania glass, and tridymite posses the same short-range order.

The correspondence of the positions and magnitudes of the details in the RDF's obtained for silica glass and tridymite-like particles indicates that the data are consistent with a structure in which nearly all of the atoms comprise parts of tridymite-like regions having dimensions ranging up to at least 20Å. Details at large r suggest the possibility of a small amount of cristobalite-like ordering. The relatively large details in the outer portion of the RDF for silica glass from the neutron diffraction data may arise from the oxygen atoms, the dominant neutron scatterers, lying on the periphery of the ordered regions. However, the larger sample used for the neutron diffraction experiment may, in fact, be more highly ordered.

If the interpretation that nearly all atoms are part of ordered regions is correct, it is required that these regions be efficiently bonded together in a manner analogous to twinned crystals, but with a fairly large number of relative orientations and small distortions so that isotropic properties would ensue. Differences in the inner regions of the RDF's of silica glass and tridymite computed from the x-ray diffraction

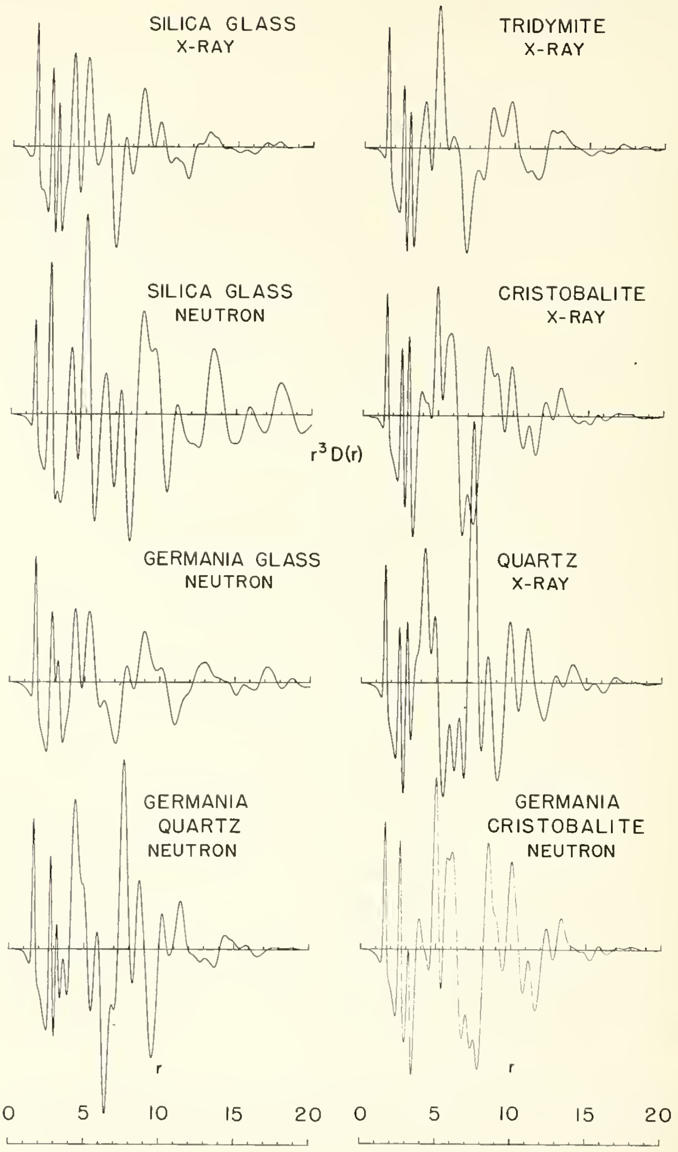

Fig. 1. Radial distribution functions for silica and germania glasses and comparision functions derived from the broadened powder patterns of crystalline polymorphs.

data can be related to the junctures between the ordered regions. The three shortest distances throughout the glass samples are nearly identical to the corresponding distances in all of the crystalline modifications where the silicon atoms are tetrahedrally bonded. The contribution to the RDF from distances between atoms in different ordered regions would be progressively less as r increases, and after about 6Å they would not contribute any appreciable details.

While radial distribution functions of glasses do not alone provide enough information for a unique structure determination, the comparisons with the functions calculated from crystalline phases of nearly the same density as the glasses imply a great similarity between glasses and crystals on the atomic level.

---

[1] N. Valenkov and E. Porai-Koshits, *Z.Krist.* 91, 195 (1936).

[2] W. H. Zachariasen, *J. Am. Chem. Soc.* 54, 3841 (1932).

[3] C. Carraro, M. Domenici and T. Zucca, in *Physics of Non-Crystalline Solids*, J. A. Prins, Ed. (North Holland Publ. Co., Amsterdam, 1965) pp. 152-161

[4] E. H. Henninger, R. C. Buschert and L. Heaten, *J. Phys. Chem. Solids* 28, 423 (1967).

[5] E. Lorch, *J. Phys.* C 2, 229 (1969).

[6] R. L. Mozzi and B. E. Warren, *J. Appl. Cryst.* 2, 164 (1969).
R. L. Mozzi, Ph.D. Thesis, Massachusetts Institute of Technology (1967).

[7] G. A. Ferguson and M. Hass, *J. Am. Ceram. Soc.* 53, 109 (1970).

[8] I. L. Karle and J. Karle, *J. Chem. Phys.* 17, 1052 (1949); 18, 957, 963 (1950).

[9] P. D'Antonio, C. George, A. H. Lowrey and J. Karle, *J. Chem. Phys.* 55, 1071 (1971).

[10] R. A. Young and Ben Post, *Acta Cryst.* 15, 337 (1962).

[11] W. A. Dollase, *Zeit. Krist.* 23, 617 (1967).

[12] W. A. Dollase, *Acta Cryst.* 23, 617 (1967).

[13] We thank Mr. L. Paollela for his aid in collecting the neutron diffraction data. The research was supported in part by the Advanced Research Projects Agency.

PRECISION MEASUREMENT OF THE THERMAL NEUTRON SCATTERING AMPLITUDE FOR SILICON

C. S. Schneider
(U. S. Naval Academy, Annapolis, Md.)

Measurements have been completed this year on the refractive shifts of a nearly monochromatic (3.2Å) neutron beam resulting from passage through a right angled prism of silicon. This first result, b_N(Si) = 4.152(2) fm, is in good agreement with Shull's determination from the Pendellosung effect in Bragg reflection from silicon and corrected for the Foldy charge interaction: b_N(Si) = 4.1491(10)fm.

The spectrometer has since been resuspended, by cables from above replacing pneumatic tubes below, to improve the angular stability. The wavelength has also been increased to about 4.2Å so that better advantage may be taken of the full range of the torsion goniometer used in defection measurements.

A precision (1/4 second arc) indexing goniometer head has replaced the continuous sine-arm goniometer used for prism orientation and for initial wavelength calibration; in this second mode the indexing head is seated on a sine-arm which is driven by the computer-automated stepping motor. With these improvements in the double crystal spectrometer, it seems quite feasible to obtain an accuracy of .001 fm in neutron scattering amplitude determination. Since the prism determination includes only the nuclear force contribution of the nucleus, due to the forward scattering and unpolarized neutron spin, there are no corrections necessary for other interactions possible when neutrons pass through matter. In particular, there is no Foldy charge contribution to the measured amplitude so a comparison of this determination with Shull's uncorrected value gives new experimental verification of the existence of the Foldy interaction.

It is for later experiments to extend these comparisons to higher accuracy leading to a possible clarification of the present discrepancy between the recent Ringo-Krohn determination and the Foldy-predicted amplitude of interaction between the neutron and electron.

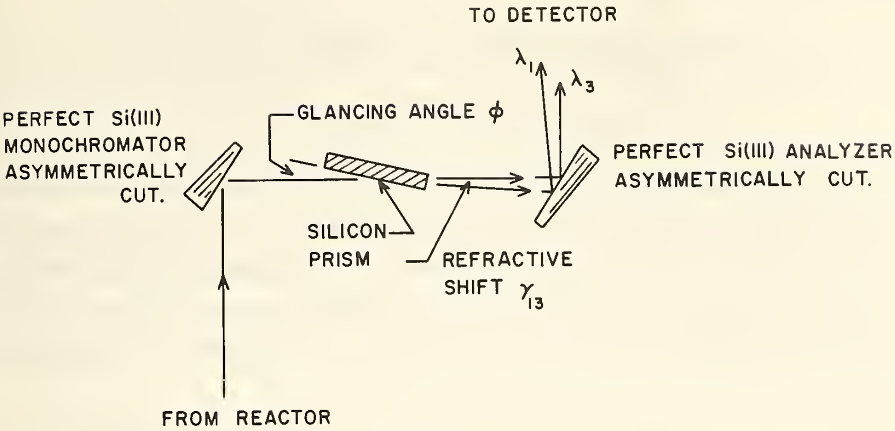

Fig. 1. Schematic diagram of neutron optics in double perfect crystal spectrometer.

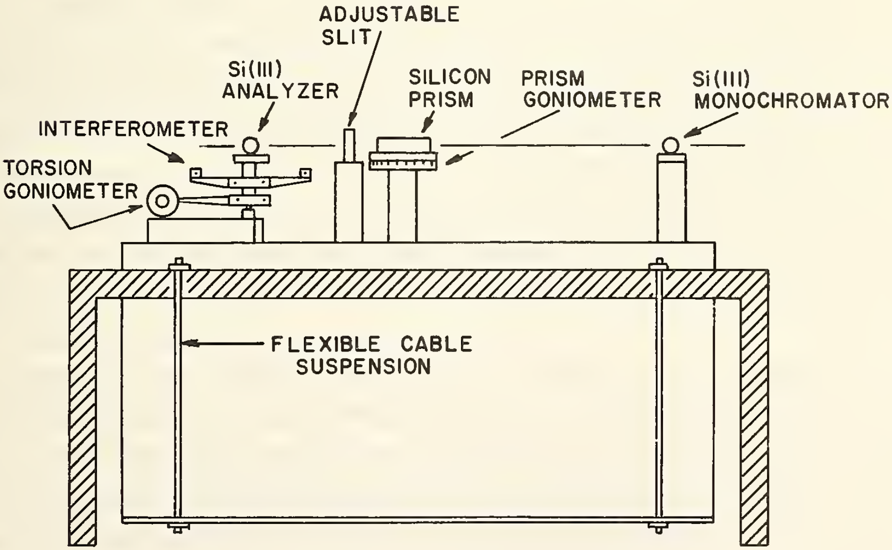

Fig. 2. Schematic diagram of control systems in double perfect crystal spectrometer.

D. NON-RRD NBS PROGRAMS

ACTIVATION ANALYSIS SECTION: SUMMARY OF ACTIVITIES

P. D. LaFleur
(Analytical Chemistry Division)

The Activation Analysis Section of the Analytical Chemistry Division is physically located in the NBS Reactor Building. A complete description of the Section's activities may be found in its annual progress report, NBS Technical Note 588. Therefore, only a brief summary of some of the work will be included here, with an emphasis on the NBSR characterization work.

1. Standard Reference Materials (SRM)

Much of the section's efforts have been directed toward the development of high precision and high accuracy in neutron activation analysis, with a primary aim being the analysis and certification of NBS Standard Reference Materials.

a. Biological SRMS - The biological SRMs analyzed include Orchard Leaves (SRM 1571) and Bovine Liver (SRM 1577) mentioned in last years's report, and several new materials as well. These new biological materials include Mercury in Tuna (SRM 1578), Tomato Leaves, as well as preliminary work on a standard blood serum SRM.

b. Environmental SRMs - The environmental SRMs analyzed by neutron activation analysis this year include Mercury in Coal (SRM 1630), and preliminary analyses for trace elements in gasoline, residual fuel oil, coal and fly ash.

c. Other SRMs - A wide variety of other types of SRMs were analyzed by neutron activation analysis. A few of these materials include stainless steel, high purity iron, molybdenum concentrate, graphite, and titanium. Some of the elements determined in one or more of the above materials include gold, silver, rhenium, nickel, aluminum, iron, vanadium, chromium, manganese, tantalum and titanium.

2. Cooperative and Service Analyses

In addition to the analyses on SRMs, a large number of additional analyses were made on non-SRM materials. These include cooperative analyses, where the analysis is made on samples furnished by other laboratories. In the past year such samples have included high purity silicon, high purity iron, ion exchange resin, alveolar macrophages, and single crystal magnesium oxide. A few of the elements determined include gold, cobalt, iridium, manganese, scandium, zirconium, hafnium, tungsten, and europium.

3. Radiochemical Separations

Many of the analytical determinations made by the section require a radiochemical separation to obtain the accuracy and precision necessary for certification as standard material. To this end, there is always research on radiochemical separations taking place, striving to improve existing procedures or to develop new and better ones. Work this year includes additional development of procedures using di(2-ethylhexyl) phosphoric acid (HDEHP) as an extractant, and a new volatilization procedure in which a rapid quantitative separation of zinc, arsenic, selenium, cadmium and mercury after neutron activation is performed.

Considerable work has been done in the application of reversed phase chromatography using HDEHP on an inert base as the stationery phase, for separations of the individual rare earth elements.

4. ^{252}Californium Neutron Source

Further studies on the applicability of ^{252}Cf sources to neutron activation analysis include the evaluation of the ^{207m}Pb isotope ($T_{1/2}$= 0.8s) for the rapid screening of paint samples for lead content. This procedure presently requires repetitive irradiation and counting cycles for marginal results. However, with a considerably upgraded ^{252}Cf source, this analysis procedure may provide a very useful screening technique.

5. Nuclear Track Technique

Further investigations into the applicability of the nuclear track technique are in progress. Currently the elements which may be quantitatively determined using this technique include nitrogen, lithium, boron, uranium, and thorium. During the past year analyses by this technique included lithium and nitrogen in biological samples, boron in graphite, and uranium and boron in lunar samples.

6. Characterization of the NBSR

Since the initial startup of the NBSR in 1967, an extensive program of reactor characterization has been in progress. This program has been largely carried on through the efforts of the Activation Analysis Section, primarily because of the striving of our group for the highest possible precision and accuracy.

Many of the results shown here were published in part in the Activation Analysis Section's previous progress report, NBS Technical Notes 508 and 548, but have been recently updated or supplemented. Figure 1 shows the results of the flux dropoff for each of the five pneumatic tube facilities (rabbits). Three of the rabbits have linear flux dropoffs, with two non-linear. RT-4 shows the greatest dropoff, over 40% from end-to-end. Figure 2 shows the circumferential flux variation in each of the rabbit facilities. These results show very little side-to-side variation for RT-1 through RT-3, with a slight variation (< 4%) for RT-4. However, RT-T, the thermal column rabbit, has side-to-side variation approaching 20%. Some preliminary results for the integral fast neutron spectra for RT-1 through RT-4 are shown in Fig. 3. These results, made using threshold foils, seem to indicate a curve shape very similar to that of a pure fission spectrum. Further studies are in progress to elucidate the spectral shapes at neutron energies < 2MeV. The flux distribution of the vertical thimble G-2 is shown in Fig. 4 with copper-cadmium ratios [Cu(Cd)] shown for several locations. The circumferential flux distribution in G-2, while not shown was found to be less than ± 3% outside of the core area (including core gap area), but up to ±20% within the core area.

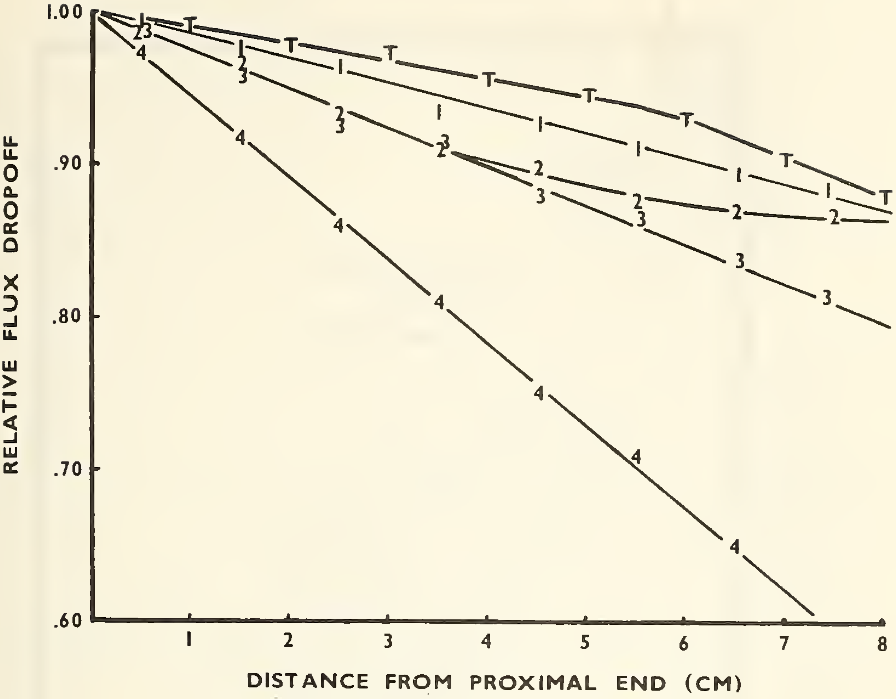

Fig. 1. Axial neutron flux drop off

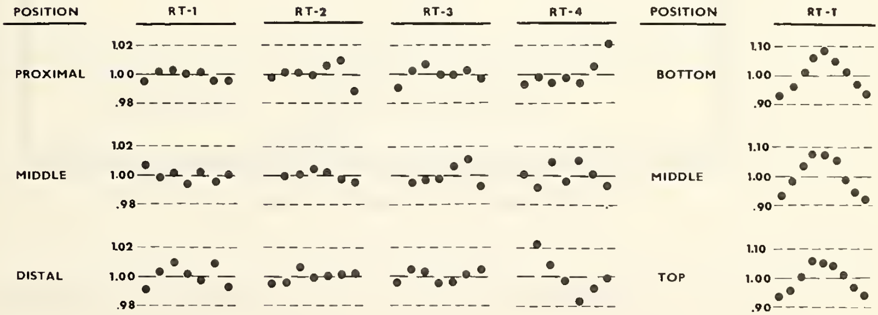

Fig. 2. Relative circumferential flux distribution for NBSR pneumatic tubes.

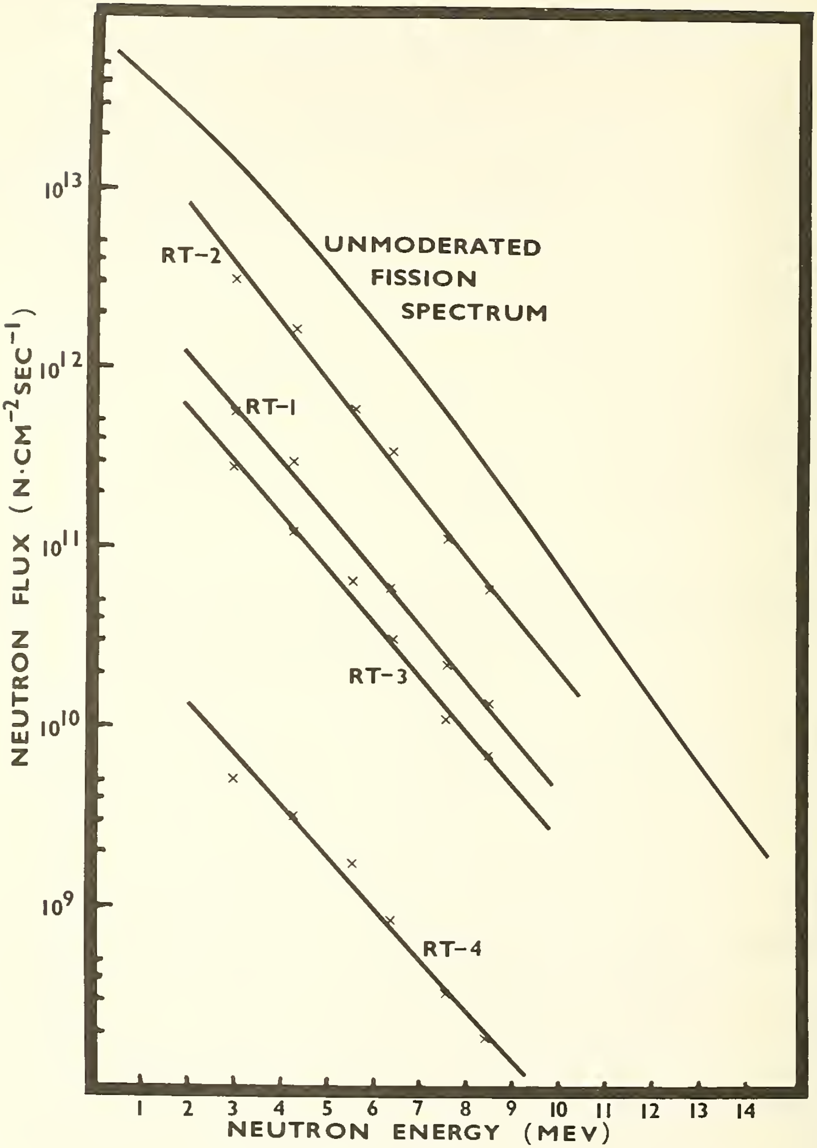

Fig. 3. Integral fast neutron flux data as determined by preliminary threshold foil measurements in the NBSR pneumatic tubes, compared to an unmoderated ^{235}U fission spectrum.

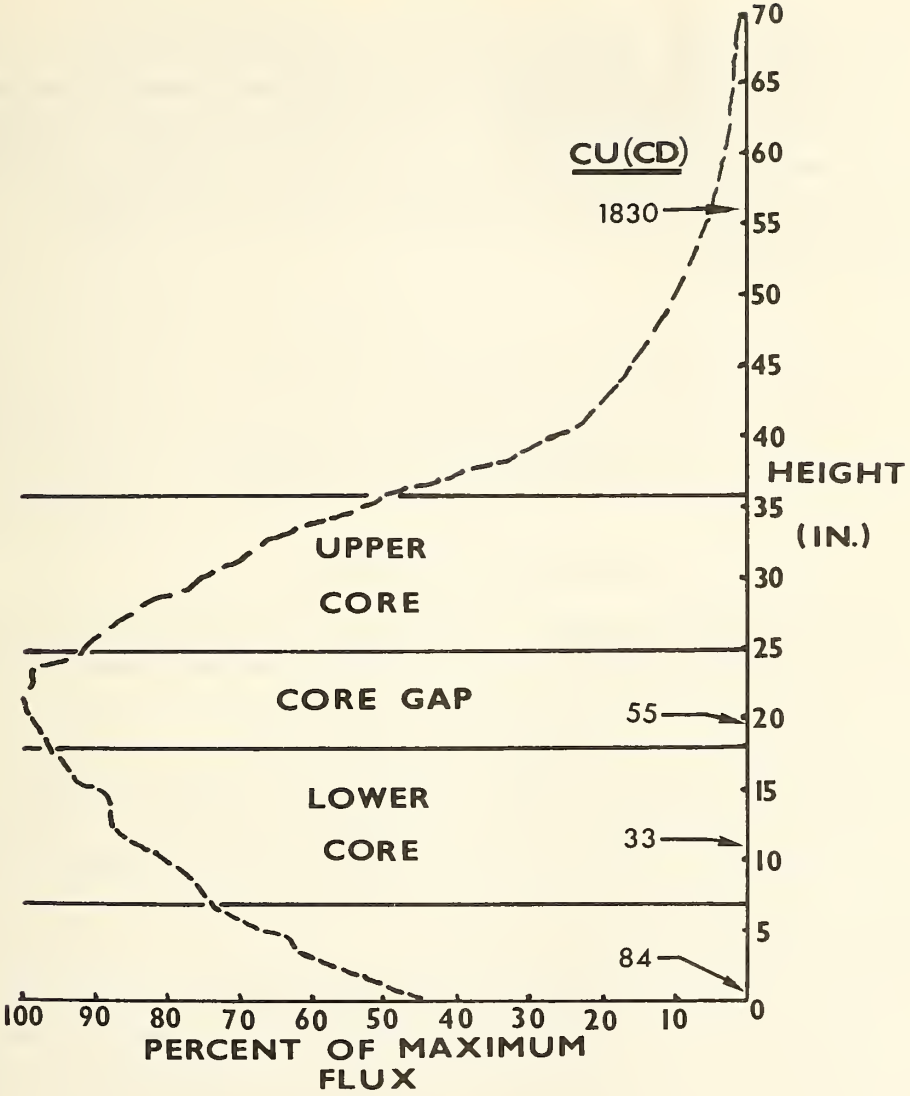

Fig. 4. Neutron flux distribution in vertical thimble G-2.

7. Conclusion

The Activation Analysis Section of the Analytical Chemistry Division has been involved with the analysis of a wide variety of sample types for a large number of different elements. Work is continuing in most of these areas, as well as on a number of fundamental studies in the field of activation analysis.

THE CAVITY FISSION NEUTRON SOURCE

A. Fabry
(CEN-SCK Laboratory, Mol, Belgium)

and

J. A. Grundl
(Nuclear Radiation Division)

Extensive neutron transport computations of wall-return flux intensity and spectrum have been carried out by a visiting staff member from the CEN-SCK Laboratory at Mol, Belgium. These computations, part of a joint effort to establish intense fluxes of pure fission neutrons, make it possible now to estimate reliably the wall-return background at the cavity Fission Neutron Source Facility. A paper presenting the results of these computations will be presented in November at the Washington Meeting of the American Nuclear Society. The following is an excerpt from the published summary of this paper:

> "Wall-Return Neutron Fluxes for High- and Intermediate-Energy Cavity Neutron Sources." A. Fabry (CEN-SCK), D. J. Jenkins (ORNL).
>
> Spherical cavities in graphite thermal columns of nuclear reactors provide an ideal environment for the production of comparatively intense, energy distributed neutron fields, i.e., either intended pure fission neutron spectrum sources or intermediate-energy standard neutron spectra. Cavities of 50 cm diameter are used in various laboratories; a 30 cm diameter cavity is operated at NBS and a 1 meter diameter cavity has recently been implemented at CEN-SCK.

Numerical computations of graphite wall-return neutron spectra have been performed by means of the discrete ordinates multigroup method in one-dimensional spherical geometry. The evaluated nuclear data files KEDAK, ENDF/B version 2, and ENDF/B version 3 have been used and the convergence of the S_n multigroup multitable treatment has been established systematically.

Within the cavity, a good approximation of the wall-return is

$$\phi_W(r,\mu, E;r_s) = \phi_W(E).$$

This relationship is correct to better than 2% for $r, r_s \leq R/2$ where R is the cavity radius and r_s the radius of a thin, fission spectrum source shell. This fundamental property has led to the development of an experimental method for determing wall-return backgrounds. A comparison of such experiments with theory will be discussed.

MEASUREMENTS WITH THE NBS DOUBLE FISSION CHAMBERS

J. A. Grundl
(Nuclear Radiation Division)

A number of fission rate measurements with the NBS double fission chamber have been performed for both the NBS Neutron Standards Program and for the AEC's Interlaboratory LMFBR Reactor Rate Program (ILRR). Fission rate determinations with the chambers in the thermal beam at the NBSR thermal column have been an essential support for all of these efforts. The activities at the thermal column may be briefly summarized: (1) performance maximization and check-out of two chambers, one for absolute fission rate measurements for the ILRR Program at the CFRMF reactor in Idaho, and the second for intercomparison measurements in the ΣΣ Standard Neutron Facility at the CEN-SCK Laboratory (Mol, Belgium); (2) thermal neutron weighing of ^{239}Pu, ^{235}U, and normal-U fission foils; (3) intercomparison of the NBS double fission chamber with fission track detectors developed at the Argonne National Laboratory.

EXTREME-ANGLE EMISSION OF LONG-RANGE ALPHA PARTICLES IN THE THERMAL NEUTRON FISSION OF ^{235}U

I. G. Schroder
(Nuclear Radiation Division)

An experiment has been performed in order to seek a correlation between the kinetic energy of long-range alpha particles emitted at extreme angles ($0° \leq 0 \leq 30°$, $180° \leq 0 \leq 150°$) with respect to the line of emission of the light fission fragments and the kinetic energy of the fisson fragments. An annular surface barrier detector (alpha detector) subtended an angle of ±30° at the target (^{235}U) with respect to a fission fragment detector placed behind the annular detector. An annular aluminum foil was introduced between the alpha detector and the source. This let through alpha particles $\gtrsim$ 6 MeV but stopped all fission fragments. A coincidence circuit (15ns resolving time) demanded coincidence between the two detectors. The output from these was displayed on a 2-dimensional PHA. The results obtained show that extreme-angle alpha particles have higher than average kinetic energies (>20 MeV) and rate of emission. Furthermore, these alpha particles are associated with fission fragments in the region of minimum kinetic energy between the light and heavy fission fragments.

A SEARCH FOR DOUBLY RADIATIVE N-P CAPTURE

R. G. Arnold and B. T. Chertok
(American University, Washington, D.C.)

and

I. G. Schroder
(Nuclear Radiation Division)

and

J. L. Alberi
(Harvard University, Cambridge, Mass.)

It has been suggested[1] that the long-standing discrepancy of 24 mb between the measured and the calculated thermal np capture cross sections might be ascribed to captures leading to emission of two photons. An experiment has been performed. Gated prompt- and delayed-coincidence γ spectra were obtained with two 2" x 2" NaI(Tℓ) detectors using a H_2O target and a D_2O target for background exposed to a beam of thermal neutrons from the NBS reactor. The result is that no two photon captures are observed at the 1 mb level, so the long-standing discrepancy still remains. Analysis of data is in progress to reduce this upper limit in order to test for the presence of an orthogonality breaking $^3S \rightarrow {}^3S + \gamma$ transition. A calculation[2] predicts an upper limit of 42μb for $^3S \rightarrow {}^3S + 2\gamma$.

---

[1] R. J. Adler, B. T. Chertok, and H. C. Miller, *Phys. Rev. C2*, 69 (1970).

[2] R. J. Adler (in press).

PARITY VIOLATION IN NEUTRON-CAPTURE γ-RAYS

J. L. Alberi and Richard Wilson
(Harvard University, Cambridge, Mass.)

and

I. G. Schroder
(Nuclear Radiation Division)

The program to study parity violation due to the weak interaction in the overall nucleon-nucleon interaction (weak forces between nucleons) is continuing in collaboration with Harvard University. The results obtained with the reaction ^{113}Cd (n,γ) ^{114}Cd have been reported.[1]

We have measured the circular polarization of γ rays from thermal neutron capture in ^{113}Cd and find a $P_\gamma = (6.0 \pm 1.5) \times 10^{-4}$ for the combined 8.51- and 9.04-MeV transitions. This value was measured using a transmission Compton polarimeter and pulse-counting technique. The value confirms the existence of parity-nonconserving terms in the inter-nucleon force. A search is being conducted for other nuclei which have neutron capture states which are no longer eigenstates of parity and, therefore, exhibit small parity impurities similar to those in cadmium.

---

[1] *Phys. Rev. Letters* 29, 518 (1972).

IN-CORE FAST-NEUTRON MEASUREMENTS USING A ^{3}HE SEMICONDUCTOR SPECTROMETER

J. C. Glynn
(U.S.A.E.C., Washington, D. C.)

and

F. J. Munno
(University of Maryland, College Park, Md.)

and

I. G. Schroder
(Nuclear Radiation Division)

The need to accurately determine reactor spectra (>0.5 MeV) has become increasingly important with the advent of fast breeder reactors. This need is particularly true in the study of fast fluence effects on structural materials and, in the calculation of spectral-dependent parameters (Doppler coefficients). However, the inability of fast-neutron spectrometers to operate in reactor environments (sensitivity to high gamma fields) has made an accurate in-core determination of reactor spectra unfeasible. To circumvent this problem a collimating system was designed and built to scatter neutrons from the core of the NBS reactor and extract a neutron beam which, in turn, could be related to the in-core spectrum.

A ^{3}He semiconductor fast-neutron spectrometer was chosen to study the emergent spectrum because of its high resolution, fast response, and well-controlled geometry. The incident beam was parallel to the surface of two semiconductor detectors and collimated such as not to strike either. This minimized gamma sensitivity and fast-neutron damage. The sensitive volume between the two detectors could only "see" a scatterer placed at the bottom of the collimating assembly and adjacent to a fuel element. Three different scatterers - carbon, aluminum, and lead - were chosen to maximize the effect of the differential scattering cross section on the experimental data. Figure 1 shows the data obtained for the carbon and lead scatterers after corrections for background, detector efficiency, and resolution.

Calculations were made to determine both the scalar and vector fluxes. By performing a series expansion of the vector flux, the expansion coefficients can be calculated, in principle, from the data obtained from each

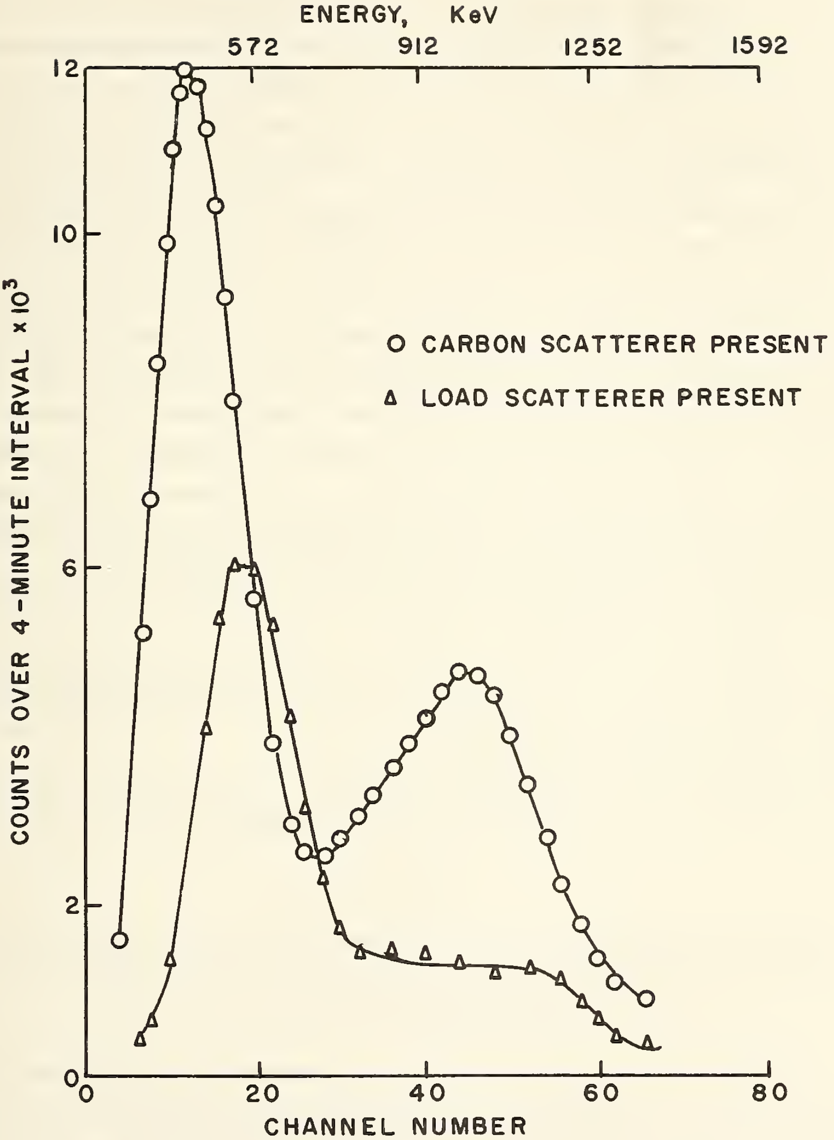

Fig. 1. Spectrometer response.

scatterer. However, the errors in the known differential cross sections and the experimental uncertainties masked the small differences obtained in the data. To obtain the scalar flux, the assumption was made that anisotropies in the flux were the same at all energies.[1,2] With the additional assumption that a negligible ΔE occurs for a neutron in an elastic collision with lead, an average angle of scatter was estimated based on the difference between the low energy peaks in Fig. 1. The data for carbon were then corrected for the neutron energy loss during scattering and the scalar flux calculated directly, as carbon is a highly isotropic scatterer. These results indicate that an in-core flux can be measured to an accuracy of 25%. To reduce this uncertainty, further knowledge of both scattering cross sections and collimator characteristics is needed. As a by-product of this study, an intense external reactor beam has been obtained which can be of great value to study fast-neutron spectrometers and can provide a facility where experimentalists can intercompare different instruments.

---

[1] R. J. Cerbone and K. D. Lathrop, "Sn Calculation of Highly Forward Peaked Neutron Angular Fluxes Using Asymmetrical Quadrature Sets," *Nucl. Sci. Eng.*, 35, 139 (1969).

[2] D. R. Metcalf and P. F. Zweifel, "Solution of the Two-Group Neutron Transport Equation - I, II," *Nucl. Sci. Eng.*, 33, 307 and 318 (1968).

PRECISION MEASUREMENT OF THE COMPTON WAVELENGTH OF THE ELECTRON

W. C. Sauder, E. G. Kessler and R. D. Deslattes
(Quantum Metrology Division)

The purpose of this experiment is to determine the Compton wavelength by means of precision crystal diffraction spectroscopy of the radiation emitted in two-photon annihilation of positronium. This will yield a non-quantum electrodynamic determination of the fine structure constant at the one ppm level.

Activity in the past year has consisted principally of assembling the apparatus in the Reactor Building. A two-axis, Laue case transmission crystal diffraction spectrometer, perhaps the most critical element in the experiment, is now in place in the experimental area. This instrument which was designed and fabricated at NBS is capable of Bragg angle sensitivities of better than 10^{-4} arc-sec. The spectrometer rests upon an air-supported table in a temperature-controlled chamber located in the NBS Reactor Building. This location for the experiment was chosen in order to make (relatively) straight-forward the transfer of the necessary 20 kilocurie ^{64}Cu source from the reactor vessel to the experimental area.

The installation of the spectrometer and its peripheral equipment (detector assembly, source positioning machinery, electronics, etc.) is nearly completed, so that in the near future a preliminary measurement of the 412 keV line from ^{198}Au can be undertaken. Other nuclear gamma lines also will be measured.

The source cryostat that will provide a 7 K annihilation environment for positronium formed subsequent to the $\beta+$ decay of the high intensity copper source has been designed and presently is under construction. The coming year should see the first of the annihilation data forthcoming from the experiment.

^{60}Co GAMMA RAY ANISOTROPY THERMOMETRY

H. Marshak, R. J. Soulen and D. B. Utton
(Heat Division)

Work is continuing on the comparison of a Josephson junction noise thermometer to a ^{60}Co γ-ray anisotropy thermometer. In order to measure the hyperfine splitting directly we are attempting a nuclear magnetic resonance-oriented nuclei experiment. A very thin (3 mil) ^{59}Co single crystal disk shaped sample was irradiated in the NBS reactor to produce the ^{60}Co activity. Results of our first measurement were negative and indicated that our sample was too thick. The experiment will be repeated with a thinner sample.

STUDIES OF GASSEOUS FISSION PRODUCTS

F. J. Schima and L. D. Miller
(Nuclear Radiation Division)

Early in 1972, the direction of the ARPA-supported program was reoriented along the lines of specific radioisotope standardization. Several aspects of this prior reactor related research have been successfully concluded and these were:

1. ^{81}Kr Decay Studies

A foil source of ^{81}Kr was prepared by means of the isotope separator from the gas sample. This foil source has an activity level of about 100 dps. The K x-ray intensity was measured by comparison with standard sources of ^{57}Co and ^{75}Se using the Si(Li) detector. The measured ratio of the intensity of the 276 keV gamma to the K x-ray intensity was found to be 6.8 ± .8% which implies a branching ratio of about 3.7%. The gamma transition energy was measured as 275.99 ± .01 keV. This is in excellent agreement with recent energy measurements for the first excited state in ^{81}Br.

2. ^{129m}Xe Decay Studies

Considerable data have been obtained on the gamma decay of the ^{129m}Xe. The half-life has been measured as

$$T_{\frac{1}{2}} = 8.92 \pm .03 \text{ days}$$

over a period of 4.2 half-lives. The two gamma transitions have been measured as

E(isomeric)	196.38 ± .11 keV
E(ground state)	39.50 ± .17 keV

E. SUMMARY OF REACTOR OPERATIONS

During the period October 1, 1971 through September 30, 1972, approximately 5100 hours of reactor time was provided to users. This is equivalent to about 51,000 megawatt-hours of energy produced. Leaks in the main heat exchanger and operations with minimum staffing reduced reactor on-line time to 58% for this period which is the same as last year but below previous years. Excellent fuel burnup of about 45% was again achieved this year through utilization of heavier loaded elements. A summary of operating statistics together with those of previous years are presented in the following table:

NBSR Operating Summary

	Nov. 1969 to Nov. 1970	Oct. 1970 to Oct. 1971	Oct. 1971 to Oct. 1972
Reactor Operations to date, MWh	78,213	123,761	175,161
Reactor Operations for year, MWh	59,186	51,175	51,400
Hours Reactor Critical	6,000	5,440	5,200
Number of Days at 10 MW	247	213	214
On-line time at 10 MW	67%	58%	58%
Number of fuel elements used	44	24	26
Average U-235 Burnup	34%	48%	45%
Number of Refueling Operations	11	6	6
Number of Unscheduled Shutdowns	3	10	11
Number of Irradiations	1,500	3,000	4,000
Number of Visitors	4,000	4,000	3,400

Over a period of 15 months, 11 heat exchanger leaks developed, nine of which were during the last 10 months. These leaks resulted in a substantial loss of operating time and in a very costly degradation of the heavy water in the primary system. A chronological history of the leaks is presented in the following table.

Schedule of Reactor Shutdowns
Caused by Heat Exchanger Leaks

Date Leak Occurred	Length of Shutdown - Days	Repair Time - Days	Period of Operation Between Leaks - Days	No. of Tubes Leaking	No. of Tubes Plugged
6/3/71	46	36		1	33
			9		
7/28/71	8	8		1	3
			114		
11/28/71	5	5		2	2
			60		
1/27/72	4	4		1	1
			73		
4/13/72	7	5		1	1
			8		
4/28/72	60	7		0*	6
			3		
6/29/72	4	2		1	1
			9		
7/12/72	5	2		1	10
			52		
9/7/72	4	2		1	3
			7		
9/18/72	3	2		1	6
			6		
9/27/72	2	2		1	1

*Leak was so small that it could not be positively identified.

Nine of the 11 leaks involved only a single tube, one involved two tubes and on one occasion the leak was so small that the leaky tube could not be positively identified. To date 67 of 1285 tubes have been plugged. Of these, 11 have definitely been identified as leakers. The remainder were plugged because they were suspect or thought to be potential leakers based on eddy-current, helium, or freon testing or based on the pattern that the location of the identified leaks followed. Of the 11 leaky tubes that were found, seven were in the 14th row, two were in row 13, one in row 21, and one in row 35. There is a total of 60 rows of tubes. In all 21 of 46 tubes were plugged in row 14, seven of which were leakers, and six of 45 tubes were plugged in row 13, two of which were leakers. In all cases where the leaks were identified the leaky tube was easily found by ultrasonic testing.

Delivery of two new stainless steel heat exchangers (one to serve as a backup) is scheduled for April 1973. Installation is presently planned for the summer of 1973 in order to minimize the impact of the anticipated two-month shutdown on the experimental program since the reactor is operated on a curtailed schedule during the summer. The exact date will depend on the condition of the present all aluminum heat exchanger.

During the repair of the leak of April 28, 1972, light water was inadvertently introduced into the primary heavy water system resulting in degradation of the heavy water from its original purity of 99.5% to about 96 - 97%. Light water was being used to flush the heat exchanger, which had been previously drained and isolated, in order to remove traces of tritiated heavy water and permit access to the heat exchanger. The diaphragm on the main isolation valve of the heat exchanger did not seat properly permitting seepage of light water into the main heavy water storage tank through an open drain line. Power operation could not be sustained with the degraded water and the entire water content of the primary system had to be replaced by reactor grade heavy water. It took approximately 45 days to obtain the new heavy water resulting in a total reactor shutdown of almost two months including the time used for repair of the leak.

A portion of the lost time was recovered through early performance of required maintenance and surveillance tests thereby reducing scheduled future shutdowns. Also because the new heavy water had very low tritium activity, immediate access to the heat exchanger was possible. Leak repair time was reduced to only two days resulting in a gain of several days of operating time over that previously needed for the repair.

F. SERVICE PROGRAMS

Service and irradiation programs have again shown substantial increase over previous years. In all, approximately 4,000 irradiations involving 40,000 samples were performed this year. These irradiations covered a wide range of people-oriented projects, research and application programs and radioisotopes production. Highlights of these programs are presented in following sections.

THE USE OF NEUTRON ACTIVATION ANALYSIS IN SCIENTIFIC CRIME DETECTION

Forensic Staff
(U. S. Treasury Department, Washington, D. C.)

The primary mission of the Forensic Laboratory is the examination of physical evidence by scientific techniques. The evidence is related in a large number of cases to activities of ATF agents who enforce the 1968 Gun Control Act and the Organized Crime Act of 1970. The Forensic Laboratory also offers its services to State, Local and County agencies in cases of mutual interest. Because of the increased services the Forensic Laboratory has been called upon to provide, the Laboratory staff has more than doubled in the past two years. The number of irradiations at and use of the NBS reactor facilities has similarly significantly increased.

The ATF Forensic Laboratory is equipped with atomic absorption, UV, IR, x-ray diffraction and fluorescence, and an emission spectrograph which are used to examine evidence in destructive device investigations. Evidence connected with Arson/Firebomb cases are examined by gas-liquid chromatography.

The ATF Laboratory examines hundreds of cases each year by NAA at the NBS facility. The Laboratory is equipped with three 400 channel analyzers, a 4096 ADC computer coupled data acquisition system with a 50 cm^3 GeLi detector, and an off line computer system for the analysis of gunshot residue data. A dual 4096 ADC Computer system will be acquired shortly.

In the past 12 months, the ATF Forensic Laboratory has examined 600 bomb/incendiary cases and analyzed 12,000 gunshot residue samples representing some 1500 cases. Neutron activation analysis was also used in several hundred cases to examine a wide variety of evidentiary material including drugs, hair, paint, soil and illicitly distilled spirits.

Court testimony has been given by Forensic Laboratory experts in robbery, rape, homicide, and income tax fraud cases.

Plans are being made to move a part of the Forensic Laboratory NAA activities to the NBS reactor site in order to more fully utilize the facility by measuring short lived radionuclides.

THE USE OF ACTIVATION ANALYSIS IN SCIENTIFIC CRIME DETECTION BY THE FEDERAL BUREAU OF INVESTIGATION

Neutron Activation Analysis Unit
(Federal Bureau of Investigation, Washington, D.C.)

The FBI Laboratory uses neutron activation analysis (NAA) extensively as a means of elemental analysis of metals, biological materials and gunshot residue lifting mechanisms.

The capability of analyzing a specimen nondestructively is very important. Often the small metal fragments found on a tool or on a suspect's person are introduced as evidence at a trial. If a destructive method of analysis was employed this is not possible and must be explained to the court if necessary.

The sensitivity for many elements makes NAA ideal for analyzing the minute metal fragments so often associated with cutting tools or pry bars used in burglaries. For instance, a fragment of copper-colored metal weighing 80 micrograms was removed from the jaws of a wire cutter. The wire cutter was confiscated from a man accused of selling stolen wire to a junk dealer. The metal fragment was significantly different in composition from the stolen wire submitted to the Laboratory. By neutron activation analysis it was possible to quantify selenium, gold, silver and antimony in the copper fragment nondestructively.

The FBI Laboratory uses NAA in situations where classical chemical methods of analysis are available but are time consuming and cumbersome. For instance, the detection and quantifying of platinum and rhenium in an aluminum matrix was accomplished easily and quickly by NAA.

The FBI Laboratory has purchased a low energy photon detector. Work will be conducted on the detection and quantifying of some of the rare earths and other elements such as mercury which have isotopes which decay with photon emissions less than 300 keV.

U. S. POSTAL SERVICE ACTIVATION ANALYSIS PROGRAM

G. R. Stangohr, J. Upton, and M. Beckman
(U. S. Postal Service, Washington, D. C.)

During the past year, the U. S. Postal Service Crime Laboratory in Washington, D. C., has continued to use the nuclear reactor facility at NBS for forensic neutron activation analysis. Items of evidence which were irradiated at NBS included glass, hair, rope, paint, safe insultation, and paper. Much of this evidence was derived from cases involving kidnapings, armed hold-ups, burglaries, mail bombs, and frauds.

One important case involving two separate kidnapings was successfully resolved by using NAA to associate the rope used to tie each of the kidnaped victims with the rope recovered from the suspect's home. In another case, utilization of NAA assisted in providing evidence to smash a burglary ring by matching paint particles found in a suitcase used to carry burglary tools with paint from damaged safes from burglarized post offices covering a wide geographic area.

ACTIVATION ANALYSIS PROGRAM OF THE FOOD AND DRUG ADMINISTRATION AT THE NBSR

J. T. Tanner and M. H. Friedman
(Food and Drug Administration, Washington, D.C.)

1. Mercury in Foods

A continuing program at FDA has been the analysis of mercury in foods. Recently part of this study was published[1] which deals with foods commonly eaten. The current part of this study involves a more complex sampling of foods. In this case 77 different foods were collected and divided into 12 different categories. Of these, 9 categories were analyzed for mercury: dairy products; fish, meat, and poultry; cereals and grains; potatoes; leafy vegetables; legume vegetables; root vegetables; garden fruits; and fruits. These foods were collected throughout the country and should approximate the average mercury intake by the USA consumer. These food samples were analyzed by neutron activation analysis (NAA) at the National Bureau of Standards research reactor at Washington, D.C., USA. Because the mercury content of these samples was quite low, a chemical separation had to be used to enhance the 279 keV γ-ray of ^{203}Hg with respect to the background. The procedure consisted of anion-exchange chromatography and sulfide precipitation previously described.[1] No samples in this study were found to contain more than 50 ppb Hg; in fact, most of the samples contained substantially less than 20 ppb Hg. Thus, most foods consumed in the USA today appear to be relatively free from mercury.

2. Instrumental Neutron Activation Analysis of Bromine in Pig Tissue

Another continuing program of FDA is the analysis of bromine as an indicator of brominated vegetable oil (BVO) in pig tissue and organs. Brominated vegetable oils are edible oils in which some or all of the double bonds are saturated by bromine. They are used in the manufacture of soft drinks to increase the specific gravity of the essential oil components so that they remain in suspension which prevents the formation of rings of essential oil at the intersection of the surface of the liquid and the bottle.

Recent studies in Canada have shown that prolonged use of high doses of brominated vegetable oil causes physiological damage. The use of brominated vegetable oil as a food additive has therefore been suspended until studies are completed to determine what would be a safe limit.

The purpose of this study is to determine what amount of brominated vegetable oil can be used safely as a food additive. To answer this question pigs were fed brominated vegetable oil, the amount of bromine present in different tissues was measured and correlated with observed physiological changes. The physiological changes and the correlation with the measured amount of bromine will be reported elsewhere.

Neutron activation has a number of advantages as a method of quantitatively analyzing the samples for bromine. The analysis is done completely instrumentally; no reagents are used and so this method of analysis is completely free from reagent contamination. To the extent that the sample does not appreciably attenuate the neutron flux or the gamma rays leaving the sample the method is free of matrix effects. For all biological materials and most other non-biological matrices these conditions are easily satisfied.

3. Rapid Instrumental Analysis for Mercury in Biological Materials by Neutron Activation

Most measurements of mercury in biological materials by neutron activation analysis (NAA) rely on the 279 keV peak of ^{203}Hg ($t_{1/2}$ = 46.6 days) rather than on the x-rays that are produced when ^{197}Hg($t_{1/2}$ = 64.1 hours) captures an orbital electron, thus decaying to ^{197}Au. After irradiation, however, the intensity of the K x-rays from the decay of ^{197}Hg is much higher than that of the 279 keV ^{203}Hg gamma ray and offers the possibility of a more sensitive instrumental analysis. Measurements of the ^{197}Au $K_{\alpha 2}$, $K_{\alpha 1}$, $K'_{\beta 1}$, $K'_{\beta 2}$ x-rays (the respective energies are 66.99, 68.81, 77.9 and 80.1 keV) with the usual large volume Ge(Li) detector or

NaI(Tl) crystal are hampered by a large Compton continuum in this region and by inadequate resolution. The Compton background can be lowered with a thin (5 mm) Ge(Li) detector which reduces the amount of material the gamma radiation can interact with while the low-energy x rays, because of their high photoelectric cross section, are detected with comparatively high probability. The net effect is that with a thin Ge(Li) detector one obtains an increase in the peak-to-background ratio in the x ray region where a more sensitive instrumental analysis based on ^{197}Hg is possible.

This technique was used for a toxicological study undertaken to map the distribution of mercury in the central nervous system of dogs fed with MeHgCl. Three dogs were fed daily doses of 2.0-mg MeHgCl/(kg day) for 15 days, at which point they became moribund; a fourth dog, given 10 doses of 2.0-mg MeHgCl/(kg day), became moribund 26 days after the dosage was discontinued. After the animals were sacrificed, their brains were profused, the tissues dried, sealed in quartz vials, and irradiated for 1 h in a flux of 6×10^{13} n/(cm^2 sec). Counting was done 3 days after irradiation, with a sensitivity of 0.1 ppm. No effort was made to achieve a more sensitive measurement since a sensitivity of 0.1 ppm was more than adequate for the purpose of this work.

From these results we learn what mercury levels to expect in different parts of the central nervous system, at the point of death, due to methyl mercury poisoning. The concentration of mercury found in the central nervous system of the moribund dogs ranged from 2 ppm in the lumbar spinal cord to 57 ppm in the prefrontal cortex. Thus, mercury was not found to be uniformly distributed in the central nervous system. Even though the mercury concentration was high, the smallness of the sample, sensitivity, ease of analysis, and specificity make neutron activation the method of choice for these analyses.

4. MTELMT: A Computer Language for the Reduction of Neutron Activation Analysis Data

A computer reduction program is a fixed set of instructions for doing some computation. However, because of the many variables inherent in both acquiring and reducing neutron activation analysis data a single set of instructions is not applicable to reducing all data sets. Typically then, changes must be made in the program to get the required data reduction sequence or alternately the program is set up to do part of the calculation but the final results are calculated manually. Neither approach is entirely satisfactory: 1) changing a program written in FORTRAN or ALGOL can involve so many details that it can only be done convieniently by the person who wrote the program and even then it may take a long time and 2) doing even part of a calculation manually can be quite time-consuming if there are many samples to analyze. The MTELMT language (mnemonic for multiple element) was developed to give the user a convienient way of communicating to the computer how to reduce any set of neutron activation analysis data.

The language consists of a set of commands. A CDFRMT (card format)[2] command specifies the format of data to be read from IBM cards. Once the card format has been specified, a spectrum consisting of any number of channels (up to 4096) can be read in with the command CDDATA (card data). A spectrum on tape can be read in with the command TPDATA if it is the next spectrum on the tape or with the command SRCHTP if one must search the tape for the proper spectrum. To skip over file marks on the tape, the command FLSKIP (file skip) is used and the magnetic tape is rewound with the command REWIND. To make a linear or semi-logarithmic CAL COMP plot of any spectrum with up to 4096 channels the command GRAPH1 is used. Options of the various commands are controlled by the command KNTROL. The location of peaks and input parameters for drawing the background line are input through the command INTPRM (integration parameters). Pertinent information which must be specified for each sample and standard (weight, etc.) are input with the commands SAMPLE and STNDRD. The computation of the ppm or micrograms or upper limit of the element specified by the STNDRD command is initiated by the command ANLYZM (analyze in manual mode).

The feature which makes this program so powerful is that it defines a language and the words of the language can be put together in many different ways to accomplish different tasks. Between the CDDATA, TPDATA and SRCHTP commands data can be read in from cards and tape in any sequence that is desired. Because of the CDFRMT command the program can accomodate spectra on cards in any format. The result is an extremely flexible, yet simple to use, input/output capability. With the use of the REWIND command, for data which is on the magnetic tape, in a single computer run one can analyze the data again in a different way. Between the STNDRD and the INTPRM command the pertinent information for any element can be readily input to the computer. Thus, this program can analyze for any element for which the x ray or gamma ray peaks are resolved.

The MTELMT language is on the drum of the UNIVAC 1108 computer at NBS.

---

[1] *Science* 177, 1102 (September 22, 1972).

[2] The mnemonic appears in parenthesis following the command.

DEVELOPMENT OF ANALYTICAL METHODS AND DETERMINATION OF CONSTITUENTS OF GEOLOGICAL SAMPLES

J. J. Rowe
(U.S. Geological Survey, Washington, D. C.)

The U. S. Geological Survey has been utilizing the reactor facilities of the National Bureau of Standards for the development and application of neutron activation analysis and isotope dilution techniques for the determination of trace constituents in geological materials.

The reactor has been used for the preparation of ^{76}As for use in the isotopic dilution determination of arsenic in soils as part of a study of environmental pollution. The method has been applied to the analysis of more than 5,000 samples of soils and rocks from various areas.

Instrumental neutron activation analysis has been applied to the determination of tantalum and hafnium in lunar rocks and soils. Various terrestrial materials have been analyzed for thorium, chromium, scandium, hafnium, tantalum, caesium, rubidium, antimony, lanthanum and the rare earths for geochemical studies.

Activation analysis with post-irradiation radiochemistry has been applied to the determination of gold in many rocks and minerals; selenium in sulfide minerals and tungsten in rocks and minerals.

Trace concentrations of platinum and palladium in rocks have been determined using a fire assay preconcentration and post-irradiation radiochemistry. A method has been developed for the determination of ruthenium and is being applied to the analysis of chromites and rocks. The collection of ruthenium on a plastic film before irradiation overcomes fission product interferences and permits the instrumental determination for samples containing as little as 10 ppb of ruthenium.

Epithermal irradiations have been used for the determination of gold in native silver and copper. It is planned to extend the application of epithermal irradiations to the determination of rare earths in phosphate rocks.

COMPARISON AND PREPARATION OF ^{18}FLUORINE AND ^{99m}TECHNETIUM-TIN-PHOSPHATE RADIOPHARMACEUTICALS

Major George Dunson
(Armed Forces Radiobiology Research Institute, Bethesda, Md.)

Fazle Hosain
(Johns Hopkins Medical Institutions, Baltimore, Md.)

John Harbert
(Georgetown University Hospital, Washington, D.C.)

and

Ira Godwin
(Northern Virginia Pathology Laboratories, Fairfax, Va.)

During 1970 and 1971 ^{18}F produced in the NBS reactor was used for bone lesion imaging in patients in the Bethesda Naval Hospital, Fairfax Hospital, Georgetown University Hospital, Johns Hopkins University

Hospital, Northern Virginia Pathology Laboratories, Walter Reed General Hospital, Washington Hospital Center and Washington Veterans Administration Hospital. The methods of producing the radiochemical and preparing it as a radiopharmaceutical were published in the NBS Technical Note 714, March, 1972.[1,2]

In 1971 Dr. Subrumanian of the Upstate Medical Center, Syracuse, N. Y. published articles on the use of ^{99m}Tc polyphosphate as a bone lesion imaging radiopharmaceutical.[3,4] This innovation created a need for a study to compare ^{99m}Tc polyphosphate with ^{18}F and other bone imaging radio-pharmaceuticals and to develop a method of compounding ^{99m}Tc polyphosphate that could be used by technicians in the various nuclear medicine clinics to prepare the radiopharmaceutical as needed. The study was carried out in two phases during 1971 and 1972 in approximately 300 patients in the medical facilities listed above.

Initially comparisons were made of ^{18}F, ^{67}Ga, ^{85}Sr, ^{87m}Sr and ^{99m}Tc polyphosphate and reported at the March, 1972, meeting of the Mid-Eastern Society of Nuclear Medicine.[5,6] This report indicated that both ^{18}F and ^{99m}Tc polyphosphate were superior to the other bone lesion imaging radiopharmaceuticals and that each had advantages and disadvantages. It was also reported that the published materials and methods for compounding ^{99m}Tc polyphosphate gave intermittently successful and unsuccessful results and required individual preparation by an experienced radiopharmacist.

^{18}F advantages were that physicians were sufficiently experienced with the radiopharmaceutical to easily interpret the nuclear images, technicians were familiar with dosing and instrumentation techniques and the radiopharmaceutical was always of high quality. ^{18}F disadvantages were due to its nuclear properties. It is made by nuclear bombardment of a stable parent and decays with a 2 hour half-life. Therefore, it must be prepared for patients on a scheduled basis, quickly processed and transported to using institutions. ^{18}F is a positron emitter which gives off 511 keV gamma rays upon annihilation. This energy is poorly collimated and suitable only for rectilinear imaging.

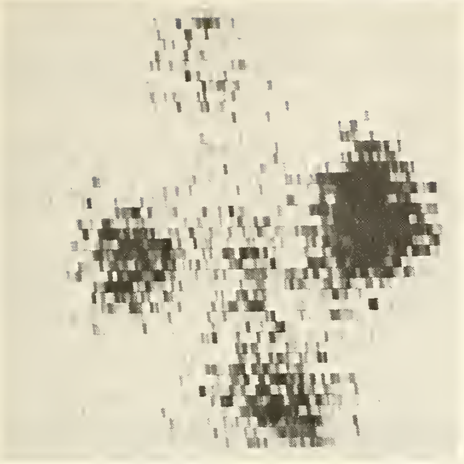

Fig. 1A. ^{18}F rectilinear image

Fig. 1B. ^{99m}Tc-tin-phosphate rectilinear image

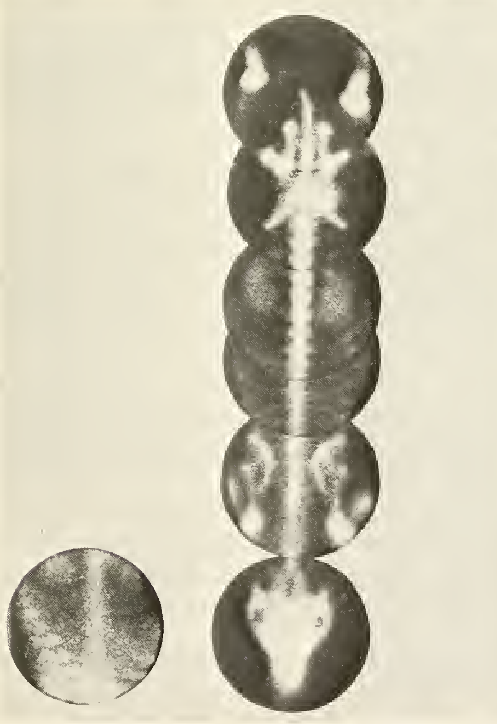

Fig. 2. ^{99m}Tc-tin-phosphate gamma camera composite image

^{99m}Tc polyphosphate advantages were due to the nuclear properties of its ^{99m}Tc component. ^{99m}Tc is a decay product of 2.7 day half-life ^{99}molybdenum. It is easily obtained as a sterile, pyrogen free, eluate of a commercial generator system that is stocked by most nuclear medicine clinics. ^{99m}Tc decays with a 6 hour half-life and gives off 140 keV gamma rays. This energy is ideally suited for both rectilinear and gamma camera imaging. Comparison of ^{18}F and ^{99m}Tc polyphosphate rectilinear images of the pelvic area are shown in Fig. 1A and 1B. Both images demonstrate sacroiliac abnormalities and urinary bladder accumulation. ^{99m}Tc polyphosphate disadvantages were due to the chemical nature of Tc and the Tc polyphosphate complex and lack of experience with ^{99m}Tc and a bone lesion imaging agent.

In the second phase of the study ^{18}F was used as a standard for patient imaging and interpretation while physicians and technicians developed interpretation, dosing and instrumentation techniques using a ^{99m}Tc-tin-phosphate kit radiopharmaceutical developed by the group radiopharmacist. This kit eliminated the chemical disadvantages of ^{99m}Tc polyphosphate because it gives a high quality successful radiopharmaceutical every time, can be stored indefinitely and can be prepared by technicians within 5 minutes when needed. Fig. 2 shows typical gamma camera images of a pig dosed with ^{99m}Tc-tin-phosphate using a kit prepared at the Armed Forces Radiobiology Research Institute (AFRRI). Patient images are of equal quality. This study led to the gradual disuse of ^{18}F by participating medical institutions as physicians and technicians gained experience in ^{99m}Tc bone imaging.

---

[1] G. Dunson, I. Godwin, J. Harbert et al, "Fluorine-18 radiopharmaceutical for Bond Lesion Localization, *NBS Tech. Bulletin 714:*70-74 (1972).

[2] G. Dunson, W. Crofford and J. Ring, :Fluorine-18 Production in the NBS Reactor, *NBS Tech. Bulletin 714:* 75 (1972).

[3] G. Subrumanian and J. G. McAfee, "A New Complex of Tc-99m for skeletal Imaging," *Radiology 99:* 192 (1971).

[4] G. Subrumanian et al, "Tc-99m Polyphosphate PP46: A New Radiopharmaceutical for Skeletal Imaging," *J. Nucl. Med. 12:* 399 (1971).

[5] G. Dunson, J. Harbert and F. Curl, "Comparison of Bone Lesion Visualization Using Tc Polyphosphate, Ga-67 Citrate and Sr-85 Nitrate, Mid-Eastern," *Soc. of Nucl. Med*, March 1972.

[6] F. Hosain, P. Dugal, G. Dunson et al, "Pediatric Bone Scanning and Relative Merits of Fluorine-18, Sr-87m Citrate and Tc-99m Polyphosphate," *Mid-Eastern Soc. of Nucl. Med.,* March, 1972.

USE OF NEUTRON ACTIVATION ANALYSIS IN THE STUDY OF COPPER IN WOUND HEALING AND HEPATIC DISEASES

G. C. Battistone
(U.S. Army Inst. of Dental Research, Washington, D.C.)

Studies on the role of copper in wound healing have continued during the past year. Although some success has been achieved in accelerating bone healing with certain copper chelates, the overall effect of the copper chelates used has been toxic in the experimental animals used. Thus far no totally acceptable copper chelate complex has been found. When non-toxic dose levels of the copper complexes were used, no observable effect was seen on the healing process.

In collaboration with the Hepatic Disease Research Branch of the Armed Forces Institute of Pathology, a study was begun during the past year to determine copper levels in various hepatic diseases in order to obtain a better understanding of the role of copper in these diseases. Data are being collected as biopsy and autopsy material becomes available. It is hoped from an accumulation of such data that copper determinations will provide greater diagnostic as well as etiological information.

TRACE ELEMENTS IN THE ENVIRONMENT AND DECAY SCHEME STUDIES

W. H. Zoller, G. E. Gordon and W. B. Walters
(University of Maryland, College Park, Md.)

During the past year our work has centered on the analysis of trace elements on atmospheric particulate material and pollution-source materials. We have used the facilities of the NBS reactor to irradiate a large number of samples followed by γ-ray spectroscopy using Ge(Li) detectors. Atmospheric particulate material from Boston, Massachusetts, Friendship Airport (near Baltimore, Maryland), College Park, Maryland and the general Washington, D.C. area have been analyzed. These studies are related to the atmospheric chemistry program at the University of Maryland. The samples were collected on filters such as Millipore, Nucleopore, Whatman and Delbag which can be pressed into pellets prior to irradiation using a Nickel-Nylon die system to eliminate contamination of the samples. Other samples were collected by cascade impactors which separate the particles into size fractions on polyethylene. The polyethylene with the collected material can then be irradiated directly and counted.

The analysis of a set of air samples collected in Antarctica during the last two years has nearly been completed. The results of these experiments have shown that the concentration of trace elements in this very clean location is nearly a factor of 10,000 less than in the rural United States. This project will continue, as more samples will be collected this year. Mr. John Ondov of the University of Maryland will go to the South Pole station to set up equipment and bring back samples which have been collected there during the past winter.

Our analyses of hydrocarbon fuels by INAA has yielded results on fractions down to the boiling point of iso-octane. These lighter fractions are sealed in quartz under vacuum prior to irradiation. We find these lighter fractions to be much lower in trace elements than heavier fractions as the distillation process leaves them behind.

Most impurities are from additives put into the fuels by the producers. Nearly twenty automobile lubricating oils have also been analyzed under this project as we need to know their compositions for our studies on automobile emissions to the atmosphere.

Experiments on different types of monitors for activation analysis have been initiated. In this project we are comparing liquid monitors with weighted solids and evaporated solutions on certain matrices. We have obtained excellent results by making monitor solutions from ultrapure weighable (i.e. non-hydrated) compounds of the elements and evaporating known quantities of the solutions to dryness on hydrophyllic filter paper. The filter material is then pressed to form pellets having the same dimensions as the pellets containing atmospheric particulates.

Some separated isotopes Fe, Cd, Gd, and Ru have been irradiated to produce isotopes whose decay schemes need to be studied in greater detail. This work will continue beyond this year and others will be added in the future. Some of these isotopes are used for tracer work on chemical separation currently being studied at the University of Maryland.

SEA AND ATMOSPHERE POLLUTION STUDIES

D. J. Bressan
(Naval Research Laboratory, Washington, D.C.)

During the year, laboratory experiments and chemical analyses have been carried out in connection with studies on sea water and atmospheric aerosol chemistry, transport and fractionation of chemicals from the sea surface to the atmosphere, and the transport and distribution of pollutants in the ocean and the atmosphere. These studies require the analysis of Hg, Pb, Ag, Fe, Mn, Sc, Na, K, S, Ca, Sr, Br, Cl and I.

The NBS reactor has been used to analyze samples of sea water, rain, fog condensate, atmospheric aerosols and atmospheric dust for microgram amounts of the above named elements. Radioactive tracers for some elements were made at the NBS facility and used in laboratory experiments at NRL. These experiments are to determine transport mechanisms, distribution and partitioning of man-made pollutants and naturally occurring elements in the natural systems under study.

This program is continuing with significant results expected for publication next year.

NEUTRON ACTIVATION ANALYSIS NAVY OIL MONITORING PROGRAM

D. A. Kubose
(Naval Ordnance Laboratory, White Oak, Md.)

The Naval Ordnance Laboratory is presently involved in a project to investigate the use of neutron activation as an analytical method in its oil monitoring program.

The Navy's oil monitoring program has been in operation for the past fifteen years. The ultimate goal of the program is the development of a method which can precisely predict and pinpoint sources of engine and transmission failures by analysis of trace components in the oil used to lubricate these parts.

The premise upon which the program is based is that excessive wear in the engine and transmission will be reflected in increased levels of trace elements in their lubricating oils. Systematic analysis of these oils should indicate when and possibly where this excessive wear is occurring. Engines and transmissions can be overhauled and/or otherwise fixed before catastrophic failure results.

The Navy is presently utilizing emission spectrometry in its oil monitoring systems. While the present method has been successful in detecting accelerated wear in engines and transmissions, it has not been able to pinpoint where this wear is occurring. This may be due in part to the inherent limitations (in terms of instrument sensitivity and versatility) of the system.

Neutron activation analysis is an extremely sensitive method which is capable of simultaneous multielement determination on a purely instrumental basis. Because of its extreme sensitivity, one can obtain detailed qualitative/quantitative trace element patterms which may allow the tracing of wear metals in the lubrication oil to its ultimate source in the engine or transmission component. The primary objective of the NOL research will be directed toward that achievement.

FEASIBILITY INVESTIGATIONS OF A FUEL BUNDLE MOTION MONITOR

J. P. Boright and R. E. Patrick
(U.S. Arms Control and Disarmament Agency, Washington, D.C.)
and
O. E. Frizzell

This program reported in the Annual Progress Report for the period ending October 31, 1972 was continued and concluded in this reporting period.

The work was expanded to include the radiation effects on the sensitivity of the solid state electronics employed in the monitor. The amplifier utilized was a radiation hardened solid state D.C. amplifier. Tests were conducted in high energy gamma fluxes up to 10^{20}R without degradation of the amplifier sensitivity or calibration.

A part of this program has been the mapping of the high energy gamma fields from the spent fuel elements. The reported values of energies by various investigators on this type of element is in the 0.8 to 1.6 MeV range. The element intensity does drop off with time but this does not present a serious obstacle since the average energy remains relatively constant and the radiation intensity can be measured and converted to dosage values. The intensity of the element drops about a decade in a 120-day period. The spent elements are renewed with fresh spent elements from reactor on a 90- to 120-day cycle.

This experiment necessitated the development of a means of measuring the intensity of the elements at different distances and locations from the element or elements. A high range gamma chamber (10mR to 10^4 R/h) and an electrometer were utilized for this purpose. An absolute calibration was not conducted since reproducibility was the experimental requirement.

A method of optical sighting was also developed in conjunction with the experiment to locate the target within ±1/4 in. on the X and Y axis under 20 ft. of water.

The experiment was concluded by a test of the completely assembled collimator, ion chambers and electronics. Spent fuel bundles were moved past the system through various background fields of gamma radiation to determine the limits of sensitivity. Various geometrical configurations of shielding material were inserted between the spent fuel bundle and detectors to determine the limits of sensitivity.

As a part of the same program demonstrations were conducted of the TV surveillance system developed at NBS[1] under similar environmental conditions under which it will be installed.

---

[1] Measurement Engineering Division (446.03), IAT.

STUDIES OF MAGNETIC PROPERTIES IN RARE EARTH ALLOYS AT CRYOGENIC TEMPERATURES

R. Segnan and D. M. Sweger
(American University, Washington, D.C.)

A Mössbauer effect source of ^{161}Dy has been prepared in a matrix of Gd_2O_3 for use in magnetic rare earth alloys studies of cryogenic temperatures. A high velocity drive (±25 cm/s) has been assembled for use in measuring resonant absorption in ^{161}Dy.

Magnetic rare earth alloys offer promise of possible use as materials suitable for high energy density electromagnetic applications. Particularly promising are Dy-Gd and Dy-Y alloys, since these tend to have quite attractive magnetic properties (for example, dysprosium has a saturation magnetization of approximately 34 kilogauss at 4.2 K).

The alloy system Gd-Dy can be investigated by Mössbauer spectroscopy by using a suitable radioisotope of either Gd or Dy. An analysis of the properties and availability of possible radioactive sources led to the selection of a ^{161}Dy isotope. The γ-ray used in this case comes from the decay of the 25.6 keV excited state to the ground state in ^{161}Dy. The excited state of ^{161}Dy can be populated by thermal neutron irradiation of ^{160}Gd.

Gadolinium oxide, Gd_2O_3, enriched to 96% ^{160}Gd in the form of a fine powder is the source material. The source is activated in the RT-4 pneumatic facility of the National Bureau of Standards Reactor in a thermal neutron flux of 1.3×10^{13} neutrons/cm^2 s. Such a flux will yield a source strength of about 3 millicuries/h gram of enriched Gd_2O_3.

The splitting of the saturation hyperfine field in ^{161}Dy is 43.7 cm/s and thus the drive must be capable of peak velocities of about ±25 cm/s. Velocities such as these are at least an order of magnitude larger than are required for most other Mössbauer isotopes. In addition, as for all drive systems, the velocity must be linear to within 1%. A modified version of the NBS Mössbauer drive was used to achieve the high velocities required for the ^{161}Dy resonance.

Measurements have been taken on four Dy-Gd alloys from 4.2K to their neèl (curie) temperatures. A saturation magnetic hyperfine splitting of 43.7 ± .1 cm/s is obtained for 1.0 ± .2 cm/s. The data for $H_{INT}(T)$ are composed to existing molecular field and spin-wave series, and it is found that spin-wave theory, when an anisotropy energy gap on the order of 24K is included in the spin wave spectrum, is in reasonably good agreement with the $H_{INT}(T)$ data below 0.5 $T_N(T_C)$. The temperature dependence of the data for quadrupole coupling is in good agreement with a theory by Callen and Callen[1] and indicates that the dominant contribution to V_{zz} is the single ion magnetocrystalline antisotrophy.

---

[1] H. D. Callen and E. Callen, *J. Phys. Chem. Solids*, 27, 1271-1285 (1966).

EFFECT OF RADIATION ON MAGNETIC MATERIALS

R. S. Sery and D. I. Gordon
(Naval Ordnance Laboratory, White Oak, Md.)

The Naval Ordnance Laboratory is a primary research and development activity of the Naval Material Command. Its mission includes research, design, development, testing, evaluation, fleet engineering support in weapons systems, etc., and investigations in related fields of science and technology.

One of the current projects of interest is that of determining radiation resistance of magnetic materials and devices including bubble memory materials for potential military applications.

The main purpose of this investigation is to determine whether or not they are invulnerable and if vulnerable how the materials and devices may be amenable to "radiation hardening."

Extensive sample irradiations have been performed to date at the NBS reactor facilities. The results thus far are preliminary and require further evaluation plus additional irradiation experiments in order to determine threshold values of doses, below which no radiation induced changes can be detected, and to give adequate statistical weight to (either confirming or contradicting) the findings obtained to date.

MÖSSBAUER SPECTROMETRY

D. A. Kubose
(Naval Ordnance Laboratory, While Oak, Md.)

The program being carried out at NOL which requires the use of the neutron irradiation facility at NBS concerns work in Mössbauer Spectrometry. The NBS facility has been used to produce radioactive Mössbauer sources.

In Mössbauer spectrometry, an absorber, which contains atoms of a particular nuclide, is interposed between a radioactive source and a detector. The radioactive source contains radionuclides that decay to the same nuclide that is in the absorber. Count rates are observed from the detector as a function of the relative velocity of the source as it is moved with respect to the absorber. The resultant velocity (energy) spectrum shows dips which are the result of resonant absorption of the gamma rays in the absorber. The system is extremely sensitive to small changes in gamma-ray energy that are caused by variations in the density of the valence electrons surrounding the atomic nucleus. The technique thus should find wide application as a sensitive analytical method for the determination of the chemical species of specific elements in samples, whether such elements be present in macro or tracer concentrations.

Once Mössbauer spectrometry has been successfully demonstrated, a suitable platform will be assembled such that coulomb excitation of a sample can be performed in conjunction with the NOL Van de Graaf accelerator. Upon completion of this assembly, it will be possible to use Mössbauer spectrometry as an analytical tool for the determination of the chemical species of many elements in any sample matrix. Applications will be made to the study of the chemical species of elements in seawater and in atmospheric particles.

ANGULAR CORRELATION OF POSITRON ANNIHILATION RADIATION IN METALS

A. C. Ehrlich
(Naval Research Laboratory, Washington, D.C.)

The electronic structure of the conduction electrons in alloys at any temperature and pure metals at all but the lowest temperatures cannot be studied by the experimental techniques that have been so successfully employed in studies of pure metals at low temperatures. These techniques require that the electrons have very long mean free paths and this occurs only in the purest metals at temperatures near absolute zero.

Among the very limited number of direct ways of studying the electronic structure of alloys (and pure metals at all but the lowest temperatures) is the angular correlation of positron annihilation radiation. In this method, one makes use of the fact that the small deviations from 180° made by the direction of travel of the two γ-rays which are emitted when a positron annihilates with an electron is a direct measure of the momentum of the annihilated electron. Thus, measurement of the number of coincident γ-ray pairs as a function of the angle between them provides direct information of the momentum spectrum of the electrons in a metal.

In order to provide useful information, however, the angles that must be resolved are very small ($\lesssim 10^{-3}$ radians), whereas to minimize statistical uncertainties the total number of counts must be large. To reconcile these opposing conditions, previous experimental setups have resolved only one component of momentum (one angle). To obtain more precise information, we have constructed an apparatus designed around two components of momentum while still achieving a satisfactorily high count rate. The technique requires that the specimen under study be rendered a highly radioactive positron emitter. This is most conveniently achieved by studying copper based alloys which, when irradiated in a neutron flux, become strong positron emitters. At the same time, minimizing crystallographic damage suggests the use of a thermalized (rather than a high energy) neutron flux. The RT-4 facility at the NBS nuclear reactor seems well suited to this purpose. Sufficent preliminary data has already been collected to determine that the experiment is feasible and should provide information on the electronic structure of alloys of a precision heretofore unobtainable.

BAND TAILING IN INDIUM ANTIMONIDE

John Stannard
(Naval Research Laboratory, Washington, D.C.)

Irradiation of the semiconductor indium antimonide with thermal neutrons transmutes indium into tin. Careful control of the neutron fluence allows the concentration of tin donor atoms and therefore the electrical properties of the irradiated crystals to be controlled. This has allowed the fabrication of surface active millimeter wave detectors whose impedance and physical strength are much improved over that of the state-of-the-art Rollin detector. The detectivity of these devices appears at present to approach that of the Rollin detector.

QUALITY ASSURANCE OF ALUMINUM ECAPSULATION MATERIAL

L. S. Kellogg and W. N. McElroy
(Hanford Engineering Development Laboratory, Richland, Wash.)

High Purity Aluminum for encapsulation of fission foils to be used in the Liquid Metal Fast Broader Reactor program were analyzed by the Hanford Engineering Development Laboratory. As part of the Quality Assurance program, a set of six foils was prepared and irradiated for a total of 16 hours (total fluence $\sim 8 \times 10^{17}$) in the NBS reactor RT-4 position (highly thermalized). These foils indicated a number of contaminating gamma activities. Those now identified are ^{46}Sc, ^{182}Ta, and ^{69}Co with ^{46}Sc the major contributor to the gamma spectra. Gamma energies of peaks noted but not identified at this time (in ∿keV) are: 54, 65, 99, 147, 316, 606, 324, 486, 135, and 1101. Preliminary calculations assuming ^{45}Sc(N,γ) ^{46}Sc indicate an initial concentration of ^{45}Sc of ∿0.1 ppm. The variation in impurity content (homogeneity) utilizing ^{46}Sc for the measurements was found to be <3% relative.

G. STAFF ROSTER

RRD ORGANIZATION CHART

REACTOR RADIATION DIVISION
(Division 314)

R. S. Carter, Chief
T. M. Raby, Deputy Chief

E. Maxwell, Admin. Officer*
E. Simms, Receptionist

Technical Support

R. Casella
M. Ganoczy
V. Myers
F. Shorten

314.01

Reactor Operations
T. M. Raby, Chief
J. F. Torrence, Deputy

D. Ahalt, Sec'y.
J. Bowers, Admin. & Tech. Ass't.

D. Allison
R. Beasley
M. Bell
N. Bickford
H. Brake
D. Cea
A. Chapman
H. Dilks
J. Ring
R. Scheide
R. Stiber
D. Wilkison
B. J. Young

314.02

Engineering Services
J. H. Nicklas, Chief

R. Weller, Sec'y.*

P. Beachley
R. Conway
J. Darr
O. Frizzell
E. Guglielmo
R. Hayes
H. Jackson
J. Sturrock

314.03

Neutron S-S Physics
J. J. Rush, Chief

L. Clutter, Sec'y.

A. Cinquepalma
D. Fravel
R. Livingston*
E. Prince
A. Santoro
A. Tudgay
W. Rymes

*Temporary, Part-time

NON-RRD NBS STAFF LOCATED AT REACTOR

Division 310.08

D. A. Becker
B. S. Carpenter
W. A. Cassatt
T. Gills
P. D. LaFleur
G. J. Lutz
L. T. McClendon
E. Orvini (U. of PaVia, Italy)
G. M. Reimer
H. L. Rook
R. W. Shideler
J. E. Suddueth
R. M. Young
H. P. Yule

Division 313.00

B. Mozer
B. LeNeindre (CNRS-Bellevue, France)

Division 240.01

P. R. Cassidy
H. E. DeSpain
E. J. Embree
J. J. Shubiak

Division 242.01

R. A. Dallatore
J. A. Grundl
I. G. Schroder
A. Fabry (Cen-Sek, Belgium)

GUEST WORKERS AND COLLABORATORS

Division 221.03

H. Marshak
R. J. Soulen, Jr.
D. B. Utton

Division 221.05

R. D. Mountain
H. J. Raveche

Division 232.06

R. D. Deslattes
W. C. Sauder
E. G. Kessler

Division 242.02

L. D. Miller
F. J. Schima

Division 311.03

J. D. Barnes

Division 311.05

B. Dickens
L. W. Schroeder

Division 313.01

C. W. Reimann

Division 313.06

A. D. Mighell

Argonne National Laboratory

H. Flotow
D. C. Price
J. M. Rowe

STAFF ROSTER

Armed Forces Radiobiology Res. Inst.

Maj. G. Dunson

Federal Bureau of Investigation

D. B. Davies
J. W. Kilty
J. M. Little
G. P. Mahoney
J. P. Riley

Food and Drug Administration

M. Friedman*
R. E. Simpson
J. T. Tanner*

Harry Diamond Laboratory

D. McGarry

Northern Virginia Pathology Lab.

Ira Godwin

Naval Ordnance Laboratory

H. Alperin*
D. I. Gordon
D. A. Kubose
S. J. Pickart*
J. J. Rhyne*
R. S. Sery
R. H. Williams*

Naval Research Laboratory

D. J. Bresson
A. C. Ehrlich
G. A. Ferguson
J. Karle
J. H. Konnert
L. F. Paolella*
J. Stannard
P. E. Wilkniss

Picatinny Arsenal

C. S. Choi*
H. J. Prask*
R. S. Singh*
S. F. Trevino*

U.S. ACDA

J. D. Boright
R. E. Patrick

U.S. Army Inst. of Dental Res.

G. C. Battistone

U.S. Atomic Energy Commission

J. C. Glynn

U.S. Geological Survey

F. W. Brown
R. Finkelman
L. P. Greenland
J. J. Rowe
G. Sellers
F. O. Simon

U.S. Postal Service

M. Beckman
G. R. Stangohr
J. Upton

U.S. Treasury Department

R. L. Brunelle
P. C. Buscemi
C. M. Hoffman
F. A. Lundgren
M. J. Pro

Hanford Engineering Devel. Lab.

L. S. Kellogg
W. N. McElroy

The Ford Motor Company

W. G. Rothschild

American University

R. G. Arnold
B. T. Chertok
R. A. Segnan
R. Simon
D. M. Sweger

Carnegie Institution of Washington

L. W. Finger

Harvard University

J. L. Alperi*
R. Wilson

Interuniversitair Reactor Instituut

L. A. de Graaf

McGill University

G. Donnay
J. D. H. Donnay
R. F. Martin

Temple University

M. Green
V. P. Warkulwiz*

U.S. Naval Academy

C. S. Schneider

University of Maryland

J. Barker
P. Buhl
R. A. Cahill
T. J. Conry
E. Gladney
C. Glinka
G. E. Gordon
J. Graber
S. Harrison
A. Jones
R. Khanna
V. J. Minkiewicz
F. J. Munno
J. Ondov
L. Raber
J. Reednick
W. B. Walters
W. H. Zoller

Georgetown University Hospital

J. Harbert

Northern Va. Pathology Lab.

Ira Godwin

Johns Hopkins Medical Inst.

F. Hosain

---

*Located full-time at NBS Reactor

H. PUBLICATIONS

COLLABORATIVE PROGRAMS

ALPERIN, H. A., S. J. PICKART, J. J. RHYNE AND V. J. MINKIEWICZ, Softening of the Transverse Optic Mode in PbTe," *Phys. Letters* 40A, 295 (1972).

BARNES, J. D., "Neutron Inelastic Scattering Study of the 'Rotator' Phase Transition in N-Alkanes," *Proc. Intern. Symposium on Inelastic Scattering of Neutrons, Grenoble, France* (March 1972).

CASELLA, R. C., "Possible Failure of the Pomeranchuk Theorem Shrinkage of the Forward Elastic Peak and Oscillations," *Elementary Processes at High Energy* (Academic Press, New York, 1971), p. 578.

CHOI, C. S., AND E. PRINCE, "The Crystal Structure of Cyclo-trimethylene-trinitramine," *Acta Cryst.* B28, 2857 (1972).

CHOI, C. S., J. E. MAPES, AND E. PRINCE, "The Structure of Ammonium Nitrate (IV)," *Acta Cryst.* B28, 1357 (1972).

CHOI, C. S., AND J. E. ABEL, "The Crystal Structure of 1,3,5-Trinitrobenzene by Neutron Diffraction," *Acta Cryst.* B28, 193 (1972).

CLARK, A. E., H. S. BELSON, J. J. RHYNE, S. J. PICKART AND E. R. CALLEN, "Magnetostriction and Magnetic Anisotropy of $TbFe_2$," *Phys. Rev. Letters* (to be published).

DEGRAAF, L. A., J. J. RUSH, R. C. LIVINGSTON, H. E. FLOTOW AND J. M. ROWE, "Study of Hydrogen Diffusion in Vanadium and Tantalum Hydride by Quasielastic Thermal Neutron Scattering," *Proc. Intern. Meeting on Hydrogen in Metals, JUL-Conf-6 (Vol. 1)* (March 1972), p. 301.

DEGRAAF, L. A., J. J. RUSH AND R. C. LIVINGSTON, "Neutron Scattering Study of the Rotational Motions and Phase Transitions in Sodium and Cesium Hydrosulfides," *Proc. 5th IAEA Symposium on Inelastic Scattering of Neutrons, Grenoble, France* (March 1972).

DEGRAAF, L. A. AND B. MOZER, "Structure Study of Neutron Diffraction by Liquid Neon," *J. Chem. Phys.* 55, 4967 (1971).

DEGRAAF, L. A., J. J. RUSH, H. E. FLOTOW AND J. M. ROWE, "Quasielastic Thermal Neutron Scattering by Hydrogen in α-Vanadium Hydride," *J. Chem. Phys.* 56, 4574 (1972).

KONNERT, J., J. KARLE AND G. A. FERGUSON, "Structure of Vitreous Silica and Germania by Neutron and X-ray Diffraction," *Science* (to be published).

PUBLICATIONS

LEUNG, P. S., J. J. RUSH AND T. I. TAYLOR, "Study of Hindered Rotation in Crystals by Neutron Transmission Measurements: Comparison of Calculated and Measured Scattering Cross Sections," *J. Chem. Phys.* 57, 175 (1972).

LOGAN, D. W., S. F. TREVINO, R. C. CASELLA, W. M. SHAW, L. D. MUHLESTEIN AND R. D. MICAL, *Phonons,* (Flammarion Science Press, Paris, 1971), p. 104.

MIGHELL, A.D., AND A. SANTORO, "The Crystal and Molecular Structure of Hexakis (imidazole)cadmium(II) nitrate, $[Cd(C_3H_4N_2)_6](NO_3)_2$ and Hexakis(imidazole)cadmium(II)hydroxide nitrate tetrahydrate, $[Cd(C_3H_4N_2)_6](OH)(NO_3)\cdot 4H_2O$", Acta Cryst. B27, 2089 (1971).

MIGHELL, A. D., C. W. REIMANN, AND A. SANTORO, "The Crystal and Molecular Structure of the 2:1 Dimer Dibromobis (Pyridine N-oxide) Copper (II) [Pyridine N-oxide$)_2$CuBr$_2]_2$," *Acta Cryst.* B28, 126 (1972).

MYERS, V. W., "Klein-Gordon Equation for Charged Particle Interacting with an Electromagnetic Wave," *J. Franklin Institute* (to be published).

PRICE, D. L., J. M. ROWE, J. J. RUSH, D. PRINCE, D. G. HINKS AND S. SUSMAN, "Single Crystal Neutron Diffraction Study of Potassium Cyanide," *J. Chem. Phys.* 56, 3697 (1972)

PRASK , H., S. TREVINO, J. GAULT AND K. W. LOGAN, "Ice I-Lattice Dynamics and Incoherent Neutron Scattering," *J. Chem. Phys.* 56, 3217 (1972).

PRINCE, E., "The Configuration of the Water Molecule in Cupric Fluoride Dihydrate at 928°K," *J. Chem. Phys.* 56, 4352 (1972).

PRINCE, E., L. W. SCHROEDER, AND J. J. RUSH, "A Constrained Refinement of the Structure of Durene," *Acta Cryst.* (to be published).

PRINCE, E., A. D. MIGHELL, C. W. REIMANN, AND A. SANTORO, "Hexakis(Imidazole) Cobalt(II) Nitrate $[Co(C_3H_4N_2)_6](NO_3)_2$," *Crystal. Struct. Comm.* (to be published).

PRINCE, E., G. DONNAY AND R. F. MARTIN, "Neutron Diffraction Refinement of an Ordered Orthoclase Structure," *Am. Mineralogist* (to be published).

PRINCE, E., AND L. W. FINGER, "Use of Constraints on Thermal Motion in Structure Refinement of Molecules with Librating Side Groups," *Acta Cryst.* (to be published).

RAFIZADEH, H. A., S YIP AND H. PRASK, "Lattice Dynamics of Rhombohedral Sodium Azide," *J. Chem. Phys.* 56, 5377 (1972).

PUBLICATIONS

RAO, K. R., S. F. TREVINO, H. J. PRASK AND R. D. MICAL, "The Lattice Dynamics of KN_3," *Phys. Rev.* 4B, 4551 (1971).

REIMANN, C. W., M. ZOCCHI, A. D. MIGHELL AND A. SANTORO, "Crystal and Molecular Structure of Nitrotobis-(2,2'-dipyridyl)cobalt(III) Hydroxide Nitrate Tetrahydrate $[XCo(C_{10}H_8N_2)_2(NO_3)](NO_3)(OH)\cdot 4H_2O$," *Acta Cryst.* B27, 2211 (1971).

RHYNE, J. J., S. J. PICKART, AND H. A. ALPERIN, "Direct Observation of an Amorphous Spin Polarization Distribution," *Phys. Rev. Letters* (to be published).

ROWE, J. M., J. J. RUSH, L. A. DEGRAAF AND G. A. FERGUSON, "Neutron Quasi-elastic Scattering Study of Hydrogen Diffusion in a Single Crystal of Palladium," *Phys. Rev. Letters* (to be published).

RUSH, J. J., L. W. SCHROEDER AND A. J. MELVEGER, "The Dynamics of Sodium and Potassium Bifluoride," *J. Chem. Phys.* 56, 2793 (1972).

RUSH, J. J., L. A. DEGRAAF AND R. C. LIVINGSTON, "Neutron Scattering Investigation of the Rotational Dynamics and Phase Transitions in Sodium and Cesium Hydrosulfides," *J. Chem. Phys.* (to be published).

SANTORO, A., AND A. D. MIGHELL, "Coincidence-Site Lattices," *Acta Cryst.* (to be published).

SANTORO, A., AND A. D. MIGHELL, "Properties of Crystal Lattices: The Derivative Lattices and Their Determination," *Acta Cryst.* (to be published).

SAVAGE, H. T., AND J. J. RHYNE, "Magnetic Characteristics of Gd Doped SnTe and PbTe," *A.I.P. Conf. Proc.* 5, 879 (1972).

SCHROEDER, L. W., L. A. DEGRAAF, AND J. J. RUSH, "Neutron Diffraction Study of the Trigonal and Cubic Phases of NaSH," *J. Chem. Phys.* 55, 5363 (1971).

WANG, F. E., S. J. PICKART, AND H. A. ALPERIN, "Mechanism of the TiNi Martensitic Transformation and the Crystal Structures of TiNi-II and TiNi-III Phases," *J. Appl. Phys.* 43, No. 1 (1972).

INDEPENDENT PROGRAMS

ALBERI, J. L., R. WILSON, AND I. G. SCHRODER, "Parity Violations in Neutron Captive Gamma Rays," *Phys. Rev. Letters* (to be published).

PUBLICATIONS

BECKER, D. A., AND P. D. LAFLEUR, "Neutron Activation Analysis: Applications to Trace Element Analysis in Biological and Environmental Materials," *Proc, Conf. on Trace Substances in Environmental Health, Columbia, MO, June, 1971* (1972) pp. 447-453.

BECKER, D. A., AND P. D. LAFLEUR, "Determination of Trace Quantities of Uranium in Biological Materials by Neutron Activation Analysis Using a Rapid Radiochemical Separation," *Anal. Chem.* 44, 1508 (1972).

BECKER, D. A. "Trace Analysis for Platinum in Glasses by Neutron Activation Analysis," *Anal. Chim. Acta* 61 (1972).

CARPENTER, B. S., "The Use of the Nuclear Track Technique for Boron and Uranium Analyses in Botanical Material," *Proc. Am. Nucl. Soc. Meeting, Boston, June 1971* (1971), pp. 130-131.

CARPENTER, B. S., "Determination of Trace Concentrations of Boron and Uranium in Glass by the Nuclear Track Technique," *Anal. Chem.* 44, 600 (1972).

CARPENTER, B. S., AND P. D. LAFLEUR, "Observing Proton Tracks in Cellulose Nitrate," *Intern. J. Appl. Radiation and Isotopes* 23, 157 (1972).

CARPENTER, B. S., "Quantitative Applications of the Nuclear Track Technique," *The Microscope* 20, 175 (1972).

CARPENTER, B. S., AND P. D. LAFLEUR, "Nitrogen Determination in Biological Samples Using the Nuclear Track Technique," *Proc. Am. Nucl. Soc. Meeting, June, 1972* to be published).

DUCE, R. A., W. H. ZOLLER, and A. G. JONES, "Atmosphere Particulate and Gas Sampling at McMurdo and South Pole Stations," *Antartic J. of U.S.*) (1971), 133.

FABRY, A., and J. D. JENKINS, "Calculations of the ΣΣ Facility with ENDF/B-Versions II and III and Comparison with Experiment," *Proc. Am. Nucl. Soc., Washington, November, 1972* (1972), p. 940.

FABRY, A., AND J. D. JENKINS, "Wall Return Neutron Fluxes for High- and Intermediate-Energy Cavity Neutron Sources," *Proc. Am. Nucl. Soc., Washington, November, 1972* (1972), p. 975.

FRIEDMAN, M. H., J. T. TANNER AND E. MILLER, "Rapid Instrumental Analysis for Mercury in Biological Materials by Neutron Activation," *Transactions of the Am. Nucl. Soc.* 15, 150-151 (1972).

GLADNEY, E. S., W. H. ZOLLER, R. A. DUCE, AND A. G. JONES, "Vanadium, Aluminum and Manganese in Atmosphere Particulate from McMurdo and South Pole Stations," *Antartic J. of U.S.* (1972).

PUBLICATIONS

GLYNN, J. C., F. J. MUNNO, AND I. G. SCHRODER, "In-core Fast-Neutron Measurements Using a ^{3}He Semiconductor Spectrometer," *Trans. Am. Nucl. Soc.* 15, 537 (1972).

GOTTFRIED, D., J. J. ROWE, AND R. I. TILLING, "Distribution of Gold in Igneous Rocks," *Geological Survey Professional Paper 727* (1972).

GRUNDL, J. A., V. SPIEGEL, JR., AND C. EISENHAUER, "Measurement of ^{235}U and ^{238}U Fission Cross Sections for ^{252}Cf Spontaneous Fission Neutrons," *Proc. Am. Nucl. Soc., Washington, November, 1972* (1972), p. 945.

JONES, A. E., N. CHAED, G. L. DUNSON, AND F. HOSAIN, "Clinical Evaluation of Orally Administered Fluorine-18 for Bone Scanning," *J. Radiology* (to be published).

LAFLEUR, P. E., "Retention of Mercury When Freeze-Drying Biological Materials," *Anal. Chem.* (to be published).

LINCOLN, D. N., M. H. FRIEDMAN, AND J. T. TANNER, "Application of Neutron Activation Analysis to the Determination of Mercury in Food Products: A Bibliography," *F.D.A. By-Lines* 2, No. 2., 88-89 (1971).

LUTZ, G. J., "Determination of Lead in Environmental Samples by Photon Activation Analysis," *Proc. Am. Nucl. Soc. Topical Meeting, Aug. 1971* (1972), pp. 144-149.

LUTZ, G. J., R. J. BORENI, R. S. MADDOCK, AND J. WING, "Activation Analysis: A Bibliography through 1971," *NBS Techn. Note 467* (1972).

MARGOSIS, M., AND J. T. TANNER, "Neutron Activation Analysis: Logistics and Economics," *F.D.A. By-Lines* 2, No. 5, 215-224 (1972).

MARSHAK, H., AND R. J. SOULEN, JR., "The Temperature Scale Defined by ^{60}Co γ-ray Anisotropy and Noise Thermometry," *Proc. of LT-13, Boulder, Colorado* (to be published).

MASTERS, L. W., AND G. J. LUTZ, "Determination of Thallium by Photon Activation Analysis," *Anal. Chim. Acta* 56, 365 (1971).

ROOK, H. L., P. D. LAFLEUR AND T. E. GILLS, "Mercury in Coal: A New Standard Reference Material," *Environ. Letters* 2, 195 (1972).

ROOK, H. L., T. E. GILLS, AND P. D. LAFLEUR, "Method for Determination of Mercury in Biological Materials in Biological Materials by Neutron Activation Analysis," *Anal. Chem.* 44, 1114 (1972).

PUBLICATIONS

ROOK, H. L., "Rapid, Quantitative Separation for the Determination of Selenium Using Neutron Activation Analysis," *Anal. Chem.* 44, 1276 (1972).

SCHRODER, I. G., "Emission of Long-Range Alpha Particles in the Sub-Thermal, Thermal, and Resonance-Neutron Fission of Pu^{239}," *Nucl. Phys.* (to be published).

SEITZ, M. G., R. M. WALKER AND B. S. CARPENTER, "Improved Methods for Measurement of Thermal Neutron Dose by the Fission Track Technique," *J. Appl. Phys.* (to be published).

SOULEN, R. J. JR., AND H. MARSHAK, "The Use of Josephson Junctions for Noise Thermometry Below 1 Kelvin," *Proc. Applied Conductivity Conf., Annapolis, Md.* (May 1972).

TANNER, J. T., M. H. FRIEDMAN, AND D. N. LINCOLN, "Mercury Content of Common Foods Determined by Neutron Activation Analysis," *Science* 177, 1102-1103 (1972).

THOMPSON, B. A., AND E. C. MILLER, "Determination of Trace Elements in Ruby Laser Crystals by Neutron Activation Analysis," *J. of Research, NBS--A. Physics and Chemistry* 75A, 429 (1971).

THOMPSON, B. A., AND G. J. LUTZ, "Characterization of Ancient Bronze Artifacts by Neutron and Photon Activation Analysis," *Radiochem and Radioanal. Letters* 9, 343 (1972).

THOMPSON, B. A., AND P. D. LAFLEUR, "Gamma Ray Spectroscopy," *Encyclopedia of Chemistry, Third Edition* (to be published).

YULE, H. P., "Study of Gamma-Ray Spectrum Distortion by Mathematical Smoothing," *Anal. Chem.* 44, 1245 (1972).

YULE, H. P., "A Conversational Text Editor for a Laboratory Minicomputer," *Anal. Chem.* (to be published).

ZOLLER, W. H., G. E. GORDON, E. S. GLADNEY, AND A. G. JONES, "The Sources and Distribution of Vanadium in the Atmosphere," *Advances in Chemistry* (to be published).

☆ U. S. GOVERNMENT PRINTING OFFICE :1973—511-324 (204)

FORM NBS-114A (1-71)

U.S. DEPT. OF COMM. **BIBLIOGRAPHIC DATA SHEET**	1. PUBLICATION OR REPORT NO. NBS TN-758	2. Gov't Accession No.	3. Recipient's Accession No.
4. TITLE AND SUBTITLE NBS REACTOR: SUMMARY OF ACTIVITIES OCTOBER 1971 TO SEPTEMBER 1972			5. Publication Date March 1973 6. Performing Organization Code
7. AUTHOR(S) Robert S. Carter			8. Performing Organization
9. PERFORMING ORGANIZATION NAME AND ADDRESS NATIONAL BUREAU OF STANDARDS DEPARTMENT OF COMMERCE WASHINGTON, D.C. 20234			10. Project/Task/Work Unit No. 11. Contract/Grant No.
12. Sponsoring Organization Name and Address Reactor Radiation Division National Bureau of Standards Washington, D.C. 20234			13. Type of Report & Period Covered 10/1/71 - 10/1/72 14. Sponsoring Agency Code

15. SUPPLEMENTARY NOTES

16. ABSTRACT (A 200-word or less factual summary of most significant information. If document includes a significant bibliography or literature survey, mention it here.)

This report summarizes all those programs which depend on the NBS reactor. It covers the period from October 1971 through September 1972. The programs range from the use of neutron beams to study the structure and dynamics of materials through nuclear physics and neutron standards to sample irradiations for activation analysis, isotope production and radiation effects studies.

17. KEY WORDS (Alphabetical order, separated by semicolons)
Activation analysis; crystal structure; diffraction; isotopes; molecular dynamics; neutron; nuclear reactor; radiation

18. AVAILABILITY STATEMENT ☒ UNLIMITED. ☐ FOR OFFICIAL DISTRIBUTION. DO NOT RELEASE TO NTIS.	19. SECURITY CLASS (THIS REPORT) UNCLASSIFIED	21. NO. OF PAGES 140
	20. SECURITY CLASS (THIS PAGE) UNCLASSIFIED	22. Price $2.10 Domestic Postpaid $1.75 GPO Bookstore

NBS TECHNICAL PUBLICATIONS

PERIODICALS

JOURNAL OF RESEARCH reports National Bureau of Standards research and development in physics, mathematics, and chemistry. Comprehensive scientific papers give complete details of the work, including laboratory data, experimental procedures, and theoretical and mathematical analyses. Illustrated with photographs, drawings, and charts. Includes listings of other NBS papers as issued.

Published in two sections, available separately:

- **Physics and Chemistry (Section A)**

Papers of interest primarily to scientists working in these fields. This section covers a broad range of physical and chemical research, with major emphasis on standards of physical measurement, fundamental constants, and properties of matter. Issued six times a year. Annual subscription: Domestic, $17.00; Foreign, $21.25.

- **Mathematical Sciences (Section B)**

Studies and compilations designed mainly for the mathematician and theoretical physicist. Topics in mathematical statistics, theory of experiment design, numerical analysis, theoretical physics and chemistry, logical design and programming of computers and computer systems. Short numerical tables. Issued quarterly. Annual subscription: Domestic, $9.00; Foreign, $11.25.

TECHNICAL NEWS BULLETIN

The best single source of information concerning the Bureau's measurement, research, developmental, cooperative, and publication activities, this monthly publication is designed for the industry-oriented individual whose daily work involves intimate contact with science and technology—*for engineers, chemists, physicists, research managers, product-development managers, and company executives.* Includes listing of all NBS papers as issued. Annual subscription: Domestic, $6.50; Foreign, $8.25.

NONPERIODICALS

Applied Mathematics Series. Mathematical tables, manuals, and studies.

Building Science Series. Research results, test methods, and performance criteria of building materials, components, systems, and structures.

Handbooks. Recommended codes of engineering and industrial practice (including safety codes) developed in cooperation with interested industries, professional organizations, and regulatory bodies.

Special Publications. Proceedings of NBS conferences, bibliographies, annual reports, wall charts, pamphlets, etc.

Monographs. Major contributions to the technical literature on various subjects related to the Bureau's scientific and technical activities.

National Standard Reference Data Series. NSRDS provides quantitative data on the physical and chemical properties of materials, compiled from the world's literature and critically evaluated.

Product Standards. Provide requirements for sizes, types, quality, and methods for testing various industrial products. These standards are developed cooperatively with interested Government and industry groups and provide the basis for common understanding of product characteristics for both buyers and sellers. Their use is voluntary.

Technical Notes. This series consists of communications and reports (covering both other-agency and NBS-sponsored work) of limited or transitory interest.

Federal Information Processing Standards Publications. This series is the official publication within the Federal Government for information on standards adopted and promulgated under the Public Law 89–306, and Bureau of the Budget Circular A–86 entitled, Standardization of Data Elements and Codes in Data Systems.

Consumer Information Series. Practical information, based on NBS research and experience, covering areas of interest to the consumer. Easily understandable language and illustrations provide useful background knowledge for shopping in today's technological marketplace.

BIBLIOGRAPHIC SUBSCRIPTION SERVICES

The following current-awareness and literature-survey bibliographies are issued periodically by the Bureau:

Cryogenic Data Center Current Awareness Service (Publications and Reports of Interest in Cryogenics). A literature survey issued weekly. Annual subscription: Domestic, $20.00; foreign, $25.00.

Liquefied Natural Gas. A literature survey issued quarterly. Annual subscription: $20.00.

Superconducting Devices and Materials. A literature survey issued quarterly. Annual subscription: $20.00. Send subscription orders and remittances for the preceding bibliographic services to the U.S. Department of Commerce, National Technical Information Service, Springfield, Va. 22151.

Electromagnetic Metrology Current Awareness Service (Abstracts of Selected Articles on Measurement Techniques and Standards of Electromagnetic Quantities from D-C to Millimeter-Wave Frequencies). Issued monthly. Annual subscription: $100.00 (Special rates for multi-subscriptions). Send subscription order and remittance to the Electromagnetic Metrology Information Center, Electromagnetics Division, National Bureau of Standards, Boulder, Colo. 80302.

Order NBS publications (except Bibliographic Subscription Services) from: Superintendent of Documents, Government Printing Office, Wash-

U.S. DEPARTMENT OF COMMERCE
National Bureau of Standards
Washington, D.C. 20234

OFFICIAL BUSINESS

Penalty for Private Use, $300

POSTAGE AND FEES PAID
U.S. DEPARTMENT OF COMMERCE
215

U.S.MAIL